DOCTORAL THESIS

Industrial Wood Drying

Airflow Distribution, Internal Heat Exchange and Moisture Content as Input and Feedback to the Process

Tommy Vikberg

LULEÅ UNIVERSITY OF TECHNOLOGY

DOCTORAL THESIS

Industrial Wood Drying

Airflow Distribution, Internal Heat Exchange and Moisture Content as Input and Feedback to the Process

Tommy Vikberg

Division of Wood Science and Engineering
Department of Engineering Sciences and Mathematics
Luleå University of Technology
Skellefteå, Sweden

Printed by Luleå University of Technology, Graphic Production 2015

ISSN 1402-1544
ISBN 978-91-7583-394-1 (print)
ISBN 978-91-7583-395-8 (pdf)

Luleå 2015

www.ltu.se

Abstract

The aim of this work was to provide knowledge that can help to further develop the industrial wood drying process. Specifically, the focus was on the following tasks:

- To investigate methods of determining the average green[i] moisture content (MC) of wood batches prior to the drying process.

- To investigate methods of improving the determination of the MC of individual boards after drying.

- To examine methods to decrease the energy expenses[ii] in industrial wood drying.

To determine the average green MC of batches, two different methods were investigated. The first method utilized three dimensional scanning together with discrete X-rays. By determining the green densities of the heartwood and sapwood separately, and assuming both a fixed MC in the heartwood and a certain relation between the heartwood and sapwood basic densities[iii], the MC of the sapwood was determined. Of the investigated logs, 70% were correctly sorted into high or low MC groups. Unfortunately, the material used in the study did not contain any logs that exhibited significant drying of the sapwood, so the ability to identify that kind of log could not be investigated.

In the second method, the average basic density was estimated as a function of the log diameter, and the maximum error when calculating the average MC with a system determining volume and mass by other means was derived. The maximum error of a wood package with an average MC of 70% became as high as 14% MC, caused mainly by the variation in the basic density of the wood. The determination of the average MC of single packages was not therefore reliable, but the method could still provide valuable information about the average MC of a drying batch consisting of several packages, as well as providing an indicator of long-term MC trends.

In the investigation of methods to improve the MC determination of individual boards after drying, two other approaches were used. In the first approach, possible

[i] With "green" the state of un-dried wood is intended.
[ii] With energy expenses the energy-related costs are intended, i.e. savings can be due to decreased total heat demand or by using a cheaper fuel type to generate the heat.
[iii] Basic density is defined as the dry mass divided by the fully swollen volume.

improvements by combining measuring techniques, i.e. X-ray, microwave and visual grading, were investigated. It was found that the proportion of boards for which the MC could be determined within 1% MC from the reference MC, determined by the oven-dry method, increased from 72 to 79% by adding X-ray to the microwave data. It was also found that the lowest visual grade had the highest proportion of boards with an assessed MC deviating by more than 1 percentage point from the reference MC assessed by the oven-dry method.

In the second approach, the possibility of increasing the measurable board width was investigated by introducing a function that compensates for the interference patterns caused by the closeness of a board edge. The function was developed through finite element simulations and it was shown that the measureable board width could be increased by approximately 32 mm, which can make a considerable difference when trying to detect a MC gradient, i.e. wet cores, as well as when wood of small dimensions is cross fed over the measurement device. The absolute magnitude of the improvement is however dependent on the measurement device, and it should not be considered as a general improvement.

Ways of decreasing a sawmill's energy expenses related to wood drying were also investigated in two of the appended publications. In one of them, possible heat savings by introducing a new kiln layout were investigated. By installing a door between the two zones of a two-zone continuous kiln, it is possible to run the two zones at very different temperature levels. This makes it possible to dehumidify the air in the high-temperature zone through condensation and to reintroduce the latent heat of evaporation to the low-temperature zone of the kiln. In the investigated case, heat savings of roughly 30% could be achieved in comparison to a traditional kiln with no heat exchanger.

In the second publication, the airflow distribution in an industrial batch kiln as function of the air circulating fan speed was investigated. Although it does not affect the total heat demand to any great extent, the cost savings can be large due to the price difference between heat generated by electricity and heat generated by burning residuals, i.e. bark and sawdust. In the investigation, the air velocity was measured simultaneously at 20 positions through the load with the air circulating fans running at a number of different speeds. It was found that the airflow distribution did not change remarkably when the fan speed was altered. When the airflow had been measured at a certain fan speed, the effect of changing the fan speed could be estimated, within 10% of the measured value, by using the fan affinity laws.

Preface

The work presented in the following pages was performed at SP Technical Research Institute of Sweden and Luleå University of Technology in Skellefteå. I would like to express my warmest gratitude to my present and past colleagues for all the joy and profession we have shared. I sincerely appreciate the work of my present and past supervisors, Jonas Danvind, Lena Antti, Johan Oja, Lars Hansson, Diego Elustondo, Margot Sehlstedt-Persson and Tom Morén of whom the last two deserve an extra award for standing my company for so long. With the six appended papers in this thesis, the paper to supervisor ratio is approaching 1.

All the collaboration with the industrial partners throughout the work, and the resulting firewood to heat my house, have also been greatly appreciated.

And to you Sara, who literally skipped a prom in the castle to have a pizza with me instead, the bad judgement you showed that night, and every day since then, of which I have been heavily favoured, is greatly appreciated. You are adorable!

Last, but not least, I would like to send a big hug to my parents, siblings and everyone else who has been supporting me as a person.

Jävrebyn, September 2015

Tommy Vikberg

List of appended publications

I. Skog, J., Vikberg, T. & Oja, J. (2010) Sapwood moisture-content measurements in Pinus sylvestris sawlogs combining X-ray and three-dimensional scanning. Wood Material Science and Engineering, 5(2):91-96.

II. Vikberg, T. & Elustondo, D. (2015) Basic density determination for Swedish softwoods and its influence on average moisture content of wood packages estimated by measuring their mass. Wood Material Science and Engineering. http://dx.doi.org/10.1080/17480272.2015.1090481.

III. Vikberg, T., Oja, J. & Antti, L. (2012) Moisture content measurement in Scots pine by microwave and X-rays. Wood and Fiber Science, 44(3):280-285.

IV. Vikberg, T., Hansson, L., Schajer, G. S. & Oja, J. (2012) Effects on microwave measurements and simulations when collecting data close to edges of wooden boards. Measurement, 45(3):525-528.

V. Vikberg, T. & Morén, T. (2015) Internal heat exchange in progressive kilns. PRO LIGNO. Accepted for publication.

VI. Vikberg, T., Hägg, L. & Elustondo, D. (2015) Influence of fan speed on airflow distribution in a batch kiln. Wood Material Science and Engineering, 10(2):197-204.

The author´s contribution to the appended publications

Publication No.	
I:	A script in Matlab that made it possible to measure density in the computed tomography images was partly developed by me. The corresponding measurements and a minor part of the writing were also done by me.
III, IV & V:	I made a major contribution to the planning of the work, did the experimental work, the analysis and the main part of the writing.
II & VI:	I contributed to the data collection, and did a major part of the analysis and writing.

Contents

1 Introduction

1.1 Background

Wood is a resource of great importance for the Gross National Product of many countries. For Sweden, with 57% of the land area classified productive forest and an annual harvest of approximately 80 million m^3sk[iv] (Nilsson et al. 2014), wood has become one of the most important industrial sectors (Lundberg 2013). Of the total timber stock in the productive forest, Scots pine (*Pinus sylvestris* L.) accounts for 39.2%, Norway spruce (*Picea abies* (L.) Karst) for 41.5%, Birch for 12.0% and other species for the rest (Nilsson et al. 2014). Of the harvested volume, Scots pine accounts for 33%, Norway spruce for as much as 50% and other species for the rest (Nilsson et al. 2014). A natural result is that Scots pine and Norway spruce are the two species of greatest commercial interest.

Of the harvested forest, 45% of the volume is brought to sawmills as sawlogs. After all the process stages at the sawmill, the volume yield of sawn timber is 47% (Anon. 2015a). The single largest expense for a sawmill is the purchase of sawlogs, which probably accounts for more than 60% of the total cost (Lindholm 2006). To be able to sell the sawn timber at a high price on the global market, the sawmill companies must ensure that the final customers receive a product of an appropriate quality. Wood drying is one of the essential steps in the sawmill process where the quality parameters are considerably affected.

In the drying process, the freshly sawn timber, which contains a lot of water, is dried to a moisture content (MC) suitable for the intended end-use of the wood product. The drying process is the most time- and energy-demanding process at a sawmill and it also has a great impact on parameters that affect the selling price of the sawn timber. Such parameters are the MC distribution within single pieces of wood and between pieces of a whole batch, the stress distribution, colour, checks and distortion of the sawn timber.

In the last decades, industrial drying has made great progress through the increased knowledge and awareness of both sawmill managers and kiln operators as to how to operate a kiln to achieve the best drying results. The research and development performed by sawmills, kiln manufacturers, universities and institutes has also played

[iv] m^3sk- cubic metre standing volume, i.e. the stem volume above the stump including bark.

a major role in that progress. As a result, the kiln design, process control, and drying schedules have been considerably improved. The drying temperatures for example are in general at least 20°C higher today than they were in the 1970´s, implying faster drying, a reduced risk of checking and, most of all, less risk of mould growth (Belin et al. 1984, Wamming et al. 2003). There has also been a trend towards designing kilns with a higher capacity in terms of supplied heat, ventilation, water spraying and larger air circulating fans. In addition to the ability to achieve faster drying, this has also created a margin so that the complete kiln capacity need not be used during the entire drying process (Wamming & Persson 2010).

In process control, adaptive control systems have been introduced as an alternative to the traditional drying schedule (Larsson & Morén 2003). In such systems, the actual development of the climate in the kiln is fed back to the control system which in turn "adapts" to the current state. The idea of oscillating the drying climate (Samuelsson & Söderström 1991, Anon. 2015b), mainly to save energy but also to increase the drying quality, has also been revived. Models for simulating the drying process have been developed and improved and these models have proven to be a valuable tool to predict the outcome of drying in a given climate (Hukka 1996, Salin 2001, 2002, 2010). To predict the outcome with high accuracy as well as to determine a suitable drying climate throughout the process, it is important to supply the drying model with adequate input. As the kilns at sawmills usually have slightly different designs, and since their technical status also differs, a system that feeds back the drying outcome to the kiln operator is also valuable.

The main question in the development of drying technology today is how the drying process can be further developed by the application of new technologies, improved measurement techniques and simulators. The work presented in this thesis is an attempt to contribute, at least in part, to the further development of the drying technology.

1.2 Aim

The aim of this work is to provide knowledge that can contribute to the further development of the industrial wood drying process. The focus was more specifically on the following areas:

- methods to determine the average green MC in sawn timber batches prior to the drying process,
- methods to improve the determination of the MC of individual pieces of sawn timber after drying, and
- methods to decrease the energy expenses in industrial wood drying.

1.3 Objectives

The specific tasks selected for the work described in this thesis were:

- To develop and evaluate a model to estimate the green MC of sapwood in logs at the log sorting station using a three dimensional scanner and a discrete X-ray. The hypothesis was that by assuming a fixed MC in the heartwood of the log and a certain relation between the basic densities of heartwood and sapwood, the MC of sapwood can be determined. The method could be used to identify logs where the sapwood has started to dry. Such information would make it possible to adapt the drying schedule.
- To generate functions for the basic density of the wood as a function of the log diameter at two sawmills in Sweden and to investigate the potential of a method of estimating the green MC of wooden packages by predicting the basic density for a certain log diameter and measuring the sawn timber dimension and mass (or green density). The idea is that, with more reliable data on green MC as input to a drying simulation, the drying time and final MC could be predicted with greater accuracy. This would make the logistics easier and the final drying result would rely less upon the experience of the kiln operator.

- To investigate whether it is possible to improve the accuracy in the determination of the MC of dried sawn timber by combining different measuring techniques, i.e. X-ray, microwave and visual grading.

- To investigate the possibility of increasing the fraction of a board surface on which reliable microwave measurements can be obtained by utilizing a compensation function developed through finite element simulations. The function compensates for interference patterns caused by the board edge and, ideally, each measured quantity would appear as if it were collected from a board with two infinite dimensions, i.e. width and length. The idea is that if the measurable board width could be increased, a larger number of reliable measurements could be obtained and the opportunity to detect MC gradients would increase.

- To investigate potential heat savings by introducing a new kiln layout consisting of a wall between the first and second zone in a two-zone progressive kiln.

- To determine the influence of the air circulating fan speed on the airflow distribution in a batch kiln. Because of the price difference between heat generated by electricity and heat generated by burning the residuals, decreasing the air circulating fan speed would decrease the sawmill's costs but, if this caused an uneven airflow distribution, it might result in an uneven drying result (which should be prevented).

1.4 Limitations

All the work was carried out with a focus on the Swedish sawmill industry, and only Scots pine (*Pinus sylvestris* L.) and Norway spruce (*Picea abies* (L.) Karst.) were considered. The results and approach can, however, probably be transferred to other species, if the relevant parameters of the specific species are utilized. The work also has an industrial focus, where consideration has been given only to methods which can be used at industrial production speeds in an industrial environment. The collaboration with industries in the research, as well as the limited budget for different projects also limited the chances of making a comprehensive study. As an example, the airflow distribution was measured only in one batch kiln with its specific design, so that it is not possible to draw general conclusions.

1.5 Outline

This work is a compilation thesis with six appended papers. In chapter 1, a brief introduction is given and the aim, objectives and limitations are stated. In the second chapter, the contents of the appended publications are placed in a wider context. Since each of the appended publications has its own introduction, materials and methods, results and discussion and conclusions, the reader is recommended to read these publications for more detailed information. Chapter three presents a discussion on a more general level. The main conclusions from the work are summarized in chapter four, and some suggestions for further work are presented in chapter five.

Of the appended publications, *Publications I & II* are related to the average green MC of wooden batches prior to the drying process, *Publications III & IV* describe how to improve the MC determination of individual pieces of sawn timber after drying, and *Publications V & VI* examine methods to decrease the energy expenses in industrial wood drying.

2 Industrial wood drying of Swedish softwoods

2.1 Overview of the sawmill process

Since there are almost as many different strategies for running a sawmill as there are sawmills, this section can only be a simplified and brief explanation of the sawmill process.

When the logs enter the sawmill, they are measured and sorted in the log sorting station, Fig. 1. Besides sorting with respect to species at sawmills utilizing more than one species, the sawmills commonly sort the timber into diameter classes and sometimes also according to length and quality. These classes are commonly denoted log-classes. To measure a log's outer shape, an optical (3D-) scanner is commonly used and some sawmills also use X-ray scanners as a complement to make it possible to sort the logs according to their inner properties.

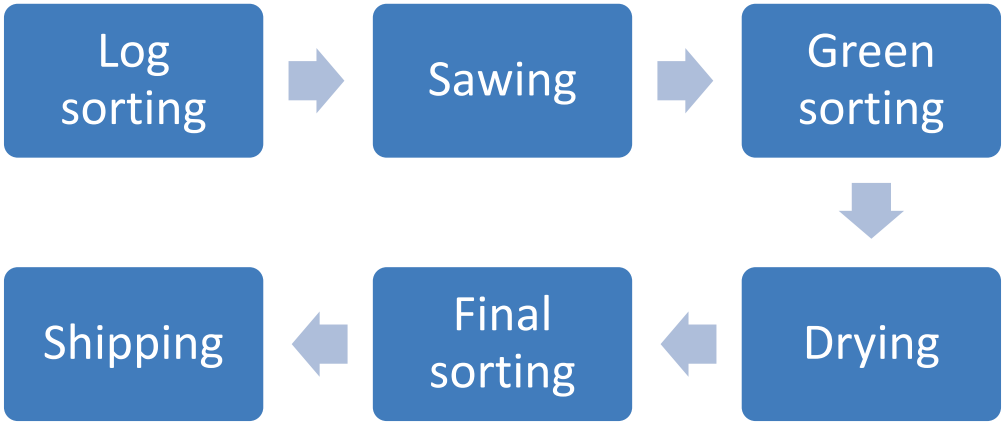

Fig. 1. Overview of the process stages in a typical Swedish sawmill.

In the sawing process, one log-class at a time is sawn into boards and the boards are then directly sorted according to cross-sectional dimensions. This stage is called "green sorting". Some sawmills also sort with respect to other parameters such as heartwood content and grain deviation. When a sufficient number of boards are sorted into a group, they are stacked to form a package for drying, stickers being put

between each layer of wood (Fig. 2) to allow air to flow through the package in the drying process.

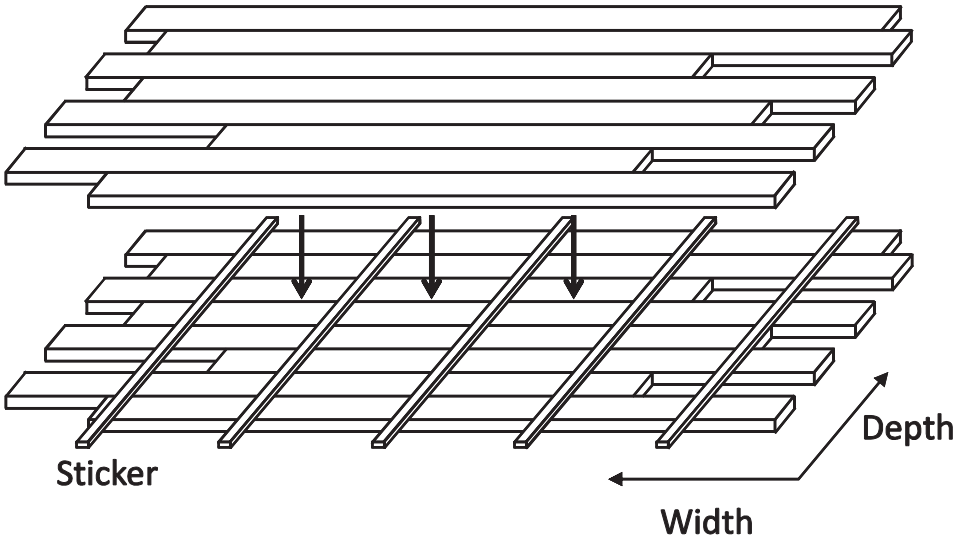

Fig. 2. Stacking of a wood package, layer by layer, prior to drying. The dimensions of a package are commonly denoted width, depth and height.

After drying, the stickers are removed from the packages and the sawn timber is transported through a final sorting station where visual quality or strength grading as well as length trimming takes place. In the final sorting, the boards are usually cross-fed at a production speed of the order of 200 pieces per minute. As the last step in the final sorting station, the sawn timber is collected into packages which are wrapped in plastic ready to be delivered to the customer.

2.2 Why drying wood?

The living tree contains a large amount of water which of course remains in the sawn timber when the log is sawn. To decrease the risk of biological decay, to improve the mechanical properties, to make the sawn timber dimensionally stable in its final use, and to decrease the density (and thereby simply prevent a lot of water from being transported back and forth), the sawn timber needs to be dried. Wood is also a hygroscopic material with an equilibrium MC (EMC) that depends on its surrounding climate (i.e. the weather conditions). The EMC is lower than the MC of a living tree (Tamminen 1962, 1964). Wood that is used in any application above ground, i.e. is not soaked in water, will therefore start to dry and sooner or later reach its EMC. The

question “why drying?” can therefore be reformulated as “why artificial drying?” Some of the reasons for artificial drying have been summarized by Esping (1992):

- In artificial drying, the kiln operator is in charge of the process.
- Artificial drying is faster than seasoning in the timber yard – i.e. the time from sawing to shipping can be weeks instead of months. This results in less restricted equity and a greater possibility of having a flexible and market-adapted production.
- Artificial drying works throughout the year – even when the outdoor climate is very humid or cold. This gives a more steady cash flow and reduces the need for sawmill storage area.
- Artificial drying considerably reduces the risk of mould growth.
- A low MC suitable for e.g. furniture production can only be reached through artificial drying.
- Artificial drying can reduce the number of checks and the distortion of the sawn timber.

2.3 Moisture in wood

The MC of a certain volume of wood is defined as the ratio of the mass of water in the wood to the mass of the dry wood:

$$u = \frac{m_{H_2O}}{m_{dry\ wood}} \tag{1}$$

where u is the MC and m is the mass. Water in the living tree or in freshly sawn (green) wood can be found either as free water in the lumen or as bound water within the cell walls. A common approach, explained through different binding energies for water in the lumen and in the cell wall, is that the lumen is emptied before the bound water in the cell wall begins to leave the wood. The MC at which there is no water in the lumen but the cell walls remain fully saturated is called the fibre saturation point (FSP), and is usually stated to be 27-30% MC at room temperature (Kollmann &

Cote 1968, Esping 1992, Dinwoodie 2000). A basic sketch of water in a softwood lumen is given in Fig. 3.

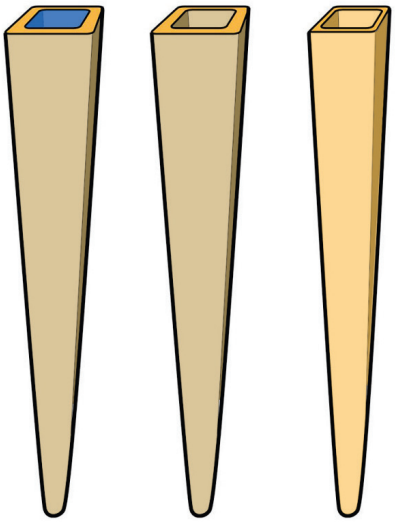

Fig. 3. Schematic picture of water in a wood cell. To the left, the cell wall is fully saturated and the lumen is also entirely filled with water. In the middle, the cell is at the fibre saturation point, i.e. no water in lumen but saturated cell walls. To the right, the MC is below the fibre saturation point, the cell walls contain less water and have started to shrink.

The actual growth of a living tree takes place in the cambium, which is located between the xylem and phloem in the outer part of the stem, Fig. 4.

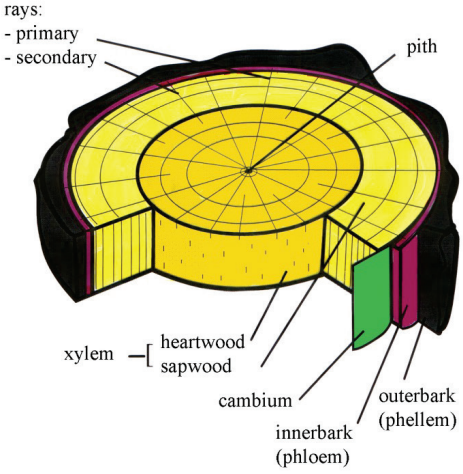

Fig. 4. A schematic representation of the wood macrostructure in the cross section of softwood.

The sapwood is the outer, newly generated part of the trunk that, in the living tree, contains some living cells, reserve material (e.g. starch) and the water-transporting cells. When a pine or a spruce tree grows older, there is no longer a need for the tree to use the entire stem for water and nutrient transportation from the ground, and heartwood begins to develop. Heartwood is the inner and central part of the trunk, and, in the living tree, it contains only dead and non-water-transporting cells, from which the reserve materials have been removed or converted into extractives. In the living tree, the MC is therefore much lower in the heartwood and it also shows less variation between different individuals than the sapwood (Tamminen 1962, 1964). This fact has been used for making a rough estimate of the basic density of the heartwood and the sapwood green MC, presented in *Publication I*.

Publication I

In the sawmill industry, the use of fixed drying schedules is very common. The result of this drying is normally satisfactory when the kiln operator is experienced and the sawn timber is normal with respect to green MC and basic density. However, when the properties of the sawn timber differ from the normal level, the choice of a suitable drying schedule to reach the target MC is often a problem. With better in-data of the properties of the sawn timber and utilizing drying simulators, it should however be possible to overcome this problem.

The objective of *Publication I* was to develop and evaluate a model to estimate the green MC of sapwood in logs at the log sorting station using a three dimensional scanner and a discrete X-ray. The work was done by utilizing data from the computed tomography (CT) scanned logs of the Swedish pine stem bank (Grundberg et al. 1995). The stem bank contains a total of 560 Scots pine sawlogs for which cross-sectional CT images are available every 10 mm within knot whorls and every 40 mm between knot whorls, giving a good knowledge of the green density of the logs. For each log, a reference value for the green sapwood density was calculated by taking the average over the sapwood in a knot-free cross-section taken approximately 400 mm from the log's butt-end. In the stem bank, CT images of disks cut from the butt-end of each log and conditioned to 9% MC are also available. In these images, the average sapwood density was calculated to determine a reference value for the dry sapwood density.

The CT data of the green logs were also used to simulate industrial X-ray and 3D log scanner data. By assuming a fixed MC in the heartwood and a certain relation

between the basic densities of the heartwood and sapwood, the sapwood MC could be predicted. The predicted sapwood MC from the industrial data was eventually compared to the reference values measured directly in the CT images. An example of a CT image of a green Scots pine log is shown in Fig. 5. The figure shows how easy it is to distinguish between the heartwood and the sapwood in a CT image, as the green sapwood contains considerably more water; the higher the density the brighter is the picture.

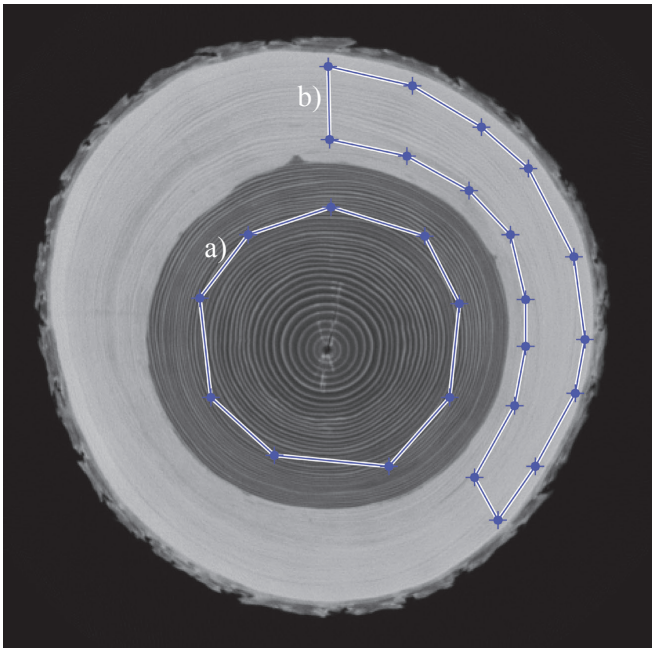

Fig. 5. Example of a computed tomography image of a cross-section of Scots pine. The blue-marked areas are used for measuring the density of a) heartwood, and b) sapwood.

Because none of the green logs in the stem bank exhibited any significant drying of the sapwood, the ability to identify such logs could not be investigated. However, the results were promising because it was possible to correctly sort 70% of the logs into either a high- or a low-MC group. Of course, there are sources of error in both the reference and predicted values. In the reference, the uncertainties are attributed to the actual MC of the conditioned disks, the volumetric swelling coefficient, the magnitude of the FSP and the difference in dry sapwood density between the butt-ends and at a distance 400 mm from the butt-end. To be able to compare the magnitudes of the errors in the reference and in the predicted values, the errors can be derived with aid of the final expressions for the MC. For the reference MC, this expression reads:

$$u_g = \frac{\rho_{g,g}(1+\alpha_{max})(1+u_9)}{\rho_{9,9}(1+\alpha_{max}\frac{u_9}{FSP})} - 1 \quad (2)$$

where u is the MC, the subscripts g and 9 refer to the green state and conditioned to 9% MC respectively, ρ is the density and the first subscript denotes the MC when the mass is measured and the second subscript denotes the MC when the volume is determined. α_{max} is the maximum volumetric swelling coefficient. With the assumption of independent variables, the propagation of errors was then estimated as:

$$\Delta u_g \approx \sqrt{\left(\frac{\partial u_g}{\partial u_9}\right)^2 (\Delta u_9)^2 + \left(\frac{\partial u_g}{\partial \alpha_{max}}\right)^2 (\Delta \alpha_{max})^2 + \left(\frac{\partial u_g}{\partial FSP}\right)^2 (\Delta FSP)^2} \quad (3)$$

This equation was evaluated with the measured mean densities and the values for α_{max} = 14.2% (Esping 1992) and FSP = 28% (Kollmann & Cote 1968). The uncertainty in u_9 was assumed to be 1% whereas the uncertainties in α_{max} and FSP were estimated to be 2% in both cases (Tamminen 1962). This resulted in a rough estimation of the propagated mean error, Δu_g, of 3% MC. The single largest error is however probably that associated with the difference in dry density between the butt-end and the wood at a distance of approximately 400 mm from the butt-end, where the green measurements were made. The magnitude of this error could not unfortunately be estimated due to a lack of data.

In the prediction, a small error is introduced when the industrial X-ray log scanner and 3D data from the stem bank are simulated. However, the largest error arises when an attempt is made to predict the dry sapwood density from the green heartwood density. Its magnitude can be estimated by considering the following expression for the sapwood MC:

$$u_{g\ Sapwood} = \frac{\rho_{g,g\ Sapwood} - \rho_{0,g\ Sapwood}}{\rho_{0,g\ Sapwood}} \quad (4)$$

where

$$\rho_{0,g\ Sapwood} = k\frac{\rho_{g,g\ Heartwood}}{1+u_{g\ Heartwood}} \quad (5)$$

where k is the ratio of the basic density of heartwood to that of sapwood. By deriving the corresponding propagation of error formula and examining the variation in the heartwood MC and in the ratio of the heartwood and sapwood basic densities from the data published by Tamminen 1962, the error in the prediction was found to be approximately 25% MC. In this estimation, the error introduced when simulating the industrial X-ray log scanner data and 3D data from the stem bank was neglected.

The derived error can be compared to the root mean square error of 21% MC from the experimental data. This is shown together with the relation between the sapwood MC achieved by the CT images and the simulated 3D X-ray in Fig. 6. The derived errors are excluded from the figure for two reasons: firstly, its magnitude is based on data achieved by other researchers, and secondly, including the errors in the figure would have made it very difficult to read.

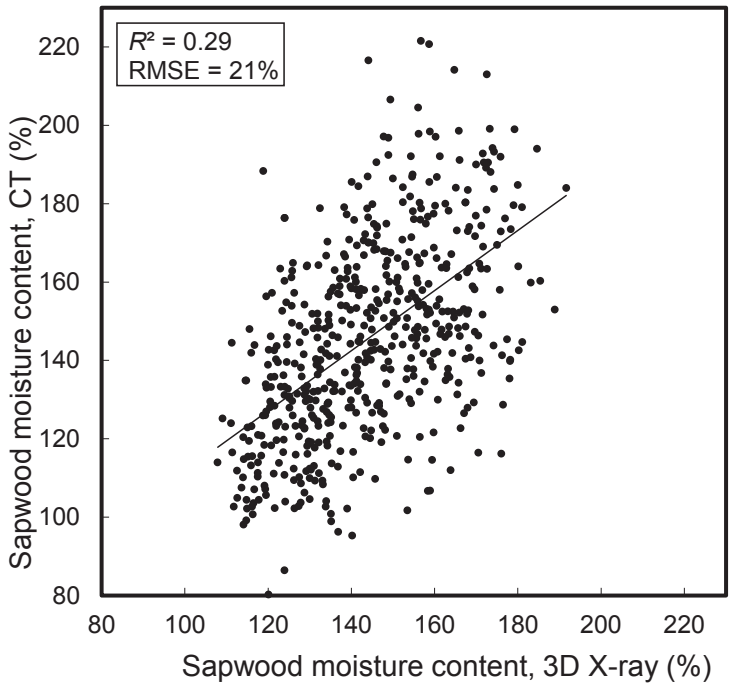

Fig. 6. Relation between the sapwood MC achieved by measuring in the computed tomography pictures and from simulated 3D X-ray data.

As seen in Fig. 6, the sapwood MC varies a lot between different individual logs and the error in the estimation is large. The method can however still be sufficiently

accurate to find the average MC of large batches and especially to detect batches of pre-dried wood originating from a given harvesting area.

To justify sorting into different MC groups in the log yard (prior to sawing), each group has to be sufficiently large. In practice it might therefore be equally valuable information if the average MC of a batch were determined just prior to drying instead of at the log sorting. This approach would also have the benefit of including changes in MC that occur in the log yard and the fact that the exact position of the sawing pattern in the log does not need to be determined by simulations (i.e. the fraction of heartwood/sapwood in the boards which considerably affects their average MC).

An approach where the average MC of a whole wood package was considered was therefore studied in *Publication II*.

Publication II

The basic problem addressed in *Publication II* is the same as that addressed in *Publication I*, with the same objective of being able to estimate the green MC of sawn timber.

The fundamental assumption adopted in *Publication II* was that the basic density of the centre-yield boards could be estimated as a function of the log diameter with sufficient accuracy to make it possible to determine the MC by an additional measurement of the total mass. In this study, specimens from both Scots pine and Norway spruce were studied. The Scots pine specimens were collected at a sawmill in Northern Sweden, while the Norway spruce specimens were collected both at the sawmill in Northern Sweden and at a sawmill in Central Sweden. In total, specimens were taken on 64 different occasions over a time span of two years. On each occasion, 30 oven-dry specimens consisting of clean wood (i.e. no knots or resin pockets) were taken from three different packages. From each package, 5 specimens were cut approximately 40 cm from the butt-end of boards and 5 specimens were cut approximately 40 cm from the top-end of boards. In addition, the dimensions of each oven-dry specimen were measured with a calliper in order to be able to calculate the basic density of the specimen. On each occasion, the diameter interval of the log-class from which the sawn timber originated was also recorded.

Since it was found in *Publication I* that separate models needed to be developed to determine the relation between sapwood and heartwood basic density for butt- and upper-logs, this was also investigated in *Publication II*. Here, an analysis of

covariance of the basic density of Scots pine specimens taken from the sawn timbers butt- and top-end was carried out. The null hypothesis was that the estimated relationship between basic density and log diameter was the same, with $\alpha = 0.05$ as rejection criterion. The analysis showed that the null hypothesis could be rejected, i.e. that there was a statistically significant difference in the relationship of the two positions.

Figs. 7 and 8 shows the distributions of the basic density versus log-class diameter for the Scots pine top- and butt-end specimens respectively.

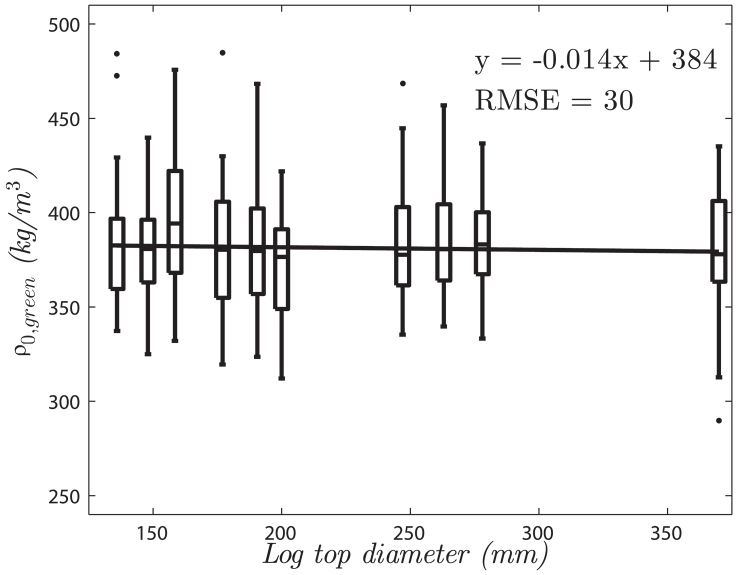

Fig. 7. Basic density of oven-dry specimens collected close to the top-end of the pine boards as a function of the logs' top diameter. Since the log-classes are sorted into diameter groups, it appears as if only certain diameters are present. In the figure, the median values are shown as lines in the boxes and the boxes extend from the 25th to the 75th percentiles. The lengths of the whiskers are maximum 1.5 times the interquartile length and observations outside this range are represented by dots. In the figure, the regression line that minimizes the squared errors of all the observations is shown together with its equation. The calculated root mean square error is also given in the figure.

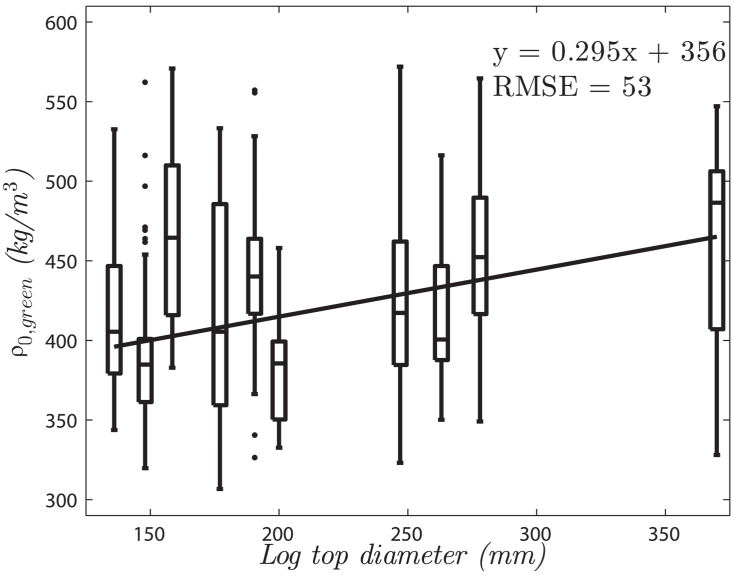

Fig. 8. Basic density of oven-dry specimens collected close to the butt-end of the pine boards as a function of the logs' top diameter. For further information, see the legend for Fig. 7.

The deviation between the fitted line and the mean values of the basic density of each log-class in Fig. 8 can be explained by the different proportions of butt-logs present in each log-class. Especially the second and sixth log-classes from the left probably contained few butt-logs, since the sawmill from which the specimens were collected tries to exclude butt-logs from those two log-classes. When specimens are collected at the top-ends of the boards, there is not the same need to differentiate between butt- and upper logs since the specimens are in any case taken at least 3 to 4 meters from the trees stump.

The magnitude of errors in the estimated MC, was achieved by maximum error estimation. The analysis starts with the expression of MC as a function of the measured total volume (V), the mass of the package, and the estimated average density:

$$\mathrm{u}(\mathrm{m},\rho,\mathrm{V}) = \frac{\mathrm{m}_u - \rho_{0,u}\mathrm{V}_u}{\rho_{0,u}\mathrm{V}_u} = \frac{\mathrm{m}_u}{\rho_{0,u}\mathrm{V}_u} - 1 \tag{6}$$

and differentiation of this equation gives:

$$\Delta u \approx \left(\frac{\partial u}{\partial m}\right)\Delta m + \left(\frac{\partial u}{\partial \rho}\right)\Delta \rho + \left(\frac{\partial u}{\partial V}\right)\Delta V = \frac{1}{\rho V}\Delta m - \frac{m}{\rho^2 V}\Delta \rho - \frac{m}{\rho V^2}\Delta V. \quad (7)$$

In these equations, the index is omitted to prevent the equations from becoming confusing. Since the mass, volume and basic density all are positive numbers, Equation (7) was then rewritten to give the maximum error estimator:

$$|\Delta u|_{max} \lesssim (u+1)\left(\frac{|\Delta m|_{max}}{m} + \frac{|\Delta \rho|_{max}}{\rho} + \frac{|\Delta V|_{max}}{V}\right) \quad (8)$$

which shows that the error in u is proportional to the relative errors in the measured/predicted mass, basic density and volume. In addition, the equation shows that the error can be separated into two components: One component that increases in proportion to the MC and a second component that is independent of the MC.

The magnitude of the error depends on how the quantities are measured, but to obtain an idea of the total maximum error, a maximum relative error of 1% in the measured mass was assumed. This is a reasonable assumption if the mass is measured with load cells. The accuracy of each cross sectional dimension was assumed to be within 0.2 mm and the accuracy of the length was assumed to be within 3 mm. The maximum relative error in the volume for a package with small dimensioned boards (i.e. 28x100 mm^2) with an average length of 4 m is then 1%. The magnitude of the relative error in the basic density was determined by calculating the pooled estimator of the variance of the basic density from all log-classes of top-end pine, butt-end pine and spruce at the given sawmill. Packages were then simulated by taking each board's basic density from a normal distribution with this variance. Each package consisted of only 100 different boards. The reason for this small number is that several boards are usually sawn from each log and the basic densities of boards originating from the same log are approximately the same. As an estimator of the maximum relative error in basic density, the maximum deviation between a single package and the total mean basic density was used. A total of 500 000 packages were simulated.

The square roots of the pooled estimators of the basic density variances were 30, 50, and 32 kg/m^3 for top-end pine, butt-end pine, and spruce respectively at the sawmill in Northern Sweden, and 37 kg/m^3 for spruce at the sawmill in Central Sweden. The corresponding maximum relative errors in basic density were 4, 6, 4 and 5%. The magnitude of the maximum relative error in basic density shows that it is not

necessary to invest in systems determining the mass and volume with extremely high accuracy.

If the green MC is approximately 70%, then the total maximum errors according to equation (8) become 11, 14, and 11% MC for respectively top-end pine, butt-end pine, and spruce at the sawmill in Northern Sweden, and 12% MC for spruce at the sawmill in Central Sweden. The corresponding maximum errors after drying to an average MC of 10% become 7, 9, 7 and 8% MC (n.b. these reported errors are in percentage points and not percentages of the mean MC).

To measure quantities such as basic density, dimension, positions, grades and so on, many different measuring devices are installed in a modern sawmill. Different devices have their pros and cons depending on the method which they use to determine a given quantity (Bucur 2003a, 2003b). One way to improve the precision of predicted values is to combine the measured quantities from several devices (Skog & Oja 2009). This is already implemented in many commercial measuring devices, but this approach could also combine measuring devices from different suppliers, provided that only individual data are collected and a new calibration is made for the combined data.

In *Publication III* the accuracy of MC measurements of dried boards was investigated by combining X-rays, microwaves and a visual grading.

Publication III

It is difficult to determine the MC of individual boards and many different measurement methods have been utilized (Vikberg 2010). If it were possible to determine the MC on individual pieces of sawn timber with high accuracy, the results could be utilized as valuable feedback to the drying process. For example, the MC distribution in the kiln could be used to indicate a possible reduction in the air circulating fan speed, and the MC distribution in individual pieces of sawn timber could be used to evaluate whether the conditioning phase at the end of the drying is sufficiently comprehensive.

The objective of *Publication III* was therefore to investigate whether it is possible to improve the accuracy in the MC determination of dried sawn timber by combining different measurement techniques, i.e. X-ray, microwave and visual grading.

The tested material consisted of 195 pieces of Scots pine. The pieces were divided into five different groups according to visual appearance. Typical characteristics of the five groups, denoted “Normal”, “Fine”, “Knot”, “Check” and “Defect”, are shown in Figs. 9-13 with three representative boards from each group. In the figures, only those parts of the boards from which data were collected (i.e., the centre 600 mm of the boards) are shown. Each of the five groups were conditioned to two different MC levels, and a calibration set was used containing a total of 45 boards with the same characteristics as the boards denoted “Normal”. The boards in the calibration set were conditioned to three different MC levels. To prevent any influence of the dimensions of the boards, all the pieces were planed to the same dimensions.

Fig. 9. Three characteristic boards from the group “Normal”.

Fig. 10. Three characteristic boards from the group “Fine”.

Fig. 11. Three characteristic boards from the group "Knot".

Fig. 12. Three characteristic boards from the group "Check". Because the checks are difficult to identify in the picture, they have been indicated with red lines.

Fig. 13. Three characteristic boards from the group "Defect". Notice the grain deviation over large areas.

The microwave measurements were performed with equipment manufactured by Satimo using a frequency of 9.375 GHz, see Fig. 14. It was found that the edges of the sawn timber affected the results considerably, and the boards were therefore stacked close to each other. The outermost boards were only placed there as dummies to decrease the edge effects, and they were not included in the subsequent analysis of the measurement data.

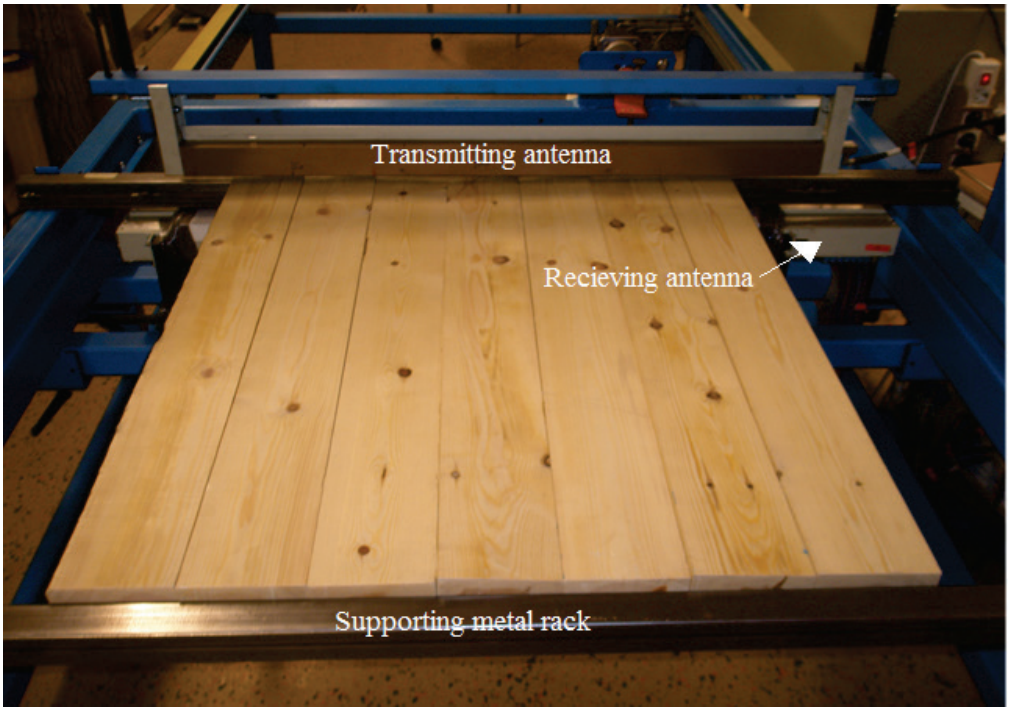

Fig. 14. Satimo microwave equipment. The transmitting and receiving antennae and one of the supporting metal racks are marked in the figure. The outermost boards were only used to decrease the problem of edge-effects as addressed in Publication IV.

The densities of the boards were assessed with a medical CT-scanner as described by Lindgren (1992). For the analysis, two different models were created, one utilizing only the microwave data and one utilizing both the microwave and the CT data. The results are summarized in Table 1 as the fraction of boards for which the difference between the assessed MC and the reference MC determined by the oven-dry method was less than 1% MC.

Table 1. Percentage of pieces for which the difference between the measured MC and the MC determined by the oven-dry method was less than 1 percentage point. In the header, the model in which only the microwave measurements were utilized is denoted mw, and the model utilizing both the microwave and CT measurements is denoted mw&CT. The superscript with a star refers to the same quantity but with the average group error subtracted from each single prediction, i.e. the best possible result with the actual calibration but with an optical device sorting it into the correct group.

Group	mw (%)	$mw\&CT$ (%)	mw^* (%)	$mw\&CT^*$ (%)
Normal	65	83	73	90
Fine	85	93	90	93
Knot	70	73	86	86
Check	78	78	78	83
Defect	63	68	66	74
All wood	72	79	78	85

It can be seen that the absolute deviation in MC was less than 1 percentage point for a larger proportion of boards when the average group error was subtracted from each estimated MC value (columns denoted by "*"). This indicates some discrepancy between the boards used in the calibration and the boards used in the prediction, and it shows the difficulty of achieving a good calibration. It can also be seen in the table that it is more difficult to predict the MC of boards with a large amount of visual inhomogeneities, i.e. the group “Defect”, than that of more uniform wood, i.e. the group “Fine”. This is an interesting result, since the low grade of the “Defect” group also implies a lower quality demand in terms of MC.

The problem in resolving data in the vicinity of the board edges was solved in this work by placing the boards tightly together and discarding the data from the outermost boards shown in Fig. 14. The problem of collecting reliable data in the vicinity of the board edges was addressed in *Publication IV*.

Publication IV

In a real application at a sawmill, the determination of the MC of the dried board should be performed in the final sorting where the boards are cross-fed piece by piece at a high production speed. To be able to make as many reliable measurements as possible when the board passes a sensor, it is very important to try to minimize the influence of the board edges. The influence of the board edges also makes it more difficult to detect differences in MC between the outer parts and the core of the boards, i.e. wet cores.

The objective of the work described in *Publication IV* was to investigate the possibility of increasing the fraction of a board surface from which reliable microwave measurements can be achieved, by utilizing a compensation function developed through finite element simulations.

An abrupt change in the physical properties of an object often leads to problems in obtaining reliable data in this region. The border between air and wood is such a problematic area, i.e. the region in the vicinity of a board edge. This problem arises for several non-invasive measurement techniques. The influence of the board edge on an electromagnetic field can be visualized by comparing Figs. 15 and 16. The exact distribution of the electromagnetic field depends on the shape of the wood as well as on its dielectric properties, which depend in turn on a number of factors (Torgovnikov 1993), such as the wood's MC, basic density, chemical content, grain direction and temperature. It also depends on the layout and frequency of the measurement device. Finally, the surroundings in which the measurement device is placed also affect the electromagnetic field. Figs. 15 and 16 should therefore only be considered as a basic illustration of a system such as the one investigated in *Publication IV*.

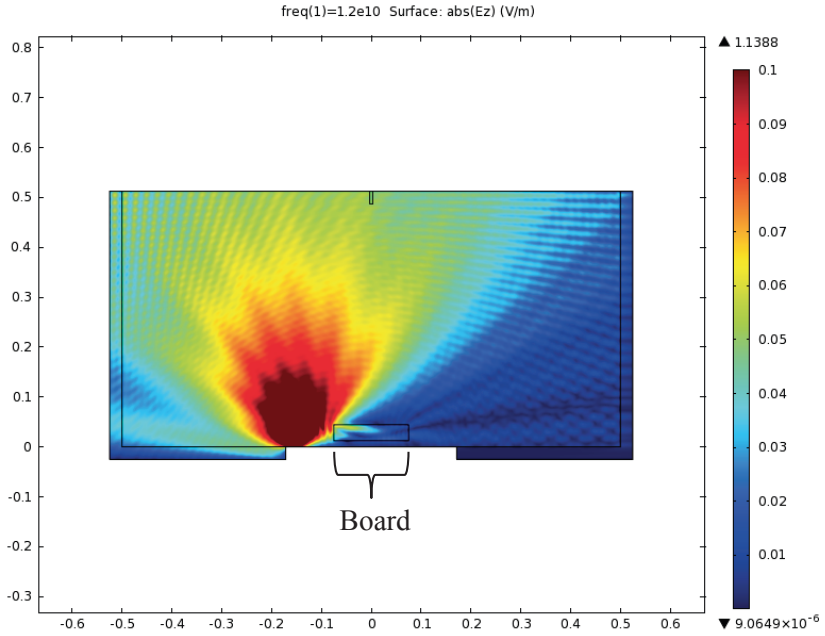

Fig. 15. Absolute magnitude of the electromagnetic field strength in the z-direction of a 12 GHz microwave system. The microwave transmitter is located at some distance outside the board (beneath the spot where the magnitude of the field is greatest) and it can be seen that the field is quite symmetric around the transmitter. The exact position of the board is marked in the figure.

Fig. 15 shows that the electromagnetic field is reasonably symmetric when the board is at some distance from the transmitting antenna. In Fig. 16, however, a couple of distinct fringes are visible when the transmitting antenna is located beneath the board but close to its edge.

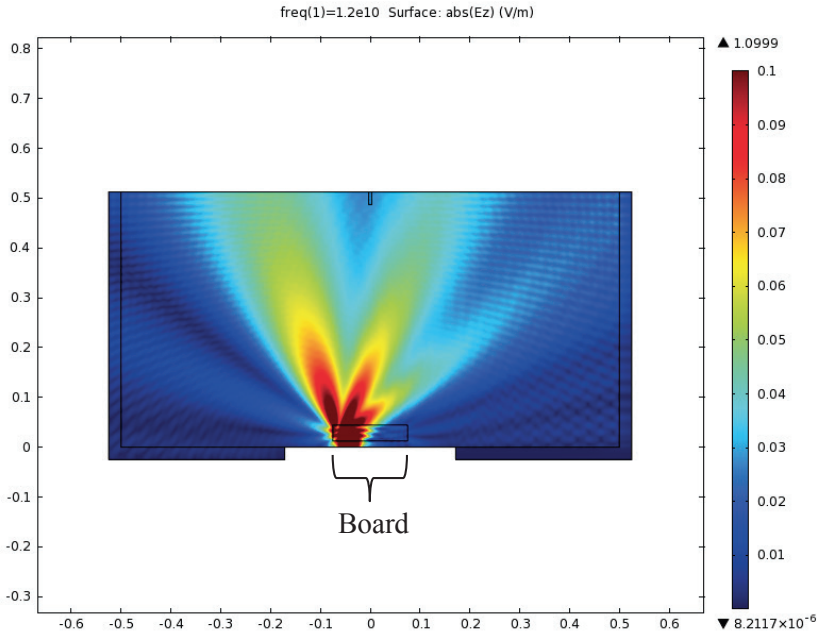

Fig. 16. Same as Fig. 15 but with the microwave transmitter located beneath the board but close to its edge. The position of the board is marked in the figure. Notice the distinct fringes in the transmitted field with a field strength greater than 0.05 (V/m).

Since the distribution of the fringes changes as the board moves over the transmitting antenna, the magnitude of the electromagnetic field at a receiving antenna located above the transmitting antenna was investigated as a function of the board position. The microwave system consisted of two horn antennae with a wooden sample placed in between. A schematic sketch of the whole microwave system is shown in Fig. 17.

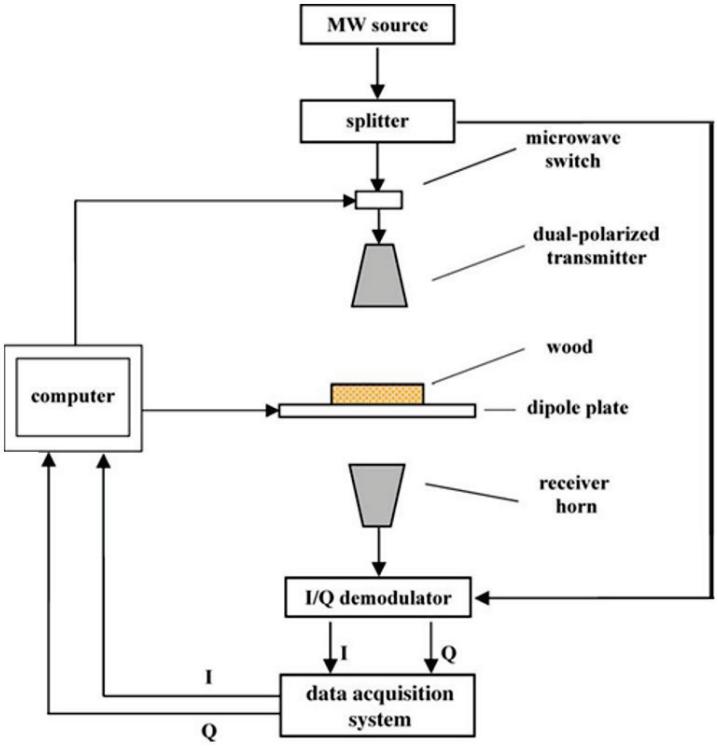

Fig. 17. Schematic diagram of the microwave system used for measuring the effects of collecting data close to a board edge.

To localize the point of measurement, the system uses a scattering dipole with two crossed directions, Fig. 18.

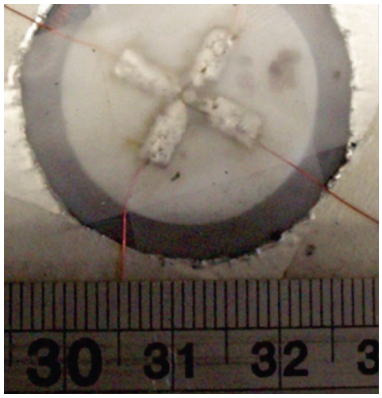

Fig. 18. Scattering dipole to localize the point of measurement.

Nine pieces of well-conditioned wood representing three different basic density classes with three different thicknesses in each class were used to check the edge effects. Each piece was measured in steps of 2 mm as it was moved over the sensor head. The simulations of the measurement system were performed in COMSOL 4.0a and the magnitudes of the attenuation and phase shift in the two principal directions of the wood, i.e. along- and cross-grain were compared to the measured magnitudes.

By comparing the simulated with the actual measured data, it was shown that it was possible to enlarge the measurable width of a board by compensating for the differences in the vicinity of the board edge, see Fig. 19. The result is only valid for the specific device investigated in this work where the measurable board width could be increased by approximately 30 mm. For small dimension boards, this increase in the measurable board width can be of great importance.

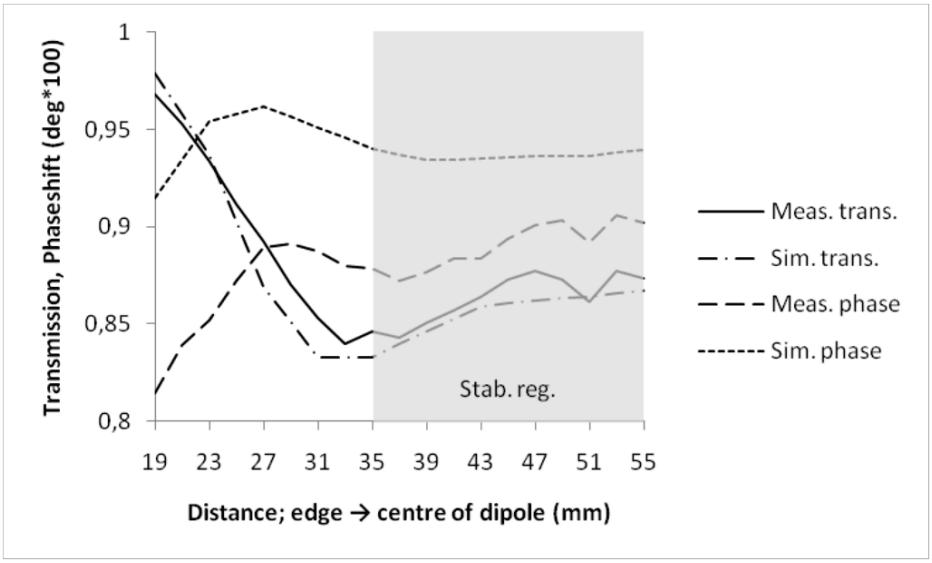

Fig. 19. Simulated and measured transmission and phase shift as a function of the distance between the board edge and the centre of the dipole. The figure shows the values achieved for one of the nine investigated boards.

In Fig. 19, it is interesting to notice the correlation between the simulated and measured transmission and phase shift.

2.4 Heat and vent kilns

There are many different types of kilns for wood drying (Campean 2010). In Sweden, however, almost all the softwood lumber produced is dried in heat and vent kilns (Staland et al. 2002). These kilns are commonly divided into two groups, batch kilns and progressive kilns. In a batch kiln, the whole kiln is loaded with wood before the drying starts and the drying proceeds until it is finished. After drying, the whole kiln is unloaded and made ready for the next batch. A sketch of a batch kiln is shown in Fig. 20.

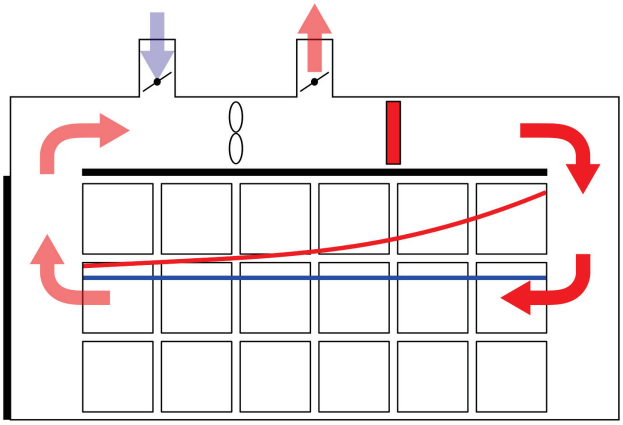

Fig. 20. Cross section of a batch kiln.

In a progressive kiln, drying is continuous, where a pile of green wood is loaded at the entry side of the kiln at the same time as a pile of dried wood is unloaded at the exit side of the kiln. Progressive kilns usually have one or two zones, although there are also kilns with more than two zones. The most extreme is the transverse continuous kiln which can be considered to have one zone for each stack of wood. Fig. 21 shows a two-zone progressive kiln with the airflow direction from the door-sides towards the centre of the kiln. This kiln layout is commonly denoted “Optimized Two-stage Continuous, OTC”-kiln.

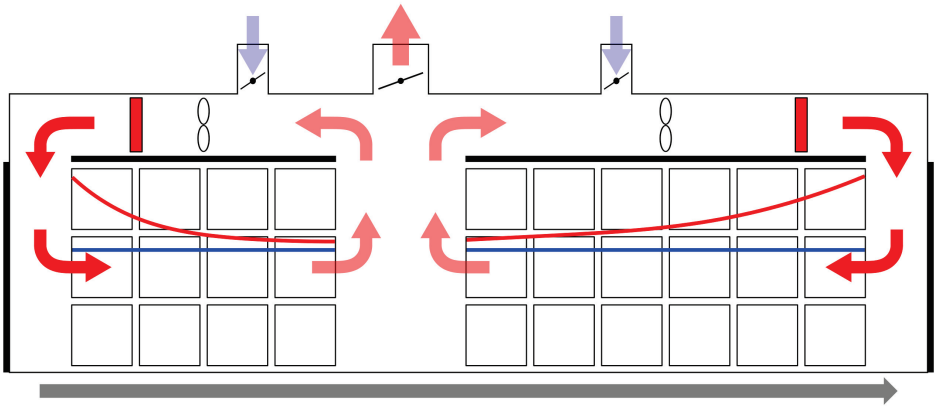

Fig. 21. Schematic sketch of a two zone progressive kiln with air entering at both the entry and exit sides of the kiln. This is called an Optimized Two-stage Continuous (OTC)-kiln. The red arrows show the direction of the air flow and the grey arrow at the bottom of the figure shows the wood feeding direction. A common ventilation outlet is located between the two zones and the ventilation inlets are located just before each air circulating fan. An air-to-air heat exchanger is usually installed on the ventilation, but this is not included in the figure.

A batch kiln with a sufficiently large capacity on the heating coils, air circulating fans and ventilation can handle a wide range of board dimensions, as well as initial and target MCs. The progressive kilns on the other hand are at their best if they are run with the same raw material to the same target MC all the time. The batch kilns are therefore better suited for products of small volumes. The continuous operation of the progressive kilns means, on the other hand, that they have the advantage of causing a more evenly distributed load on the boiler generating heat to the kiln, and a shorter payback-time on the installed heat recovery system. As the number of sawmills has decreased in Sweden while the average production of the remaining has increased in the last decades (Staland et al. 2002), a natural result has been that an increasing proportion of wood is being dried in progressive kilns.

Wood drying is the most energy-intensive process at a sawmill, where the main consumption is due to the large magnitude of the heat of evaporation, i.e. the amount of heat needed to evaporate water from the wood. To decrease the amount of energy needed to be added to the drying process, various heat recovery systems have been installed, and the concept of running kilns as clusters has been proposed (Esping 1982, Malmquist 1984, Elustondo & Oliveira 2006, Anderson & Westerlund 2014). In *Publication V* a new layout of a progressive kiln was suggested and its potential energy savings were investigated.

Publication V

The objective of *Publication V* was to investigate potential heat savings by introducing a new kiln layout consisting of a door between the first and second zones in a two-zone progressive kiln. The introduction of a door between the two zones makes it possible to run the two zones at very different temperature levels, which makes internal heat exchange through condensation of the moisture in the high temperature zone possible. A sketch of the suggested kiln layout is shown in Fig. 22. Since the intention is to dry the circulating air in the first zone through condensation, the ventilation is closed in this zone.

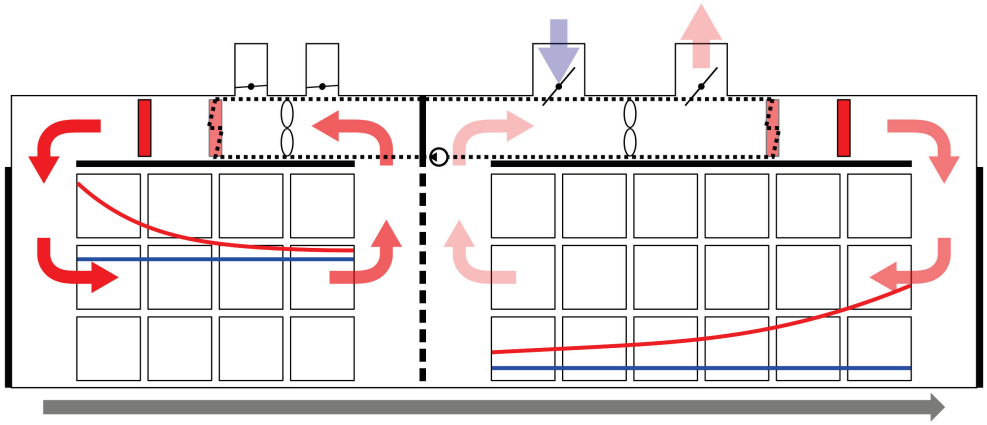

Fig. 22. Modified optimized two-stage continuous kiln, cf. Fig. 21. A heat exchanger is installed to allow heat to be transferred from the first to the second zone (piping is represented by dotted lines). A door (represented by a dashed line) is also introduced between the two zones. This means that the two zones to be run at considerably different temperature levels (indicated by the lines for temperature drop across the load in the two zones).

When dimensioning the kiln, it is important to consider the functionality of the kiln first and the potential heat recovery second. The dimensioning and drying results were simulated with aid of the commercial software Valusim, where the drying schedule for drying Norway spruce sideboards from an initial moisture content of 110% to a final moisture content of 17.4% was created according to the parameters reported in Table 2. The dimensions of the kiln were chosen so as to retain the possibility of running it without the door between the two zones. With the dimensioning of the kiln as stated and the temperature levels specified at values which ensure good drying quality, the exact magnitude of the recovered heat was determined.

Table 2. Ingoing parameters to the wood drying simulations. The reported "Air leakage" represents air passing the stack without actively participating in the drying.

Parameter	Zone 1	Zone 2
Dry bulb temperature of the air entering the wood stack (°C)	75	45
Wet bulb temperature of the air entering the wood stack (°C)	55	25
Circulating air ($kg_{dry\ air}/s$)	56	66
No. of trolley positions	3	12
Air leakage (% of $kg_{dry\ air}/s$)	25	25
Air speed in sticker space (m/s)	4.0	3.8
Sticker thickness (mm)	25	
Board thickness (nominal) (mm)	22	
Board average length (m)	4.5	
Package height (m)	1.5	
Package width (m)	6	
Package depth (m)	1.5	
No. of packages on each trolley	3	
Bolster thickness (mm)	90	
Species	Norway spruce	
Wood basic density (kg/m^3)	380	
Drying time (h)	36	
Initial moisture content (%)	110	

The resulting temperatures, moisture contents and heat demand of the drying simulation are summarized in Table 3.

Table 3. Results from the wood drying simulations. The reported temperatures are after mixing the air that passed through the packages with the air that passed the stacks without actively participating in the drying.

Parameter	Zone 1	Zone 2
Dry bulb temperature of the air after passing the wood stack [°C]	63	34
Wet bulb temperature of the air after passing the wood stack [°C]	55	25
Moisture content of the boards when exiting the zone [%]	65	17.4
Heat demand [MW]	1.5	See Fig. 23.

Although the heat demand of zone 1 was 1.5 MW, only 1.4 MW was available for zone 2. The difference is explained by the air bypassing the wood packages and not participating in the drying.

Ideally, it should be possible to recover the heat demand of the first zone, caused by the evaporation of water from the sawn timber to the air, in the condenser of the first zone. If this is not possible, some of the moist air must be vented out and this means that the energy efficiency of the kiln will drop. If, on the other hand, the heat demand in the second zone is greater than that available from the first zone, additional heat will need to be added to the second zone, which also means that the energy efficiency of the kiln will drop.

If there is no ventilation in zone 1 and/or no additional heat sink is available, the ideal case would be to design the kiln with a slightly higher heat demand in the second zone. This design would give a high energy efficiency as well as some safety margins to prevent the process from becoming unstable.

It should also be kept in mind that the air circulating fans add some heat in the second zone, and this needs to be taken into account. In practice, some additional heat is also transferred between the two zones and between the kiln and the surroundings when the loading/unloading takes place. The heat transfer due to air leakage when the doors are open was not taken into account in the drying model, but the heat transfer for heating of the wood was taken into account.

In Fig. 23 the heat demand of the second zone is shown as a function of the outdoor temperature for different outdoor relative humidities.

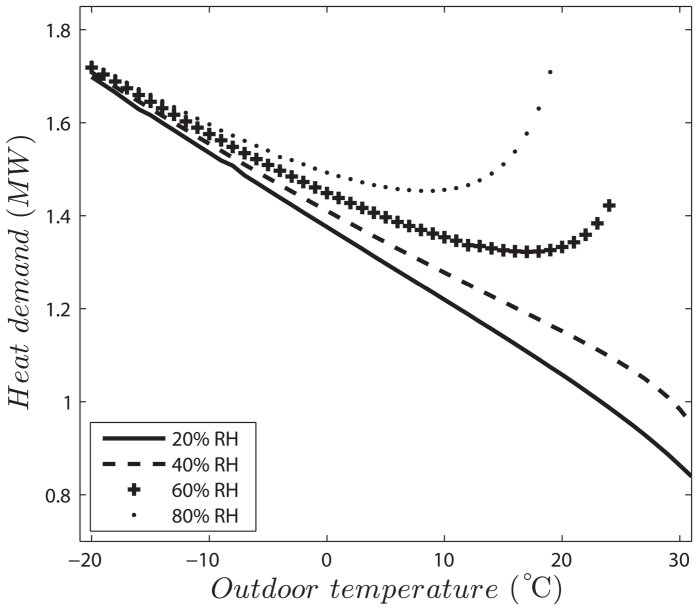

Fig. 23. Heat demand of the second zone as a function of the outdoor temperature and the relative humidity of the outdoor air.

It is interesting to notice here how the heat demand of the second zone depends on the outdoor climate. The shape of the curves can be understood by recalling the curvature of the saturation vapour density curve, i.e. at low temperatures, the air can contain very little water vapour and its relative humidity does not affect the heat demand to any great extent. At higher temperatures, the influence of the outdoor air relative humidity is greater; so that the lower the relative humidity of the outside air is, the lower is the heat demand of the second zone, since a smaller amount of air needs to be vented to maintain the desired climate in the kiln.

The low drying temperature of the second zone in comparison to that of a traditional kiln means however that the ventilation demand will always be relatively high, so that the ventilation demand is also a limiting factor affecting the kiln working range. The ventilation demand of the suggested kiln design with different external relative humidities is shown in Fig. 24.

In the same way, the total heat demand of the second zone becomes larger than in a traditional kiln when drying at a lower temperature. It therefore becomes virtually impossible to save as much as 50% of the heat used in a traditional kiln.

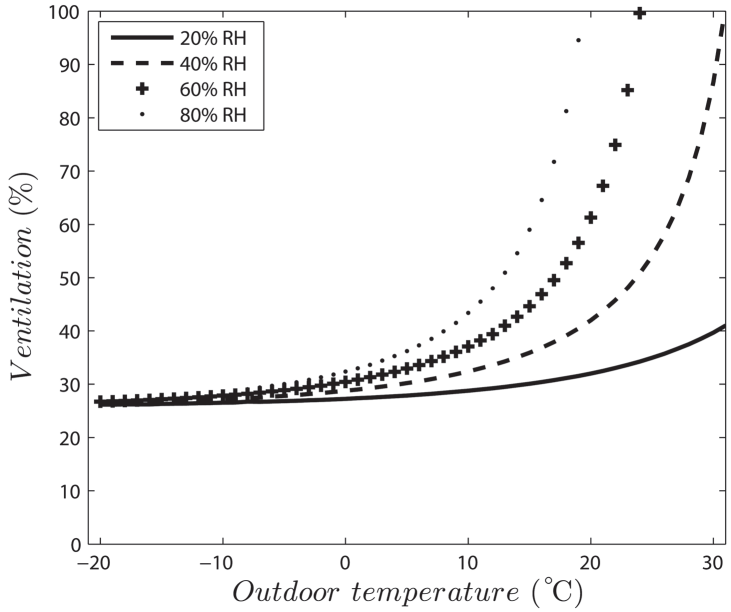

Fig. 24. Ventilation demand of the second zone as a function of outdoor temperature with different external atmospheric relative humidities.

Figs. 23 and 24 shows that the working range of the kiln is limited by both the heat demand and the ventilation demand of the second zone. The limitation due to too low a heat demand can be solved by installing ventilation in the first zone as well, but the limitation due to the need for large ventilation can only be solved by installing an additional condenser in the second zone or by increasing the drying temperature. Before any process parameters are changed, however, the drying quality and the capacity of the heat exchanger need to be taken into consideration.

At an outdoor climate of 0°C and 80% RH where the heat demand of the second zone is approximately equal to that which is available from the first zone, the total heat demand of the suggested system is roughly 1.6 MW. The heat demand for drying the same sawn timber in a conventional kiln was calculated by another simulation in the software Valusim, and the total heat demand in this simulation was roughly 2.2 MW. Of course, the temperature levels had to be adjusted in the two zones to achieve the

same drying rate since the air from the two zones is mixed in the intermediate zone. The total heat savings under ideal conditions was thus roughly 30%. The reason why the heat savings were not larger was the fact that the drying in the second zone is more energy efficient at higher temperatures (Salin 2001).

A more straightforward way to save money in the drying process is to reduce the speed of the air circulating fans. This can be done if frequency inverters are installed on the fan motors. In practice, this will not affect the total heat demand of the kiln, but since heat generated by burning residuals is usually much cheaper than heat generated by the air circulating fans, it leads to cost savings. Again, caution needs to be taken not to jeopardize the drying quality and, in practice, the fan speed can only be reduced in kilns which are over-dimensioned for a given load and drying conditions.

In wood drying, the circulating air has two purposes. First it acts as transport medium to transfer heat from the heating battery to the board surfaces where the water is evaporated, and secondly, it acts as transport medium for the moisture evaporated from the board surfaces to the ventilation. The airflow thus has a great impact on how the drying proceeds as the air flows through the wood stack (Ledig et al. 2007, Salin 2007).

Modern batch kilns are often dimensioned to be able to handle a flexible production, which means that they are dimensioned to dry thick centre boards as well as sideboards with a high initial MC. When thicker boards with a lower initial MC are dried and in the diffusion phase of drying, the fan speed can therefore be decreased, simply because the heat and mass transfer rate is lower. An uneven airflow distribution through the load can however result in an uneven MC distribution, and this should be avoided as far as possible. In *Publication VI* the question of whether the airflow distribution changes as a function of fan speed was therefore addressed.

Publication VI

Since it is normally more expensive to generate heat by electricity than by burning residuals, decreasing the air circulating fan speed would decrease the sawmill costs. An uneven airflow distribution might however result in an uneven drying result and the objective of this publication was therefore to study the influence of the air circulating fan speed on the airflow distribution in a batch kiln.

In this study, 20 hot-wire anemometers were distributed at different positions in an industrial batch kiln and the air velocity was measured for several different fan speeds with the aid of a data logger. The trial was performed twice with the anemometers in different positions, resulting in a large amount of data. The kiln contained 28 packages arranged in seven stacks with four packages in each stack. The size of each package was approximately 1.5x1.5x6 m^3 (height x depth x width denoted as in Fig. 2). Each package contained 21 layers of 50 mm thick sawn timber of Scots pine. The layers were separated by 21 mm thick stickers and the packages were separated by bolsters with cross-sectional dimensions of 95x95 mm^2. The data were collected at a frequency of 1 Hz and the air circulating fans were run at the same speed for several minutes so that each reported air velocity is the average of approximately 400 data points.

The large amount of data made it possible to analyse and interpret the data in a number of ways. The average air velocity of the gauges placed in the centre of a package is shown in Fig. 25 for a number of different fan speeds.

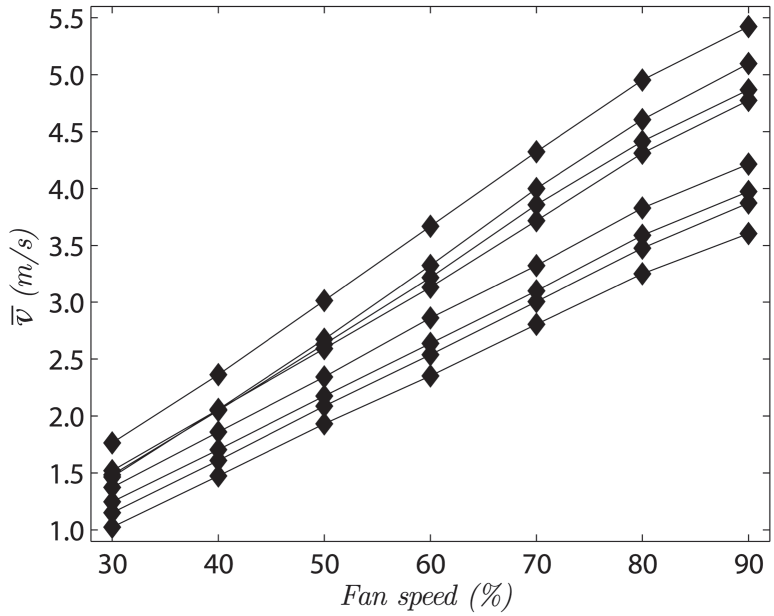

Fig. 25. Air velocity profile as function of fan speed. Each line represents the measured mean air velocity of a gauge placed in the centre of a wood package. The wood packages were placed in different positions in the kiln.

By comparing the range of air velocities for a given fan speed in Fig. 25, it can be seen that the air velocity is very different at different positions in the kiln. If, instead, the ratio of the air velocities at two different positions in the kiln is considered, it can be concluded that the airflow distribution does not change to any great extent when the fan speed is changed. This implies that, if the point with the lowest air velocity at a certain fan speed is located, this will probably be the critical point even at other fan speeds.

As it is time and labour demanding to perform industrial tests and since sawmills often have several kilns with slightly different designs, it is tempting to make all the simplifications and generalizations that are possible. One such simplification evaluated in this work was the first fan affinity law:

$$Q \propto N \tag{9}$$

where Q is the volumetric flow and N is the fan speed. With aid of this relationship, the mean air velocities of four gauges in stacks 2, 4 and 6 were estimated at air circulating fan speeds of 70%, 50% and 30%. In the estimation, the mean air velocity was assumed to be known from measurements with a fan speed of 90%. The results are summarized in Table 4.

Table 4. Measured mean air velocity of gauges placed in the middle of all the packages in stacks 2, 4 and 6 at four different speeds of the air circulating fan. The table also shows the mean air velocities at fan speeds of 30, 50 and 70 % estimated by the first fan affinity law when the air velocity at 90 % fan speed was assumed to be known. The bottom row shows the ratio of the estimated to the measured air velocity.

Measured and estimated mean air velocity (m/s)												
Fan speed	30%			50%			70%			90%		
# stack	2	4	6	2	4	6	2	4	6	2	4	6
$\bar{v}_{meas.}$	1.5	1.5	1.6	2.7	2.6	2.7	3.9	3.7	4.0	5.0	4.9	5.2
$\bar{v}_{est.}$	1.7	1.6	1.7	2.8	2.7	2.9	3.9	3.8	4.0	-	-	-
$\bar{v}_{est.}/\bar{v}_{meas.}$	1.1	1.1	1.1	1.0	1.1	1.1	1.0	1.0	1.0	-	-	-

As seen on the last row in Table 4, the ratio of the air velocity estimated by the first fan affinity law to the mean air velocity measured with the hot-wire anemometer was close to 1.

3 Discussion

One of the research questions can be stated at a more comprehensive level than in the aim and objective as: Can an increased knowledge of the average green MC of a batch prior to drying actually be utilized to improve the drying process and its final result? To answer this question, a long-term evaluation needs to be performed rather than a mere claim that it is possible to determine the MC with a certain accuracy. It should also be questioned whether this is the only way this goal could be reached or if there are other, more efficient ways, such as improved adaptive control.

To achieve as much impact as possible from the work presented in this thesis, as well as in other similar theses, industrial implementation is important. Unfortunately, a lot of research is carried out without any close collaboration with industrial partners such as equipment suppliers or sawmills, and this reduces the chance of fast implementation. As an example, none of the work presented in this thesis regarding the determination of MC in individual boards after drying was been performed in collaboration with any supplier of measurement devices. If the implementation of the ideas could lead to an increase in the accuracy of determination of the board MC, it would help the sawmills to be able to ensure the quality of their products. A lot of knowledge of wood drying could also be gained by relating the MC data to a certain kiln and position within the kiln. The feedback could for example be used to determine a suitable maximum reduction in the air circulating fan speed for each kiln and board dimension by considering the average MC of the batch as well as the MC of boards in different positions in the kiln. The data could also be used to tune the drying simulators currently implemented in the control systems of the kilns.

Another subject that deserves extra consideration is how stringent data in wood research should be analysed when the aim is to reach industrial implementation. Strictly speaking, the elimination of outliers in the data should be done with caution unless obvious mistakes have been made during the data collection. From a practical point of view, however, it might be better to have accurate models only for the majority of the boards since the individual boards with abnormal behaviour will probably end up in the chipper anyway. One method that could be utilized in this context is the determination of the Cook´s distance. This was investigated when the basic density was showed as function of the top diameter of the logs *(Publication II)*, but it was found to have very little effect on that particular data set and it was excluded from the final analysis. In order to keep the cost at a reasonable level in

terms of labour and materials, it is also important to have an extensive plan when making industrial trials in wood research. With the large variation in properties between as well as within single trees, it is important to collect samples that are indeed representative of the true population. To be able to make a correct analysis, it can also be valuable to determine additional parameters such as the sample origin in terms of distance from the stump and distance from the pith.

To determine the properties of wood, several measurement techniques, devices and assumptions are often utilized, and it is always important to determine their contribution to the total error. This can be used as an indicator of how much it is worth to invest in increasing the accuracy of a certain parameter. One such example was found in *Publication II* where the variance of the sawn timbers basic density was much larger than the typical error in determining the mass or volume. The purpose of determining wood properties should also be considered when deciding the accuracy required in such a determination. In both *Publications I & II*, the accuracy of the MC determination was found to be low but it might still provide valuable information to the kiln operator, since large volumes are handled every day and the long-term trends of a certain product might be as interesting as the exact MC of a single package.

It is often difficult and time-consuming to calibrate a measurement device, especially if wood is utilized to perform the calibration, due to the large variation in parameters between individual boards. This was discovered in the work reported in *Publications III & IV*. As many devices depend on the dielectric properties of the wood, it would save substantial time, effort and money in the long run to perform an extensive investigation of these basic properties of wood. The result could be used to investigate the maximum theoretical accuracy of any new measurement device as well as to develop a calibration dummy with well-defined dielectric properties. This dummy, preferable made of some non-hygroscopic material, could later be used for a fast and reliable calibration of the devices.

Finally, in the pursuit to reduce the cost of drying sawn timber, it is important to keep in mind that poor drying quality can become very costly. When any major change is made in the drying process, its effects on the drying quality should therefore be thoroughly investigated.

4 Conclusions

MC measurements as input to the drying process

The estimate of the green MC of sapwood in logs could be used to correctly sort 70% of the logs into a low- or a high-MC group *(Publication I)*. The uncertainty of single estimates was however large, indicated by a computed root mean square error of 21% MC. The method can still be sufficiently accurate for finding the average MC of large batches and especially for detecting batches of pre-dried wood originating from a given harvesting area.

It was found that there was a statistically significant difference in the relation between the basic density and the logs' top diameter for specimens collected close to the butt- and top-end of Scots pine *(Publication II)*. The derived maximum error in estimating the MC of a single package was also large, with errors of up to 14% MC at an average MC of 70%. Out of the contributing factors to the total error (which were the relative error in mass, volume and basic density), the large variation in basic density contributed most. It was therefore concluded that there is no reason to invest in systems to determine the mass and volume with very high accuracy. Due to the large magnitude of the maximum error estimator, the MC determination of single packages should be interpreted with care.

MC measurements as feedback to the process

The overall accuracy in predicting MC of dried boards is increased by combining microwave, X-rays and visual grading data in a single model *(Publication III)*.

Simulation of a measurement system *(Publication IV)* was shown to be a valuable tool to understand and predict a system's behaviour. By introducing a correlation function determined from simulations of the measurement system, the measurable board width could be increased, which makes it possible to achieve a larger number of reliable measurements as well as increasing the chance of detecting MC gradients, i.e. wet cores.

Internal Heat exchange during drying

By introducing a new kiln layout, a potential energy saving of approximately 30% was achieved *(Publication V)*. The direct interaction between the first and second zones as well as the influence of the outdoor climate makes the design less flexible for handling a divergent production. The increased complexity in running the drying process with the suggested kiln design also means that a full implementation in the kiln control system is required to utilize its full potential.

Airflow distribution during drying

The air distribution did not change greatly when the fan speed was altered in the investigated kiln *(Publication VI)*. It was therefore concluded that once the spot where the air velocity is lowest at a given fan speed is found, then this spot is where caution needs to be taken when reducing the fan speed. When applying the fan affinity law to estimate the air velocity at a reduced fan speed, the deviation from the measured air velocity was within 10%.

5 Future work

Measurement devices for estimating the MC prior to drying, as described in two of the appended publications, are already present in some sawmills. The next step will be to utilize the data from these devices in a long-term test to see how much the drying process gains by having this information. The collection of data prior to such an analysis would be simplified by first introducing traceable data throughout the process. This is partly installed in some sawmills but still not present over the whole production chain. By making it possible to collect traceable data from different measurement devices in a sawmill over a long period of time, it would also become possible to fully investigate the potential in combining quantities measured by different devices. The sawmills would also benefit if a calibration dummy for calibrating MC measurement devices were developed.

Although the suggested kiln design seems promising in terms of potential heat savings, a more thorough investigation is recommended prior to its construction. It is especially important to verify that the capacity of the heat recovery system becomes sufficient large. Furthermore, the kiln's flexibility in terms of different board dimensions and wood properties as well as other drying climates must also be considered.

It would also be interesting to investigate the airflow distribution in a progressive kiln, since larger blow-depths are usually used in comparison to the investigated batch kiln and no reversal of the fan's rotational direction takes place. In general, most of the research that has been done in the last decades focuses on batch kilns whereas progressive kilns are becoming more and more common. A good idea would therefore be to devote more research to the progressive drying processes.

6 References

Anon. (2015a) Virkesutnyttjande 2011 (in Swedish). In: Swedish Wood, http://www.svenskttra.se/om_tra_1/tra-som-material/fran-timmer-till-planka. Accessed 06/25 2015.

Anon. (2015b) Cleantech Timber drying. In: Alent Drying AB, http://www.alentdrying.se/TeknikE.html. Accessed 06/30 2015

Anderson, J-O. & Westerlund, L. (2014) Improved energy efficiency in sawmill drying system. Applied Energy 113:891-901.

Belin, L., Bergström, H., Dahlgren, L., Esping, B., Esping, E., Johansson, B., Lundström, H., Wallentén, B., Wimander, K., Åström, B. & Östberg, H. (1984) Trämögel, Handledning inom skogs- och träindustri (in Swedish). Sågverksindustrins kommitté för arbetsmiljöfrågor, Klippan.

Bucur, V. (2003a) Techniques for high resolution imaging of wood structure: a review. Measurement Science and Technology 14:91-98.

Bucur, V. (2003b) Nondestructive characterization and imaging of wood. Springer-Verlag, Berlin Heidelberg.

Campean, M. (2010) Timber drying methods–passing through history into the future. Proceedings of the 11th International IUFRO Wood Drying Conference, Skellefteå, Sweden, January 18-22, pp.3-16.

Dinwoodie, J. M. (2000) Timber, its nature and behaviour. E & FN Spon, London.

Elustondo, D. & Oliveira, L. (2006) Opportunities to reduce energy consumption in softwood lumber drying. Drying Technology 24:653-662.

Esping, B. (1992) Trätorkning. 1a, Grunder i torkning (in Swedish). Trätek, Stockholm.

Esping, B. (1982) Energy Savings in Timber Drying. Wood Technology Report no. 12.

Grundberg, S., Grönlund, A. & Grönlund, U. (1995) The Swedish Stem Bank. Luleå University of Technology, Report no. 1995:31.

Hukka, A. (1996) A simulation program for optimisation of medium temperature drying on an industrial scale. Proceedings of the 5th International IUFRO Wood Drying Conference, Quebec City, Canada, August 13-17, pp.41-48.

Kollmann, F. F. P. & Cote Jr, W. A. (1968) Principles of wood science and technology. Solid Wood. Springer-Verlag, Berlin.

Larsson, R. & Morén, T. (2003) Implementation of Adaptive Control Systems in Industrial Dry Kiln. Proceedings of the 8th International IUFRO Wood Drying Conference, Brasov, Romania, August 24-29, pp. 397-400.

Ledig, S. F., Paarhuis, B. & Riepen, M. (2007) Airflow within kilns. In: Perré, P. (ed) Fundamenteals of Wood Drying. COST, pp. 291-332.

Lindgren, O. (1992) Medical CT-scanners for non-destructive wood density and moisture content measurements. Doctoral thesis, Luleå University of Technology.

Lindholm, G. (2006) Sågverksbranschens kostnads- och intäktsstruktur, - undersökning, analys och trender inom svensk sågverksnäring (in Swedish). Master Thesis, Swedish University of Agricultural Sciences.

Lundberg, C. (2013) The Swedish Forest Industries, Fact and Figures 2013. Swedish Forest Industries Federation, Stockholm.

Malmquist, L. (1984) Compound-torkning av virke. En analys av torkningsskador (in Swedish). Träteknikrapport no. 62.

Meixner, J. (1972) The behavior of electromagnetic fields at edges. Antennas and Propagation, IEEE Transactions on 20:442-446.

Nilsson, P., Cory, N. & Wulff, S. (2014) Forest statistics 2014. Swedish University of Agricultural Science, Umeå.

Salin, J-G. (2001) Determination of the most economical drying schedule and air velocity in softwood drying. 3rd COST E15 Workshop, Helsinki, Finland, June 11-13, pp. 1-10.

Salin, J-G. (2002) Simulation models as an industrial tool for optimizing the drying of timber. 4th COST E15 Workshop, Santiago de Compostela, Spain, May 30–31, pp. 1-8.

Salin, J-G. (2007) External heat and mass transfer. In: Perré, P. (ed) Fundamentals of Wood Drying. COST, pp. 175-201.

Salin, J-G. (2010) Problems and solutions in wood drying modelling: history and future. Wood Material Science and Engineering 5:123-134.

Samuelsson, A. & Söderström, O. (1991) Zolon-metoden, en jämförelse med konventionell varmluftstorkning i kammartork (in Swedish). Träteknikcentrum, Report no. P 9105040.

Skog, J. & Oja, J. (2009) Heartwood diameter measurements in Pinus sylvestris sawlogs combining X-ray and three-dimensional scanning. Scandinavian Journal of Forest Research 24:182-188.

Staland, J., Navrén, M. & Nylinder, M. (2002) Såg 2000: Resultat från sågverksinventeringen 2000 (in Swedish). Swedish University of Agricultural Sciences, Report no. 3.

Tamminen, Z. (1962) Fuktighet, volymvikt mm hos ved och bark, I Tall (in Swedish). Royal College of Forestry, Report no. 41.

Tamminen, Z. (1964) Fuktighet, volymvikt mm hos ved och bark, II Gran (in Swedish). Royal College of Forestry. Report no. 47.

Torgovnikov, G. I. (1993) Dielectric properties of wood and wood-based materials. Springer-Verlag, Berlin.

Vikberg, T. (2010) Fuktkvotsmätare för träindustrin, en kartläggning av metoder för mätning av fuktkvoter i intervallet 7-18 fuktkvotsprocent (in Swedish). Technical report, Luleå University of Technology.

Wamming, T., Fjellström, P-A. & Imbaud, O. (2003) Industriell utveckling av torkning vid 90°C, 90T. -Ett alternativ till HT (in Swedish). Trätek, Report no. P 0303013.

Wamming, T. & Persson, F. (2010) Rekommendationer för reducerad fläkthastighet vid virkestorkning (in Swedish). TräCentrum Norr.

Publication I

Wood Material Science and Engineering, 2010; 5: 91–96

Taylor & Francis
Taylor & Francis Group

ORIGINAL ARTICLE

Sapwood moisture-content measurements in *Pinus sylvestris* sawlogs combining X-ray and three-dimensional scanning

JOHAN SKOG[1,2], TOMMY VIKBERG[1,3] & JOHAN OJA[1,2]

[1]*SP Technical Research Institute of Sweden, Wood Technology, Skeria 2, SE-931 77 Skellefteå, Sweden,* [2]*Division of Wood Science and Technology, and* [3]*Division of Wood Physics, Luleå University of Technology, Skeria 3, SE-931 87 Skellefteå, Sweden*

Abstract
Because today's sawmill processes are not fully adapted to the variability of the raw material, it is crucial to sort sawlogs according to material properties in order to process the wood efficiently and to obtain high-quality end-products. One material property that could be used for sorting is the moisture content (MC) of the sapwood, an important parameter for both the processing and the end-products. Most sawmills use three-dimensional (3D) scanners to sort logs and some have also invested in X-ray scanners. Previous studies have shown that, by combining raw data from 3D and X-ray log scanners, green sapwood density and dry heartwood density in Scots pine sawlogs can be estimated. In this study, the method was used to estimate sapwood MC in green logs. It was found that the MC estimate could be used to separate the logs into groups with high and low MC, correctly classifying all logs with MC below 100% as low MC logs. Out of all logs, 70% were correctly classified. The MC estimate could also be compared to the dry density-dependent maximum MC and used to identify logs that have actually started to dry.

Keywords: *3D scanning, green density, log sorting, MC, Scots pine, X-ray scanning.*

Introduction

Wood is a biological material with great variations in material properties between individual logs and within the same log. The wood industry of today deals with large volumes in an almost automatic process, which is not fully adapted to the variability of the raw material. Thus, the sawn wood also shows a great variability in material properties, and a large share of the production carries combinations of dimension and grade that do not meet customer requirements (Grönlund, 1992). To reduce the production of off-grade products, the sawlogs may be sorted according to specific material properties or predicted grade of the sawn goods before sawing. This enables the sawmill to saw each log into dimensions where the grade of the log is best utilized, thus improving the value of the sawn wood.

Sorting of logs or sawn goods according to certain material properties also helps the sawmill to adjust the process so that the wood can be processed efficiently and the highest possible quality of the end-products can be obtained. Heartwood content, wood density and sapwood moisture content (MC) are examples of properties important to the drying process. Boards with similar density and moisture-content distribution show similar behaviour during drying, and by sorting the boards according to these parameters before drying, well-adapted drying schedules can be constructed with respect to time, energy consumption and quality of the final products. If the initial MC in the batch is known, over-drying can be reduced when using fixed schedules, and the finishing time can be predicted more accurately when using adaptive schedules (Larsson & Morén, 2003).

In the green sorting, heartwood content can be measured using, for example, laser systems (Oja *et al.*, 2006), and wood density and average MC can be measured using microwave scanning (Johansson *et al.*, 2003). Using these techniques, it is possible to sort the sawn goods with respect to drying

Correspondence: J. Skog, SP Technical Research Institute of Sweden, Wood Technology, Skeria 2, SE-931 77 Skellefteå, Sweden. E-mail: johan.skog@sp.se

(Received 25 November 2009; accepted 8 April 2010)

ISSN 1748-0272 print/ISSN 1748-0280 online
DOI: 10.1080/17480272.2010.484868

properties. By this approach, however, the volumes sorted into each class is not known in advance, and consequently the production cannot be planned to achieve optimum filling in the kilns. To avoid this problem, it would be desirable to perform sorting based on drying properties earlier in the process at the log-sorting station.

In the log sorting, inner properties of logs such as heartwood content (Skatter, 1998; Oja *et al.*, 2001) and density (Oja *et al.*, 2001) can be measured using an X-ray log scanner. Most sawmills installing an X-ray log scanner already have an optical three-dimensional (3D) scanner present, and it has been shown that the combination of both scanners can be used to sort logs with improved precision (Skog & Oja, 2009). The combined 3D X-ray method has been used to measure heartwood diameter (Skog & Oja, 2009), green sapwood density and dry heartwood density in Scots pine sawlogs (Skog & Oja, 2010). However, so far no method for measuring MC in the log sorting has been presented. The hypothesis of this study is that it should be possible to use dry heartwood density to estimate the dry sapwood density, and that the dry and green sapwood densities can be combined to obtain the sapwood MC in the log. Sorting the logs based on this information would result in batches with more homogeneous material properties, which would be helpful when optimizing the processing of the logs.

The aim of this study was to develop a sapwood MC calculation model and to evaluate the feasibility of this method for the sorting of sawlogs.

Materials and methods

Calculation of reference values

The development of MC calculation algorithms requires a set of sawlogs with well-defined green and dry densities. In this study, the computed tomographic (CT) scanned logs of the Swedish pine stem bank (Grundberg *et al.*, 1995) were used. The stem bank contains a total of 560 Scots pine sawlogs (165 butt logs and 395 upper logs), for which cross-sectional CT images are available every 10 mm within knot whorls and every 40 mm between whorls, giving a good knowledge of the green density in the logs. For each log, a reference value for the green sapwood density, $\rho_{u,u}$, was calculated by taking the average over the sapwood of a knot-free cross-section approximately 400 mm from the log end.

In the stem bank, CT images of discs cut from the butt end of every log and conditioned to 9% MC are also available. In these pictures, the average sapwood density at 9%, $\rho_{9,9}$, was calculated and used to find a reference value for the dry sapwood density, $\rho_{0,0}$. This value was calculated using the relation between the density, $\rho_{u,u}$, at MC u and the dry density, $\rho_{0,0}$:

$$\rho_{u,u} = \frac{m_u}{V_u} = \frac{(1+u)\cdot m_0}{(1+\alpha_u)\cdot V_0} = \frac{(1+u)}{(1+\alpha_u)}\rho_{0,0} \quad (1)$$

where m_u is the mass, V_u is the volume, and α_u is the volumetric swelling coefficient at MC u. The swelling coefficient was calculated using:

$$\alpha_u = \alpha_{\max}\cdot u/u_{\mathrm{FSP}} \text{ for } u < u_{\mathrm{FSP}} \quad (2a)$$

$$\alpha_u = \alpha_{\max} \text{ for } u \geq u_{\mathrm{FSP}} \quad (2b)$$

where $\alpha_{\max}$ and u_{FSP} are the swelling coefficient and the MC at the fibre saturation point, respectively. The average values for Scots pine were used, $\alpha_{\max} = 14.2\%$ (Esping, 1992) and $u_{\mathrm{FSP}} = 28\%$ (Kollman & Côté, 1968).

By inserting the reference values of the green sapwood density and the dry sapwood density in eq. (1) and using the swelling from eq. (2b), the reference value for the green sapwood MC u was found:

$$u = (1+\alpha_{\max})\cdot\rho_{u,u}/\rho_{0,0} - 1 \quad (3)$$

Prediction of sapwood moisture content using the 3D X-ray method

Industrial 3D and X-ray data for the logs were simulated from the CT images (Skog & Oja, 2010). The simulated data files were then combined using the 3D X-ray technique, and the average green sapwood density of each log was calculated as described by Skog and Oja (2010).

The dry heartwood density 400 mm from the butt end of each log was also calculated from the combined data (Skog & Oja, 2010), and two linear models predicting the dry sapwood density from the dry heartwood density were developed, one model for butt logs and one model for upper logs.

Finally, a prediction of the green sapwood MC was calculated by inserting the average green sapwood density and the predicted dry sapwood density obtained using the 3D X-ray method into eq. (3).

Evaluation of results

A linear correlation between the predicted and the reference sapwood MCs was developed and predictability (R^2) and root mean square error (RMSE) were calculated. A threshold value at 145% predicted MC was used to separate the logs into two groups with lower and higher MC, respectively. Calculated MCs were also compared to the theoretical maximum MC for saturated wood (Esping, 1992):

$$u_{\max} = \frac{1560\text{kgm}^{-3} - \rho_{0,u}}{1.56 \cdot \rho_{0,u}} \quad (4)$$

where $\rho_{0,u}$ is the dry mass divided by the green volume. Using eqs (1) and (2b), $\rho_{0,u}$ was expressed in terms of the dry density, $\rho_{0,0}$:

$$\rho_{0,u} = \rho_{0,0}/(1 + \alpha_{\max}) \quad (5)$$

valid for MCs above the FSP. The average value of the swelling coefficient at fibre saturation was used, $\alpha_{\max} = 14.2\%$.

Results

For all 560 logs, the green density of the sapwood was predicted with a precision of $R^2 = 0.65$ and RMSE $= 25$ kg m^{-3} (Figure 1). The dry density of the sapwood was predicted with a precision of $R^2 = 0.47$ and RMSE $= 43$ kg m^{-3} for 553 (98.8%) of the logs (Figure 2). The seven logs that failed prediction were all large butt logs. When combining the predicted green and dry sapwood densities, the sapwood MC could be calculated with a precision of $R^2 = 0.29$ and RMSE $= 21\%$ (Figure 3).

The result when using the predicted MC to separate the logs into two groups is shown in Figure 4. The separation between the two groups is not very clear, but all logs with MC below 100% were correctly classified as dry logs. Out of all logs, 70% were correctly classified.

If the MC is plotted against the dry density (Figure 5), it can be seen that most of the observed variation in MC is caused by the varying dry density of the logs. The MC follows a curve of the same shape as the theoretical maximum value (eq. 4), as shown by the solid line in Figure 5.

By comparing the calculated MC to the theoretical maximum, it should be possible to identify logs that have low MC due to drying of the sapwood. Figure 6 shows the ratio between calculated MC and maximum MC. The reference ratio measured in the

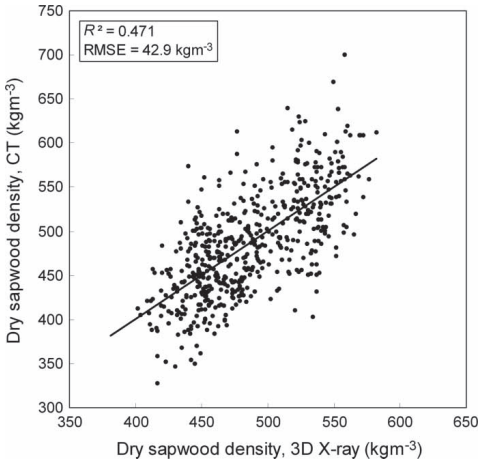

Figure 2. Sapwood dry density in 553 Scots pine sawlogs: measurements in computed tomographic (CT) images versus predictions from simulated X-ray and three-dimensional (3D) log scanner data.

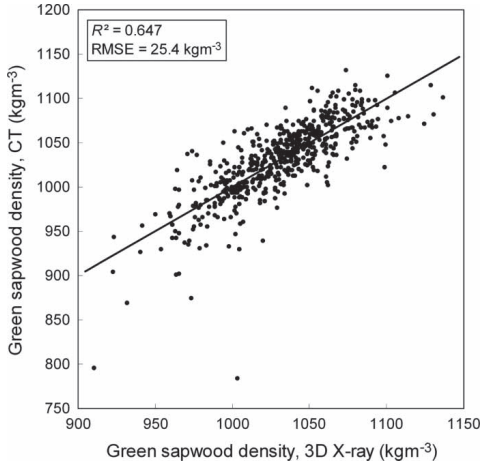

Figure 1. Sapwood green density in 560 Scots pine sawlogs: measurements in computed tomographic (CT) images versus predictions from simulated X-ray and three-dimensional (3D) log scanner data.

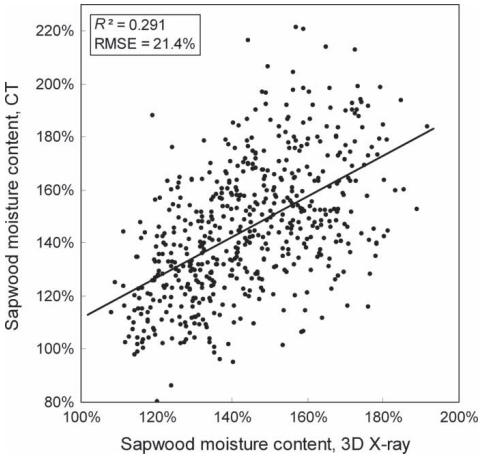

Figure 3. Sapwood moisture content in 553 Scots pine sawlogs: measurements in computed tomographic (CT) images versus predictions from simulated X-ray and three-dimensional (3D) log scanner data.

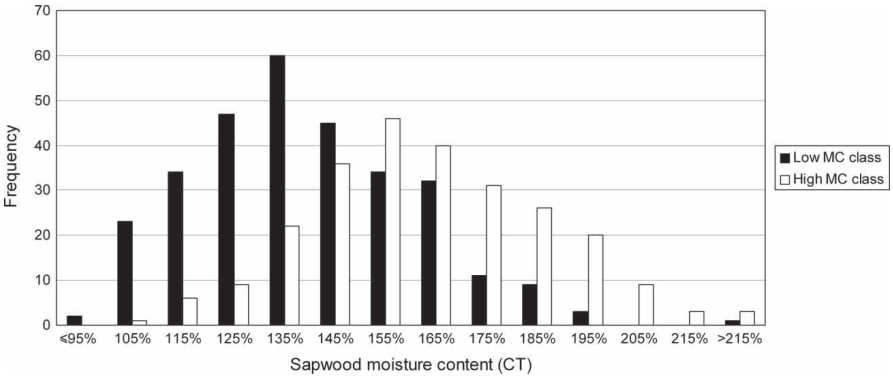

Figure 4. Observed sapwood moisture content (MC) (value from computed tomographic images) for 553 Scots pine sawlogs, separated into two classes depending on the sapwood MC predicted from simulated X-ray and three-dimensional log scanner data.

CT images could be predicted with a precision of $R^2 = 0.39$ and RMSE = 0.036.

Discussion

For Swedish sawmills, measurement of the sapwood MC would be most useful during periods when the logs may have been stored for extended periods in the forest, e.g. in spring. When the frost goes out of the ground, the roads become very soft and logs may have to be stored *in situ* for several weeks after felling until transport to the sawmills is possible. Because the logs start to dry immediately after felling, sapwood MC may vary significantly between individual logs upon arrival at the sawmill gates, depending on storage time and conditions. This predrying of the logs affects the drying properties of the sawn goods, and many Swedish sawmills need to alter their drying schedules during springtime to avoid problems with cracks and large standard deviations in the final MC. When performing this adjustment of the drying schedules, it would be of great advantage if the raw material could be sorted into batches according to the amount of predrying.

The method developed in this study offers a way of estimating the sapwood MC in sawlogs as they arrive at the log-sorting station. The RMSE of the sapwood MC estimate in the logs, 21.4% (Figure 3), is

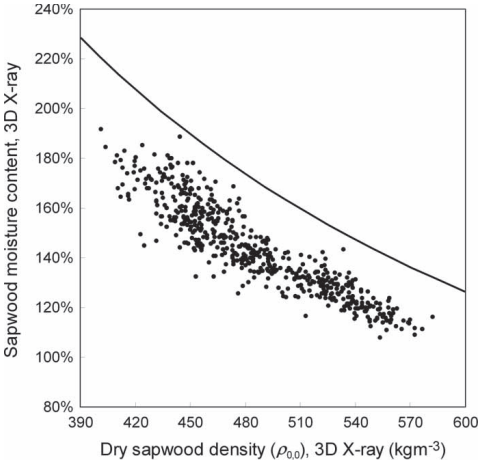

Figure 5. Predicted moisture content as a function of estimated dry density in the sapwood of 553 Scots pine sawlogs. The solid line represents the theoretical maximum moisture content of saturated wood.

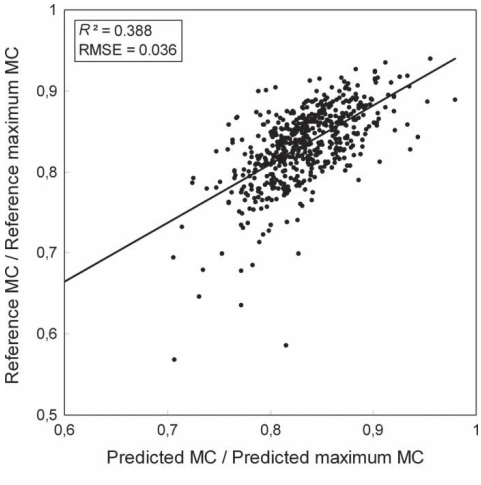

Figure 6. Sapwood moisture content (MC) relative to the theoretical maximum MC of saturated wood: measurements in CT images versus predictions from simulated X-ray and three-dimensional log scanner data for 553 Scots pine sawlogs.

significantly larger than the RMSE obtained when using the alternative method, measurement of the MC in green boards using a microwave scanner (15.9%) (Johansson *et al.*, 2003). However, sorting of logs rather than boards is desirable because it facilitates planning of the production towards batches of optimum size for the kilns. In addition, for sawmills that decide not to sort the logs according to MC, a continuous measurement of the sapwood MC in the arriving logs would be of value, as it provides an important indication about when it is time to start adjusting the drying schedules.

In most of the logs, the predicted and reference values of the green sapwood density follow a linear correlation (Figure 1). For two of the logs, however, the green sapwood density in the reference cross-section is much lower than the predicted log average. This is probably caused by a local drying of the log around the reference cross-section. These two logs are also seen as outliers in Figure 6, with reference values below 0.6.

When predicting the dry sapwood density (Figure 2), seven (1.2%) of the logs failed prediction. These were all large butt logs, which was expected, because for very large diameters, the X-ray signal becomes too weak to be detected. In this study, the dry sapwood density was predicted from the dry heartwood density using linear correlation. Because this relation varies between butt logs and upper logs, two separate correlations were used. For the reference data used in this study, the predictability between dry heartwood and dry sapwood densities was found to be $R^2 = 0.57$. The dry heartwood density, in turn, can be predicted with $R^2 = 0.83$ using the 3D X-ray technique (Skog & Oja, 2010). This means that most of the observed uncertainty in predicting the dry sapwood density ($R^2 = 0.47$) is due to the poor predictability between the dry heartwood and the dry sapwood densities.

When combining the predicted green and dry sapwood densities to find the sapwood MC, the predictability of the reference values was found to be quite low ($R^2 = 0.29$, RMSE = 21%) (Figure 3). Here, it should be noted that the reference values themselves contain some uncertainty. This is primarily because the reference MC was calculated by comparison of the dry density at the butt end and the green density 400 mm from the butt end. Dry CT images were only available at the butt end, but owing to local drying at the log ends, the green density reference could not be taken at the same position. Instead, a position 400 mm from the butt end was chosen for the green CT images to avoid the log end drying, but still to be as close to the end as possible. By choosing this position, the impact of local dry-density variations was minimized. However, especially for butt logs, there may still be a considerable dry density variation over the distance of 400 mm, causing some uncertainty in the reference values used.

The predicted MC was calculated by comparison of a dry sapwood density prediction evaluated 400 mm from the butt end of the log and the average green sapwood density of the whole log. The average sapwood density of the log was used because it was found to be the best available estimate of the green sapwood density 400 mm from the log end. This means that the prediction model tries to predict the average MC in the region around 400 mm from the log end, whereas the reference value is a mixture of two local values taken 400 mm apart. Thus, local variations at the log ends in both dry density and MC contribute to the uncertainty in the prediction of the sapwood MC presented in Figure 3.

Because the correlation between predictions and CT reference values is rather low, the method needs to be verified experimentally. If the green and dry reference densities were calculated for the same piece of wood, the MC references would be more precise, and so the actual amount of uncertainty in the predictions could be determined. Furthermore, testing the method on industrially scanned logs would show that the method is also applicable under industrial conditions.

Because the logs used in this study were all scanned directly after felling, the logs had not dried out, and most logs had an MC around the threshold value of 145% that was used for separation of the logs into groups in Figure 4. Thus, the separation between the two groups was not very clear. Figure 5 shows that most of the observed variation in MC was caused by varying dry density of the wood and not by drying of the logs. This means that sorting of the logs by MC, as illustrated in Figure 4, is not a good way to find logs that have low MC due to drying of the sapwood. Instead, the calculated MC could be compared to the theoretical maximum given by eq. (4), as shown in Figure 6. Comparing calculated and maximum MCs could prove to be a very useful way of identifying logs that have been stored for a long time before arrival at the sawmill. A proper evaluation of this method would require testing on a more diverse population of logs, containing both logs with full sapwood MC and logs with reduced sapwood MC.

In conclusion, by combining 3D and X-ray scanning in the log-sorting station, it is possible to measure the green sapwood density and to estimate the dry sapwood density and, accordingly, the MC in Scots pine sawlogs. Because the correlation with CT reference values is quite low and the reference itself contains some uncertainty, experimental verification of the simulation results is needed.

The MC estimate could be used to separate the logs into two groups with high and low MC, correctly identifying all logs with low MC as dry logs. Out of all logs, 70% were correctly classified.

The estimate can also be compared to the dry density-dependent maximum MC and used to identify logs that have actually started to dry. However, this approach needs to be evaluated for a population of dry logs, because most logs in this study were of full MC.

Acknowledgements

This work was financially supported by TräCentrum Norr, a research programme jointly funded by industrial stakeholders, the European Union (ERDF) and the county administrative boards of Norrbotten and Västerbotten.

References

Esping, B. (1992). *Trätorkning 1a—Grunder i torkning* [Wood drying 1a—Wood drying basics]. Stockholm: Trätek. (In Swedish.)

Grönlund, A. (1992). *Sågverksteknik del II* [Sawmill technology part II]. Markaryd: Sveriges Skogsindustriförbund. (In Swedish.)

Grundberg, S., Grönlund, A. & Grönlund, U. (1995). *The Swedish Stem Bank* (Res. Rep. TULEA 1995:31). Skellefteå: Luleå University of Technology.

Johansson, J., Hagman, O. & Fjellner, B.-A. (2003). Predicting moisture content and density distribution of Scots pine by microwave scanning of sawn timber. *Journal of Wood Science*, *49*, 312–316.

Kollmann, F. F. P. & Côté, W. A. (1968). *Principles of wood science and technology.* Berlin: Springer.

Larsson, R. & Morén, T. (2003). Implementation of adaptive control system in industrial dry kilns. In: *Proceedings of the 8th International IUFRO Wood Drying Conference*, Brasov, Romania, August 24–29, 2003 (pp. 397–400).

Oja, J., Grundberg, S. & Grönlund, A. (2001). Predicting the stiffness of sawn products by X-ray scanning of Norway spruce saw logs. *Scandinavian Journal of Forest Research*, *16*, 88–91.

Oja, J. Grundberg, S. Berg, P. & Fjellström, P. A. (2006). *Equipment for measuring fibre angle and heartwood content in sawn wood during transverse feed in the green sorting* (SP Rep. 2006:16). SP Technical Research Institute of Sweden. (In Swedish with English summary.)

Skatter, S. (1998). Determination of cross-sectional shape of softwood logs from three X-ray projections using an elliptical model. *Holz als Roh- und Werkstoff*, *56*, 179–186.

Skog, J. & Oja, J. (2009). Heartwood diameter measurements in *Pinus sylvestris* sawlogs combining X-ray and three-dimensional scanning. *Scandinavian Journal of Forest Research*, *24*, 182–188.

Skog, J. & Oja, J. (2010). Density measurements in *Pinus sylvestris* sawlogs combining X-ray and three-dimensional scanning. *Scandinavian Journal of Forest Research*, accepted for publication.

Publication II

Basic density determination for Swedish softwoods and its influence on average moisture content of wood packages estimated by measuring their mass*

TOMMY VIKBERG [1,2] & DIEGO ELUSTONDO [1]

[1] Luleå University of Technology, Forskargatan 1, SE-931 87 Skellefteå, Sweden, phone:+46 920 49 10 00, tommy.vikberg@ltu.se, [2] SP Technical Research Institute of Sweden, SP Wood Technology, Laboratorgränd 2, SE-931 77 Skellefteå, Sweden, phone: +46 105 16 50 00, tommy.vikberg@sp.se.

*Reformatted version of paper available at: http://dx.doi.org/10.1080/17480272.2015.1090481

Abstract

In this work, a setup with a device measuring the mass of wood packages is examined as an aid to estimate the average moisture content of wood packages. As the basic density needs to be presumed in the setup, an estimator of the basic density as function of log diameter is determined for Norway spruce (*Picea abies (L.) Karst*) and Scots pine (*Pinus sylvestris*). In total 1920 specimens were collected at two different sawmills and analysed for this purpose. Specimens collected at the butt-end of pine had the greatest variation in basic density and it is recommended that they should be omitted when sawmills create their own functions for basic density estimation. Furthermore, the variation in basic density was shown to have the greatest impact on the estimated moisture content. A maximum error estimator of the moisture content became 14 % at a moisture content of 70 % and 9 % at a moisture content of 10 %. It was therefore concluded that the described method should not be used to estimate the moisture content of packages after drying but can serve as a valuable indicator of average green moisture content of a drying batch.

Keywords: Wood drying, Sawmill, Scots pine, Norway spruce, Load cells.

Introduction

In the Nordic Countries, the two species of the greatest commercial interest are Scots pine (*Pinus sylvestris*) and Norway spruce (*Picea abies (L.) Karst*). When they grow mature, heartwood is formed in the centre of the trunk which does not actively take part in the water transport in the stem (Taylor et al. 2002). The heartwood therefore dries out and the moisture content (MC) of heartwood in a green tree is in the range of 30 to 50% whereas the MC in the sapwood is in the range of 100 to 200% for pine and spruce species (Tamminen 1962, 1964).

Since wood is a hygroscopic material, the MC of the sawn timber will be in equilibrium with its surrounding in the final use. For timber that shall be used in a dry indoor climate this implies around 8% MC and for timber used in constructions around 18% MC (Skaar 1988). It is also well known that wood shrinks when it dries to MC below the fibre saturation point and that the shrinkage is anisotropic. The result of further processing such as planning and gluing is also correlated to the MC of the timber. Consequently, the MC level of the sawn timber is one of the parameters that sawmills want to ensure their customers.

Today, all sawmills of reasonable size dry their timber in air circulating kilns (Staland et al. 2002). If it was possible to provide the kiln with the same raw material and keep the drying process exactly at a predefined schedule the outcome would always be the same. This is, however not the case, caused both by variations in the ingoing wood parameters as well as process disturbances. The single largest factor affecting the average MC of the sawn timber is the heartwood-sapwood ratio due to their different green MCs. It is also well known that the drying rate of sapwood is much higher than of heartwood and in a drying process they will eventually reach the same MC. Salin (2002a) shows that this occurs at roughly 12% MC for Scots pine with average basic density of 430 kg/m^3 and a standard deviation in basic density of 30 kg/m^3. Knowing the exact MC distribution of a drying batch or the average MC with high accuracy is therefore not important for the kiln operator. In the late spring and early summer, bad carrying capacity of many forest roads together with a dry outdoor climate can however result in a major pre-drying of the sapwood in whole drying batches.

Persson and Andersson (2014) measured average MC of freshly sawn timber batches of the same product ranging between 64% and 82% with the lowest values during the summer. They also showed by simulations that the corresponding difference in drying time to reach a final MC of 18% would be approximately 11 hours. Due to the relatively low drying rate in the diffusive regime, a few hours more or less in drying time will not affect the average final MC to a great extent. Drying to a lower MC than the target, nevertheless always represents a waste of energy and drying capacity and increase the distortion of the wood. In later production steps, when sawn timber from different drying batches are mixed, the total MC variation will also increase even if the single drying batches have only slightly different average MCs. As sawmills usually have a large number of drying kilns, even small improvements in each drying process also sum up to a major improvement in terms of drying capacity.

The extensive pre-drying of the sapwood that sometimes occurs causes problems for the kiln operators to hit the designated final MC. To stop the kiln and make an extra check with a resistive meter to determine if the target MC is reached is a possible solution but demands extra labor hours and results in decreased drying capacity. More information of the drying batch which can help the kiln operator to make the right decisions is therefore desirable. Numerous ways to provide the kiln operators with data to help them control the drying process and reach the designated final MC has been developed and tested out in the industry. Some methods are based on estimating the wood MC from measurements such as the following (Fløtaker and Trondstad 2000, Vikberg 2012):

- load cells weighting whole stacks both prior, during, and after drying
- measuring the height of the packages during drying, which is correlated to the MC through the shrinkage
- resistive measurement of the MC on a few boards per batch during drying
- capacitive measurements of the batch during and after drying

Other methods are based on computer simulation software – offline to create fixed schedules or online to adjust adjacent climate (Hukka 1996, Salin 2002b, Salin and Wamming 2008). Measurement systems that have to be implemented in each one of the kilns imply a large investment and increased demand of maintenance. One single computer can, however, be used to run all the drying simulations at a sawmill. To get a reliable result from the simulation software it is important to provide it with the correct input data in terms of species, basic density, MC, volume and kiln characteristics. Out of this, the basic density and MC are the two most difficult parameters to estimate.

Earlier work suggested extracting this information out of X-ray data from the log sorting station (Skog et al. 2010). However, if the sorted logs stay long in the log yard before they are sawn, then they will become pre-dried and the MC measured in the log sorting station will be outdated. This problem is possible to overcome by instead installing the measuring device in the green sorting. Another problem is that X-ray devices working with only one energy level lack the possibility to distinguish between wood and water substance. This could be potentially solved by using dual-energy X-ray devices (Tanaka and Kawai 2013), but the reported measurement duration with existing dual-energy X-ray systems is too long for the method to be implemented online in a sawmill (Hultnäs and Fernandez-Cano 2012, Tanaka and Kawai 2013).

If the volume of the timber and its basic density is known, then the MC could instead be measured by utilizing a balance or a single-energy X-ray. Today the volume is commonly well defined by a supplementary measuring device, thus the problem reduces to measure or estimate the woods basic density.

The aim of this study is therefore to generate functions for the wood basic density at two sawmills in Sweden. An extensive discussion is also given regarding sources of errors and their magnitude in a setup for utilizing a balance or a single-energy X-ray to estimate the average MC of a wood package.

Material and Methods

Material preparation

In this study center yield from Scots pine (*Pinus sylvestris*) and Norway spruce (*Picea abies (L.) Karst*) logs were considered. Specimens were collected at two different sawmills, one located in Northern Sweden (hereafter denoted sawmill 1) utilizing both pine and spruce and one in Central Sweden (hereafter denoted sawmill 2), utilizing only spruce. Specimens were collected at 64 occasions over a time span of two years. At each occasion, 30 oven-dry specimens were collected according to the standard SS-EN 13183-1 from three different packages. From each package, five specimens were taken approximately 40 cm from the boards' butt-end and five specimens were taken approximately 40 cm from the boards' top-end. In addition, the dimension of each oven-dry specimen was measured with a caliper for making determination of specimens' basic density ($\rho_{0,green}$) possible. To ensure high production and high volumetric yield in the sawing process, the logs are presorted in different log-classes according to the logs top diameter. The sawmill then run one log-class at the time, which implies that all specimens collected at a certain occasion originated from the same log-class. The log-class and its corresponding log diameter interval were therefore also recorded.

Basic density analysis

A fundamental assumption throughout this work was that the basic density for a certain log-diameter and species does not vary significantly over the year for trees originated from the same growth area, i.e. the timber supply area of a certain sawmill. Under this assumption, linear equations of the basic density as function of log diameter were determined for the two sawmills. The basic density of the oven dry specimens was utilized in the analysis in which the following steps were taken:

- Data was examined for explainable outliers caused by error in the measurements.
- A Lilliefors test was performed with the null hypothesis "the sample originated from a normally distributed population". In the analysis, specimens from each log diameter were considered as sampled from their own distribution. Butt- and top-end specimens were also treated separately for further examination of differences in mean basic density. As rejection criteria, α=0.05 was used. As tests for normality are quite strict, histograms were used as a complement to judge if normality could be assumed.
- A two tailed t-test was performed to compare the mean value of the butt- and top-end samples of each log-class. The variances were assumed to be unknown and not necessary equal. As a rejection criteria, α=0.05 was used.
- Linear regression was performed and the root mean square error (RMSE) of the model was calculated.
- An analysis of the covariance of the basic density of butt- and top-end samples for pine was performed with the null hypothesis that the estimated relation with the log diameter was the same. α=0.05 was used as rejection criteria.

Error estimation

The magnitude of errors in the estimated moisture content, (u) was achieved by maximum error estimation. The analysis start with the expression of u as a function of the measured total volume (V), the mass (m) of the package, and the estimated average basic density (ρ):

$$u(m,\rho,V) = \frac{m-\rho V}{\rho V} = \frac{m}{\rho V} - 1 \tag{1}$$

Equation 1 was then differentiated:

$$\Delta u \approx \left(\frac{\partial u}{\partial m}\right)\Delta m + \left(\frac{\partial u}{\partial \rho}\right)\Delta \rho + \left(\frac{\partial u}{\partial V}\right)\Delta V = \frac{1}{\rho V}\Delta m - \frac{m}{\rho^2 V}\Delta\rho - \frac{m}{\rho V^2}\Delta V \tag{2}$$

By using the fact that the mass, volume and basic density all are positive numbers and some algebra, Equation 2 was then rewritten to form the maximum error estimator:

$$|\Delta u|_{max} \lesssim (u+1)\left(\frac{|\Delta m|_{max}}{m} + \frac{|\Delta\rho|_{max}}{\rho} + \frac{|\Delta V|_{max}}{V}\right) \tag{3}$$

Equation 3 shows that the error in u is proportional to the relative errors in the measured/predicted mass, basic density and volume. In addition, the equation shows that the error can be separated in two components: One component that increases proportionally to u and a component that is independent of u.

The magnitude of the error depends on how the quantities are measured but to get an idea of the total maximum error, a maximum relative error of 1 % of the measured mass was assumed. This is a reasonable assumption if the mass is measured with load cells. The accuracy of each cross sectional dimension was assumed to be within 0.2 mm and the accuracy of the length to be within 3 mm. The maximum relative error in the volume for a package with small dimensional boards (i.e. 28x100 mm^2) with an average length of 4 m then becomes 1 %. The magnitude of the relative error in basic density was achieved by first calculating the pooled estimator of the variance (Montgomery et al. 2004) of the basic density from all log-classes of top-end pine, butt-end pine, spruce at sawmill 1, and spruce at sawmill 2 respectively. Packages were then simulated where each boards basic density was taken from a normal distribution with this variance. Each package consisted of only 100 different boards. The reason for this small number is that several boards are usually sawn out of each log and the basic density of boards origin from the same log is similar. As an estimator of the maximum relative error in basic density, the maximum deviation between a single package and the total mean basic density was utilized. In total 500000 packages was simulated.

Results and Discussion

Basic density

Out of the total number of specimens, no explainable outliers were found despite the spread was large. The Lilliefors test resulted in a rejection of the null hypothesis for 7 samples out of 60 (i.e. 30 different log-classes with the butt- and top-end samples analyzed separately). The samples for which the null hypothesis was rejected were examined with aid of histograms and it was found that the assumption that each of the specimens were collected from a normal distribution seemed reasonable.

Considering differences in basic density between butt- and top-end samples, the null hypothesis that there was no difference in the mean value could be rejected for only 4 out of 20 log-classes of spruce and 8 out of 10 log-classes of pine. Due to the result of the t-test, it was reasonable to make no distinction between butt- and top-end samples for spruce but to treat butt- and top-end samples from pine separately. A Lilliefors test was performed on the spruce samples after merging the butt- and top-end samples together, and the null hypothesis was rejected for 5 out of 20 samples. The samples for which the null hypothesis was rejected were examined with aid of histograms and it was reasonable to assume that the butt- and top-end samples were collected from the same distribution.

Box plots, together with linear regressions and the RMSE are shown in Figure 1-4. The large RMSE indicates the importance of collecting a large number of specimens to determine an accurate function for estimating the basic density.

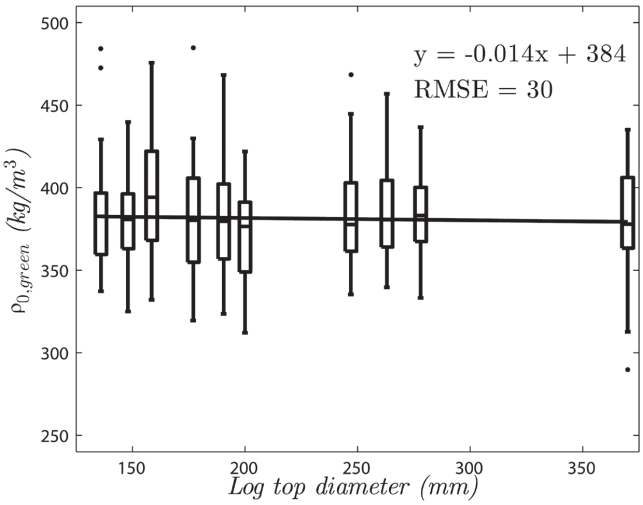

Figure 1. Box plot and linear regression for Pine basic density samples collected at the top-end of the boards. The linear equation and the root mean square error are shown in the figure. The boundaries of the box are the 25th and the 75th percentile and the line in the box is the median value. The maximum length of the whisker is 1.5 times the interquartile range and observations outside this range are represented by a dot. This is also what is shown in Figure 2 to Figure 4.

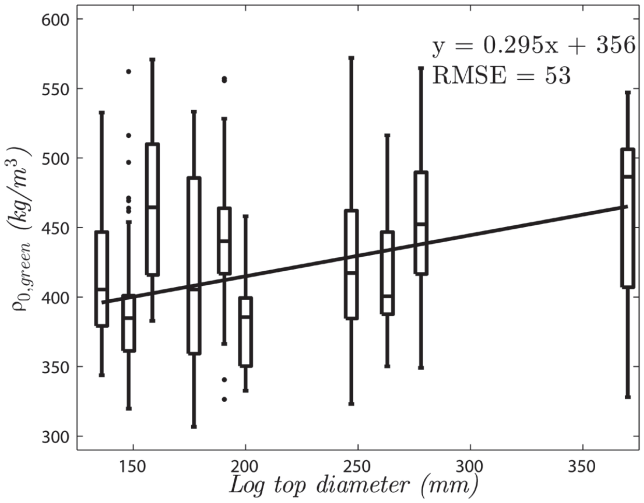

Figure 2. Box plot and linear regression for Pine basic density samples collected at the butt-end of the boards.

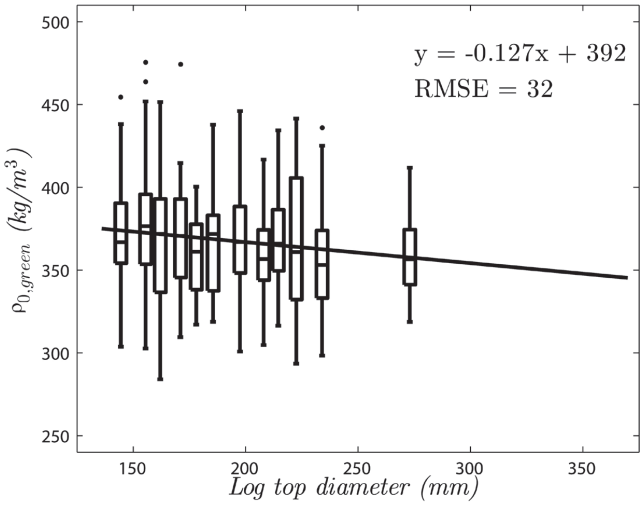

Figure 3. Box plot and linear regression for Spruce basic density samples collected at sawmill 1.

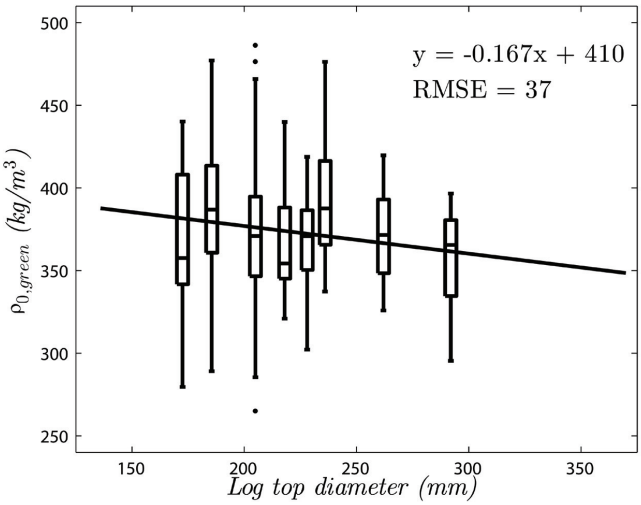

Figure 4. Box plot and linear regression for Spruce basic density samples collected at sawmill 2.

By comparing Figure 1 and 2, it can also be seen that butt-and top-end specimens from pine behave differently. A possible cause is that some of the butt-end specimens originated from the trees' butt-logs (i.e. if they were cut from the first log of the tree). Top-end specimens are on the other hand always cut at some distance from the butt-end of the living tree (i.e. at least one log-length). This affects basic density as it is well known that pine has their largest amount of extractives in the butt-end of the tree (Tamminen 1962). A further complication was caused by the fact that sawmill 1 tries to sort log-classes excluding the trees' butt-logs for some diameter intervals. In Figure 2, log-classes where sawmill 1 excluded trees' butt-logs are the 2nd and 6th log-classes counting from the left. Depending on how successful this sorting was, the proportion of butt-logs differed in these log-classes, as well as in the log-classes in which butt-logs otherwise is sorted (i.e. a mixed log-class in which the butt-log is sorted if it is classified as not being a butt-log). As the butt-log always has larger diameter than the subsequent logs from the same tree, the largest diameter log-classes will also contain a higher proportion of butt-logs. One solution could be simply excluding the butt-end specimens and using only top-end specimens for measurements. This, however, would be wrong from a drying point of view. We therefore recommend to develop functions for estimating basic density for pine from specimens cut at the top-end of the boards, but then to add a "butt-log fraction" adjusting for the amount of higher density wood in the package. The null hypothesis that there were no differences in the linear regressions for pine butt- and top-end samples was also rejected in the analysis of covariance.

Estimation of moisture content and errors

The square root of the pooled estimator of the basic density variance calculated with the values presented in Table I to IV became 30, 50, 32, 37 kg/m^3 for top-end pine, butt-end pine, spruce at sawmill 1, and spruce at sawmill 2 respectively. The corresponding maximum relative error in basic density became 4, 6, 4 and 5 %. The magnitude of the maximum relative error in basic density shows that there is no reason to invest in systems determining the mass and volume with extremely high accuracy.

If the green MC is approximately 70 %, the total maximum error according to Equation 3 thereby become 11, 14, 11, and 12 % MC for respectively top-end pine, butt-end pine, spruce at sawmill 1, and spruce at sawmill 2. The corresponding maximum errors after drying with an average MC of 10 % become 7, 9, 7 and 8 % MC (n.b. this reported errors are in percentage-units and not a percentage of the mean MC).

Table I. Pine top-end specimens.

Log top diameter (mm)	136	148	158.5	177	190.5	200	247	263	278	370
Number of specimens	30	120	15	30	30	30	60	15	30	15
Av. basic density (kg/m^3)	384	382	397	380	383	371	382	386	386	374
Std. basic density (kg/m^3)	35	26	42	38	32	27	27	31	28	39

Table II. Pine butt-end specimens.

Log top diameter (mm)	136	148	158.5	177	190.5	200	247	263	278	370
Number of specimens	30	120	15	30	30	30	60	15	30	15
Av. basic density (kg/m^3)	413	387	469	416	439	383	425	420	452	464
Std. basic density (kg/m^3)	46	38	56	68	54	34	60	51	51	64

Table III. Spruce specimens from sawmill 1.

Log top diameter (mm)	144.5	155.5	162	171	178	185.5	197.5	208	214.5	222.5	234	273
Number of specimens	60	90	60	30	30	30	120	30	90	30	60	30
Av. basic density (kg/m^3)	372	378	369	370	358	382	369	361	368	367	358	360
Std. basic density (kg/m^3)	31	34	37	36	23	30	29	25	28	43	36	27

Table IV. Spruce specimens from sawmill 2.

Log top diameter (mm)	172.5	185.5	205	218	228	236	262	292
Number of specimens	30	120	210	30	30	30	30	30
Av. basic density (kg/m^3)	370	382	374	365	365	390	369	358
Std. basic density (kg/m^3)	40	37	40	30	30	34	26	28

Conclusions

The estimation of the basic density is the largest source of error if decent equipment is used to measure the mass and volume. The large magnitude of the derived maximum error shows that the described method should not be utilized to estimate the MC of dried packages or even individual green packages. The method could however still be used to estimate the average green MC of a drying batch consisting of several wooden packages. Especially when a major pre-drying of the sapwood is present, the method can be a valuable indicator to the kiln operator when actions need to be taken to hit the designated final MC of the drying batch. Finally, because of the large variation in the basic density of butt-end specimens from pine we recommend that they should be omitted when deriving basic density estimators.

References

Fløtaker, S., and Tronstad, S. (2000) *Description and initial test of 8 principles for in-kiln measuring and end-point control of wood moisture content*, IMCOPCO (task 2.1). Norwegian Institute of Wood Technology, Oslo.

Hukka, A. (1996) *A Simulation Program for Optimisation of Medium Temperature Drying on an Industrial Scale*. In proceedings of the 5th International IUFRO Wood Drying Conference, Quebec City, Canada, August 13-17.

Hultnäs, M., and Fernandez-Cano, V. (2012) Determination of the moisture content in wood chips of Scots pine and Norway spruce using Mantex Desktop Scanner based on dual energy X-ray absorptiometry. *Journal of Wood Science*, 58(4): 309–314.

Montgomery, D.C., Runger, G.C., and Hubele, N.F. (2004) *Engineering statistics*, (New York: John Wiley & Sons).

Persson, F., and Andersson, J.E. (2014) *Automatisk övervakning och uppföljning av torkprocessen – paketvägning*, (In Swedish). Wood Centre North, Luleå University of Technology, Skellefteå.

Salin, J.G. (2002a) *The timber final moisture content variation as a function of the natural variation in wood properties and of the position in the kiln load. An evaluation using simulation models.* In proceedings of the 4th COST E15 Workshop, Santiago de Compostela, Spain, May 30-31.

Salin, J.G. (2002b) *Simulation models as an industrial tool for optimizing the drying of timber*. In proceedings of the 4th COST E15 Workshop, Santiago de Compostela, Spain, May 30-31.

Salin, J.G., and Wamming, T. (2008) Drying of timber in progressive kilns: Simulation, quality, energy consumption and drying cost considerations. *Wood Material Science and Engineering*, 3(1-2): 12-20.

Skaar, C. (1988) *Wood -Water Relations*. (Berlin Heidelberg: Springer Verlag).

Skog, J., Vikberg, T., and Oja, J. (2010) Sapwood moisture-content measurement in Pinus Sylvestris sawlogs combining X-ray and three-dimensional scanning. *Wood Material Science and Engineering* 5(2): 91-96.

Staland, J., Navrén, M., and Nylinder, M. (2002) *Såg 2000, Resultat från sågverksinventeringen 2000* (Saw 2000, Results from sawmill inventory 2000), (In Swedish). The Swedish University of Agricultural Sciences, Uppsala.

Tamminen, Z. (1962) *Fuktighet, volymvikt m.m. hos ved och bark I. Tall. (Density and Other Properties of Wood and Bark I. Scots Pine)*, (In Swedish). Research Note 41, Royal School of Forestry, Department of Forest Products, Stockholm.

Tamminen, Z. (1964) *Fuktighet, volymvikt m.m. hos ved och bark II. Gran. (Density and Other Properties of Wood and Bark II. Norway Spruce)*, (In Swedish). Research Note 47, Royal School of Forestry, Department of Forest Products, Stockholm.

Tanaka, T., and Kawai, Y. (2013) A new method for nondestructive evaluation of solid wood moisture content based on dual-energy X-ray absorptiometry. *Wood Science and Technology*, 47(6): 1213-1229.

Taylor, A.M., Gartner, B.L., and Morrell, J.J. (2002) Heartwood formation and natural durability –a Review. *Wood and Fiber Science*, 34(4): 587-611.

Vikberg, T. (2012) *Moisture content measurement in the wood industry*. Licentiate Thesis, Luleå University of Technology, Sweden.

Publication III

MOISTURE CONTENT MEASUREMENT IN SCOTS PINE BY MICROWAVE AND X-RAYS

*Tommy Vikberg**

PhD Student
Division of Wood Physics
E-mail: tommy.vikberg@sp.se

Johan Oja

Adjunct Professor
Division of Wood Science and Technology
E-mail: johan.oja@norra.se

Lena Antti

Associate Professor
Division of Wood Physics
Luleå University of Technology
SE-931 87 Skellefteå, Sweden
E-mail: lena.antti@haparanda.se

(Received November 2011)

Abstract. There is demand in the Swedish sawmill industry to improve the accuracy of moisture content measurements, both to obtain a better tool to run production and to ensure that the products meet customer expectations. In this study, 240 well-conditioned pieces of Scots pine (*Pinus sylvestris*), sorted into five different groups by visual inspection, were measured using microwaves and X-rays. Models to predict moisture content of wood were made by measurements of an additional 45 pieces of wood. Using only measured quantities from the microwave system, ie attenuation and phase shift, the root mean square error (RMSE) of the estimated moisture content was 1.00%. By adding total density from the X-ray measurements, RMSE of the estimated moisture content was lowered to 0.89%. Mean errors of the different wood groups varied from –0.65 to 0.18%.

Keywords: Wood, inline, attenuation, phase shift, knots.

INTRODUCTION

Higher production rate and less time from the felling of trees in the forest to the final product, driven by economic and qualitative factors, have led to an increased demand during the last few decades for accurate and automated measuring devices. Because wood shows great variations in properties among individuals and even within the same individual (Dinwoodie 2000), this task has proven to be a challenge. Nevertheless, it is important to obtain as high a value as possible out of the wood to sort the wood to the best designated end product and to ensure that the quality demands of the end product are fulfilled. Moisture content is one quality factor that is important in the production chain and in the final use of the wood (Esping et al 2005). Industrial tests of commercial inline moisture content meters have shown low accuracy from individual readings (Esping 2003; Nilsson 2010). All methods for measuring moisture content have their pros and cons, and most of today's meters only use one measuring technique (Vikberg 2010). Nilsson (2010) demonstrated that accuracy of moisture content measurements can be improved by taking the visual properties of wood into account. Because sawn wood is often sorted according to different qualities by visual methods using parameters such as number of knots, knot size, and wood defects, it would be straightforward to use this information together with the moisture content measurements.

* Corresponding author

Microwaves have been widely used to predict different wood parameters (Schlemm 2004; Schajer and Orhan 2006). A high microwave frequency gives high-resolution measurements, but one needs to be aware of the risk of the phase shift exceeding 2π (Hansson et al 2005). However, if wood density is known, it is likely that a model will be able to predict the number of multiples of 2π that the phase shift has expired. One way to achieve high-resolution density measurements of wood is by computer tomography (CT) (Lindgren 1992).

This study considers moisture content measurements taken with microwaves and combines these measurements with density measurements performed with a medical CT scanner. The tested material was manually sorted into five different groups based on its visual properties, and the potential for increased accuracy in moisture content measurements is discussed according to the results.

MATERIALS AND METHODS

The tested material consisted of 195 pieces of Scots pine (*Pinus sylvestris*) planed on four sides to dimensions of $44 \times 120 \times 920$ mm^3 (R, T, z). The pieces were chosen to represent different kinds of wood, and by visual inspection, they were divided into the following groups: normal, fine, knot, check, and defect. Each group was found in two different moisture content classes conditioned to approximately 13 and 16% MC. Characteristics of the different groups are as follows: the defect group contained large wood defects, such as top rupture and spike knots; the knot group contained considerably large sound knots; the check group contained checks that were easily discovered with the naked eye; the wood classified as fine had very few and small knots and most of the samples had a high amount of heartwood and an average dry density higher than the other groups; finally, the normal wood was chosen to represent the most common wood at a normal production site. From an end user's viewpoint, the fine group would be suitable for window frames, the defect group would be suitable for packaging, and the other three groups would normally be used as construction lumber. Typical magnitudes of some of the characteristic properties of the different groups were measured and are presented in Table 1.

Table 1. Typical magnitudes of some characteristics of wood in the different groups.[a]

Group	CL (mm)	CW (mm)	No. of KW	Max KD (mm)	FD (mm)	$\rho_{0,u}$ (kg/m^2)
Normal	0	0	1.7	23	0	400
Fine	0	0	1.3	7.5	0	450
Knot	0	0	2.2	34	0	400
Check	430	0.5	1.5	11	0	430
Defect	0	0	1.5	21	160	400

[a] Only the central 0.6 m of each board is considered because this was where the actual measurement took place.

CL, check length; CW, check width; KW, knot whirls; KD, knot diameter; FD, fiber disturbance; $\rho_{0,u}$, density of dry wood at MC u.

All pieces were measured with Satimo microwave equipment (Satimo Microwave Vision Sweden, Allingsås, Sweden) using a frequency of 9.375 GHz (Johansson 2001). The measured quantities were attenuation and phase shift in two directions of polarization, corresponding to parallel and cross-grain. The influence of the dielectric properties of the wood on attenuation and phase shift of the microwave was described by Hansson et al (2005), whereas Schajer and Orhan (2005) described a method to measure these quantities. Wood density, $\rho_{u,u}$, where u is moisture content of the pieces, was measured with a medical CT scanner (Siemens Somatom Emotion Duo; Siemens AB, Upplands Väsby, Sweden), as described by Lindgren (1992).

During measurements with the microwave equipment, the short ends of the boards were placed on metal supports, giving rise to some disturbance

Figure 1. Three characteristic boards from the normal group.

Figure 2. Three characteristic boards from the fine group.

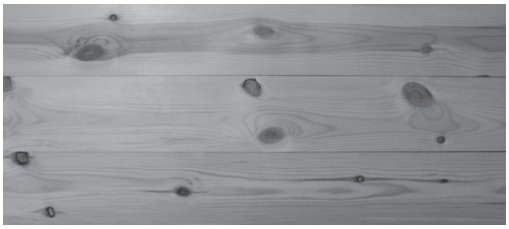

Figure 3. Three characteristic boards from the knot group.

Figure 4. Three characteristic boards from the check group (checks are outlined).

of the measured values within the vicinity of the supports. Therefore, only data from the central 0.6 m of each board were used for further analysis. To give an idea of the visual appearance of board characteristics, three representative boards of each group are shown in Figs 1-5. Only the parts of the boards from which data were collected, ie the central 0.6 m, are shown.

Before the wood pieces were removed from the conditioning chambers, each piece was sealed with glue at the ends to prevent longitudinal drying. Additionally, all boards were wrapped in plastic together with other boards from the same moisture content class to prevent large moisture content changes.

Figure 5. Three characteristic boards from the defect group. (Note large areas of grain deviations.)

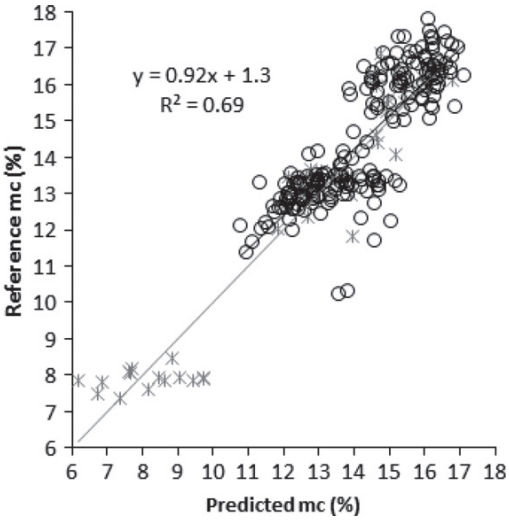

Figure 6. Predicted moisture content (MC) using a model based on measured microwave attenuation and phase shift. Stars represent calibration boards, and circles represent boards for which MC is predicted. The equation in the plot is a linear least square fit to the prediction set.

As a calibration set, 45 pieces conditioned to three different moisture content classes of approximately 8, 13, and 16% were used. Characteristics of the wood used for calibration were the same as for the normal group. The calibration set was kept relatively small to correspond to an industrial calibration procedure. The moisture content, used as the reference, of each individual piece was achieved using the oven-dry method as stated in CEN (2002).

Measured data were analyzed by constructing a partial least square regression model using

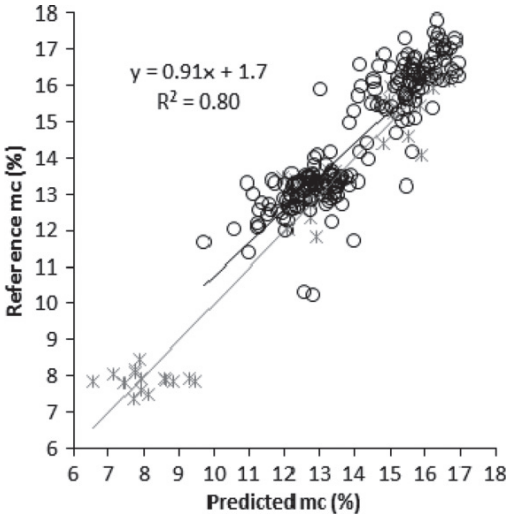

Figure 7. Predicted moisture content (MC) using a model based on measured microwave attenuation and phase shift with density from computer tomography measurements included. Stars represent calibration boards, and circles represent boards for which MC is predicted. The equation in the plot is a linear least square fit to the prediction set.

SIMCA (Eriksson et al 2006). Multivariate data analysis has already shown great potential and has been widely used in wood research (Danvind 2002; Lundgren and Hansson 2007). Two principal components were used in the model to span the space to describe significant relationships in the data. The 45 calibration boards were used for constructing the model, and prediction of moisture content for the remaining 195 pieces was analyzed. In the first model, the measured phase shift and attenuation in the two directions of polarization by means of microwaves was used; the second model also included mean density from CT measurements.

RESULTS

Results from the model predicting moisture content from the measured attenuation and phase shift in the two directions of polarization by means of microwaves are shown in Fig 6.

The calibration set in Fig 6 had a coefficient of determination (Montgomery et al 2004), R^2, of 0.92 and a root mean square error (RMSE) of 0.90%. The prediction set had an RMSE of 1.00% and, as can be seen in Fig 6, an R^2 of 0.68.

To obtain more accurate moisture content measurements, measured wood density, $\rho_{u,u}$, from the CT was used together with the microwave measurements (Fig 7).

Linear regression of the calibration boards in Fig 7 had an R^2 value of 0.94 and an RMSE of 0.77%. The different slopes of the regression lines of the calibration and prediction set show that the calibration was not suitable for all pieces of wood. RMSE of the estimated moisture content was 0.89%.

To gain an idea of possible improvements in moisture content measurements by also using an optical device, mean error and RMSE are presented for the five different groups of wood (Table 2).

As seen in Table 2, RMSE was the smallest for the most valuable wood, ie fine group.

Table 2. Mean error and root mean square error (RMSE) of moisture content measurements for the five different groups of wood.[a]

Group	$\bar{\varepsilon}_{MW}$	$\bar{\varepsilon}_{MW,CT}$	$RMSE_{MW}$	$RMSE_{MW,CT}$	$RMSE^*_{MW}$	$RMSE^*_{MW,CT}$
Normal	–0.65	–0.55	1.06	0.85	0.84	0.64
Fine	0.18	–0.21	0.64	0.61	0.62	0.58
Knot	–0.36	–0.37	1.06	0.95	1.00	0.87
Check	0.17	–0.33	1.03	0.84	1.02	0.78
Defect	–0.31	–0.59	1.12	1.13	1.08	0.97
All wood	–0.20	–0.41	1.00	0.89	0.92	0.78

[a] Values are shown when only microwave measurements were used and when they were combined with computer tomography (CT) measurements. The two last columns show RMSE after subtracting the mean error for each group, ie the best possible result if combining the measurements with a visual system.

DISCUSSION

RMSE was decreased by adding density measurements determined by CT scanning to the microwave measurements. Adding a third measurement technique would presumably further improve the results. Because the mean errors differ among the wood type groups, a visual system would also improve overall accuracy. If the measurements of a board were taken along the whole length of the board, one could filter out regions in which the signal is stable, which implies that no disturbances such as grain deviation or knots were present. In most cases, however, the boards are cross-fed through the final sorting stations in which the moisture content should be measured. In this case, connecting a visual system to the moisture content meter would be beneficial for detecting objects that are within the meter's measuring range, thus affecting the measured amount.

In the prediction set, there were two points with considerably low reference moisture content. This result was strange because these boards were placed in the same climate chamber as the rest of the pieces in the 13% MC class. There may be some errors in the reference values for those two individuals; excluding them from the prediction set would, however, not produce a remarkable change in the accuracy of the prediction model.

In this study, board thickness was not used as a parameter in the model because the boards were planed to the same dimensions. This step should normally be done because measured microwave values are related to wood and water surface density (kg/m^2), ie the thicker the board, the greater the attenuation and phase shift. A large attenuation caused by high-density wood, high moisture content, or thick boards limits the use of the described system. Generally, the limit is a moisture content of approximately 20% for a 50-mm-thick board with a dry density of 500 kg/m^3. The vicinity of the board's edges will also cause diffraction of the field, and measurements originating from those areas will be difficult to interpret correctly.

An industrial calibration procedure could be simplified if only one board dimension could be used together with preprogrammed correlations for other dimensions. This is concluded because there were problems with the calibration in this study, although only a single dimension with well-defined wood was used. Calibration procedures could also be simplified by using calibration dummies with well-defined dielectric properties.

In summary, this study shows that the accuracy of moisture content prediction was increased by combining microwave measurements with CT measurements. Mean error also differed among the wood type groups, showing the potential to further increase the measurement accuracy by adding a visual system.

REFERENCES

CEN (2002) EN 13183-1. Moisture content of a piece of sawn timber. Part 1: Determination by oven dry method. European Committee for Standardization, Brussels, Belgium.

Danvind J (2002) PLS prediction as a tool for modeling wood properties. Holz Roh Werkst 60(2):130-140.

Dinwoodie JM (2000) Timber: Its nature and behavior. Spon Press, London, UK.

Eriksson L, Johansson E, Kettaneh-Wold N, Trygg J, Wikström C, Wold S (2006) Multi and megavariate data analysis. Umetrics AB, Umeå, Sweden.

Esping B (2003) Test av kommersiella fuktkvotsmätare in-line. Trätek rapport Trätek, Stockholm, Sweden [in Swedish].

Esping B, Salin J-G, Brander P (2005) Fukt i trä för byggindustrin. Trätek, Stockholm, Sweden [in Swedish].

Hansson L, Lundgren N, Antti L, Hagman O (2005) Microwave penetration in wood using imaging sensor. Measurement 38(1):15-20.

Johansson J (2001) Property predictions of wood using microwaves. Licentiate, Luleå University of Technology, Skellefteå, Sweden.

Lindgren O (1992) Medical CT-scanners for non-destructive wood density and moisture content measurements. Doctoral, Luleå University of Technology, Luleå, Sweden.

Lundgren N, Hansson L (2007) PLS models for predicting wood properties from microwave measurements based on three dimensional FEM simulations. Proceedings, Nordic workshop on wood engineering, Luleå University of Technology, Skellefteå, Sweden.

Montgomery DC, Runger GC, Hubele NF (2004) Engineering statistics. John Wiley & Sons, Hoboken, NJ.

Nilsson M (2010) Evaluation of three in-line wood moisture content meters. MS thesis, Luleå University of Technology, Skellefteå, Sweden.

Schajer G, Orhan F (2005) Microwave non-destructive testing of wood and similar orthotropic materials. Sensing and Imaging: An International Journal 6(4): 293-313.

Schajer GS, Orhan FB (2006) Measurement of wood grain angle, moisture content and density using microwaves. Holz Roh Werkst 64(6):483-490.

Schlemm U (2004) Mass and moisture measurement by use of the microwave resonator technique. Technical bulletin, Tews Elektronik, Hamburg, Germany.

Vikberg T (2010) Fuktkvotsmätare för träindustrin: En kartläggning av metoder för mätning av fuktkvoter i intervallet 7-18 fuktkvotsprocent. Technical report, Luleå University of Technology, Skellefteå, Sweden [in Swedish].

Publication IV

Measurement 45 (2012) 525–528

Contents lists available at SciVerse ScienceDirect

Measurement

journal homepage: www.elsevier.com/locate/measurement

Effects on microwave measurements and simulations when collecting data close to edges of wooden boards

Tommy Vikberg [a,b,*], Lars Hansson [a], Gary S. Schajer [c], Johan Oja [b,d]

[a] Division of Wood Physics, Luleå University of Technology, SE-931 87 Skellefteå, Sweden
[b] Wood Technology, SP Technical Research Institute of Sweden, SE-931 77 Skellefteå, Sweden
[c] Department of Mechanical Engineering, University of British Columbia, Vancouver, Canada V6T 1Z4
[d] Division of Wood Science and Technology, Luleå University of Technology, SE-931 87 Skellefteå, Sweden

ARTICLE INFO

Article history:
Received 28 April 2011
Accepted 10 October 2011
Available online 18 October 2011

Keywords:
FEM-simulations
Board
Calibration

ABSTRACT

Parameters like strength, moisture content, density and grain direction are important when sorting wood according to their individual properties. All those parameters can be correlated to microwave measurements of phase shift and attenuation. Measurements of phase shift and attenuation are, however, affected by the vicinity of a board edge. In this article a simulation of the measurement system is used to create a compensation function for the measurements taken close to edges as if those were taken where no effects of the board edge could be noticed. It is shown, by comparison with real measurements, that by doing this the deviation between the values measured close to the board edges and those measured in the middle of the board is decreased, meaning a higher accuracy can be achieved by using the compensating function.

1. Introduction

Wood is a renewable material that can be used in a wide variation of products and applications. To get the highest possible value out of the wooden products it is important, prior to the use, to be able to characterise and sort the wood according to its specific properties. The earlier a correct classification can be done the better the remaining production chain can be adapted to the specified end product [1].

Of high importance in the wood production chain is the moisture content of the individual board. As wood is a hygroscopic material, its moisture content changes according to the surrounding climate. If the moisture content is not correctly determined after the drying process at the sawmill, there is a risk that problems will arise later when the board is in service [2]. An incorrect moisture content can result in mould growth [3], checks, twisting, shrinkage or swelling [4]. As a last step in the production chain at a sawmill, prior to the distribution to the customers, the boards are sent through a final sorting where the moisture content of each board can be measured. High energy prices and the fact that the drying capacity often is the limiting factor for the production at a mill, causes the drying process to be done in as short time as possible. If the conditioning phase in the drying is absent, or to short, the dried boards will retain a moisture gradient. This gradient will cause subsequent dimensional changes of the boards, especially those that are to be split to panels [5]. To be able to measure this moisture gradient as well as other wood parameters one would like to perform measurements close to the edges of the boards. As the boards usually are cross fed through the final sorting there is also a demand to collect data from the whole width of the board, giving a higher number of measurements to process and therefore a statistically more significant measurement result.

FEM-simulations have previously shown to be a good tool for simulating the interaction between wood and microwaves [6,7]. Simulations are also a powerful tool to use when one wants to develop a measuring device or

* Corresponding author at: Division of Wood Physics, Luleå University of Technology, SE-931 87 Skellefteå, Sweden. Tel.: +46 10 5166264.
E-mail address: tommy.vikberg@sp.se (T. Vikberg).

0263-2241/$ - see front matter © 2011 Elsevier Ltd. All rights reserved.
doi:10.1016/j.measurement.2011.10.016

understand the behaviour of an existing system. The ease of making changes in an accurate model is greater than when working with a physical system.

It is well known that diffraction of the electromagnetic field occurs close to edges of a material having a different dielectric constant than the surrounding medium [8]. Simulations are also a good way to acquire the basic understanding of fundamental principles that can be applied to complex materials such as wood, where the deviation between individuals is large. Hence, the hypothesis is that simulations of a system can be used to improve understanding of material behaviour when performing measurements close to an edge of a material. This allows the possibility to compensate the measurements to correspond better with the expected values as if those were gained from measurements of an infinite sample.

2. Materials and methods

The measurements were performed using a microwave system consisting of two horn antennas with a wooden sample placed in between. A principal sketch of the whole microwave system can be seen in Fig. 1, for a detailed description of the system used see Schajer and Orhan [9].

To localise the point of measurement, the system used a scattering dipole on which the sample under test was placed, see Fig. 2.

Verification of the linear behaviour of the system was done using four pieces of medium density fibreboards (MDF). Measurements were performed when stacking them on top of each other in different sequences and with different rotations of the fibreboards. This was done to make sure there was no anisotropy within any fibreboard as well as no difference between the different fibreboards.

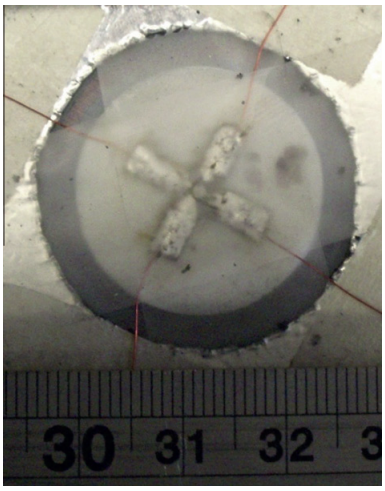

Fig. 2. Scattering dipole with two crossed directions used to localise the point of measurement.

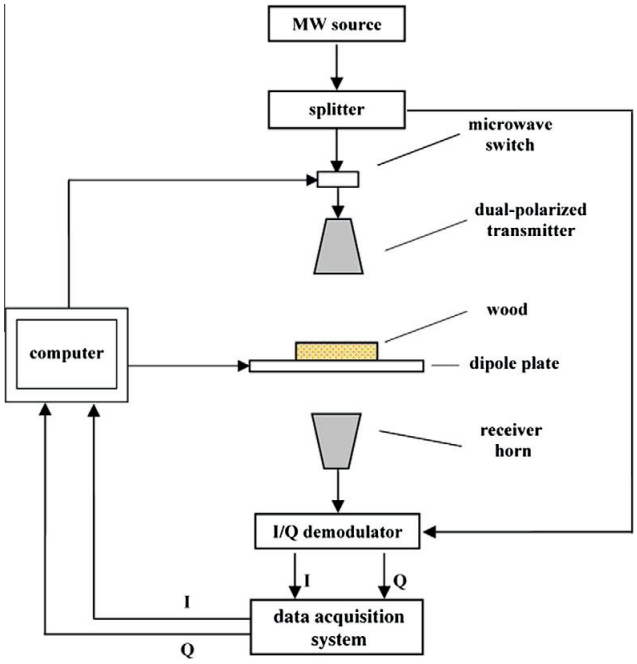

Fig. 1. Principal sketch of the microwave measuring device, [10].

In a similar way the linear behaviour of the model was verified by simulation of different thicknesses of a big slab with similar dielectric constant as the fibreboards. MDF was chosen since the dielectric constant is not dependent of the direction within the board, i.e. there should not be any anisotropy since the fibres are in random directions throughout the board.

Nine pieces of well-conditioned wood representing three different density classes with three different thicknesses in each class was used to check the edge effects. Each piece was measured in steps of 2 mm as it was moved over the sensor head. Transmission factors and the phase shifts were calculated in the principal direction of the wood. The principal direction used in the comparisons with the simulated data was from whom the higher transmission factor was achieved, i.e. perpendicular to the wood grain direction. The dielectric constants used in the simulations was taken by linear integration of tabulated values for the same principal direction, i.e. cross grain [11]. To be able to compare the simulated attenuation to the measured transmission factor, a linear regression was done to the measured and simulated values origin from the middle of the board. In this area no effects from the vicinity of the edges could be noticed.

Since the chosen wooden pieces were well conditioned and consisted of clear wood, the assumption was made that the measured transmission factor and phase shift would be uniform within the whole piece. The deviation between the measured result close to the board edge and the stable measurements in the centre parts of the board is therefore presented as an error in the measurements. Measured values are also compensated with the assumption that the measurement shows the same behaviour as the simulations, meaning a compensation of the measured values close to the board edges. All the simulations were performed in COMSOL 4.0a [12].

3. Result

Fig. 3 shows the measured and simulated transmission and phase shift near the edge of an example board.

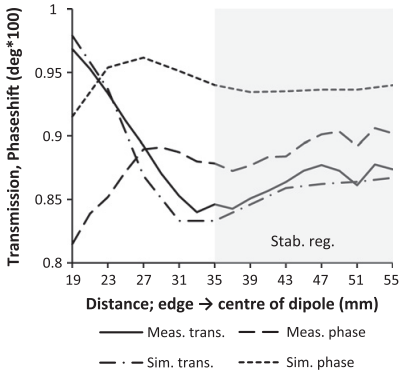

Fig. 3. Example of transmission factor and phase shift in the simulations and measurements for one piece of wood.

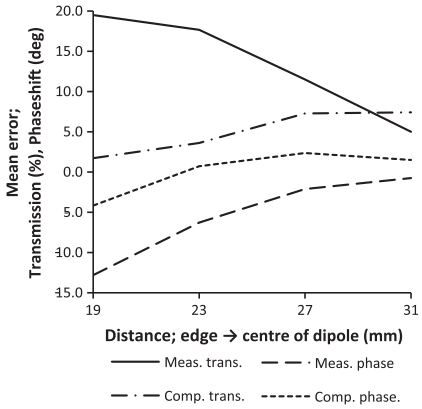

Fig. 4. Mean error for the nine measured pieces in percentage of transmission factor and in degrees for the phase shift.

Fig. 4 shows the deviation between the results measured directly and by using a compensation function. The results are compared to the average measured result from the "edge → centre of dipole" distances of 35–55 mm as the measurements where reasonably stable in this area, see Fig. 3. The compensated transmission values were determined by assuming that the simulations and measurements showed the same behaviour, i.e. if the simulations showed a difference between the stable centre values and the value at position 23 mm of 10%, the measured value at this position was changed according to this. The error was in this case calculated as the difference between the compensated value and the average measured value in the stable region.

Compensated phase shift was achieved by comparing the simulated phase shift at a particular position to the average simulated phase shift in the stable centre region and compensate the measured phase shift according to this, i.e. if the simulated phase shift at certain position was 10° higher than the simulated phase shift in the centre region the measured phase shift at this particular position

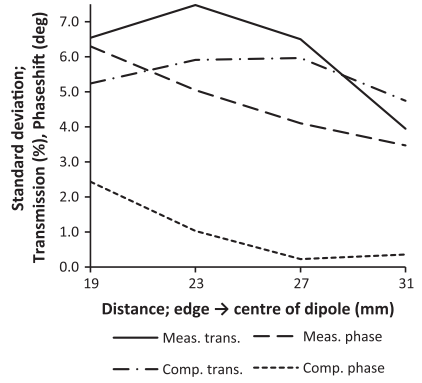

Fig. 5. Standard deviation for the nine different wood pieces in the measurements and simulations.

was subtracted with 10° and this, correlated, phase shift was compared to the phase shift measured in the centre region of the board.

In Fig. 4 it can be seen that calibration through simulated values increases the accuracy for the transmission measurements close to the board edges, i.e. for position 19, 23 and 27 mm. The corresponding standard deviation is shown in Fig. 5.

It can be seen in Figs. 4 and 5 that effective compensation can be done to reduce the effects of diffraction on wood parameter measurements made in the vicinity of a board edge by using a correlation function determined by simulating the measurement system.

4. Discussion

Performing simulations of a measurement system can become a computationally demanding task. In order to get a reliable result the grid used for the calculations has to be sufficiently small. It is therefore important to consider whether the required solutions can be found by only simulating a small part of the system, as in this case only the edge of the wood. It is also important to point out that it is not straight forward to take the results of the measurement and simulations shown here and use in another measuring system since each system interacts differently with its surroundings. The process of simulating and investigating the effects on the electromagnetic field when performing measurements close to an edge can however be used to increase the practical measuring range of any device.

From a practical point of view, a volume is always being measured rather than a point. This makes comparisons between simulations and real data somewhat difficult and a source of error that is not taken into account in this work. With a setup as described here, the measured area approximately equals the dipole size [13]. A useful method to compare simulated and measured data and not have to struggle with this problem would be to match the achieved curves according to their shapes.

Measurements has shown significant variations in dielectric constants even within the same species, density, moisture content and temperature [11]. Instead of using measured transmission in wood to make it possible to compare simulated attenuation with measured transmission factor it would be sufficient to use different materials, not necessarily wood, with well-defined dielectric constants. It would also be sufficient if those materials spanned a larger space of dielectric constants. Due to the small number of pieces used in this investigation, the difference in the magnitude of the dielectric constant between the individual pieces is a significant source of uncertainty.

It is interesting to notice, that even if the number of tested samples are small and the actual dielectric constant is a matter of concern, the simulated results and the measurements show similar behaviour. Especially the shape of the phase shift values for different distances to the board edge shows a good agreement for the whole range of sample positions. Except for the uncertainly in the magnitude of the dielectric constant, the fact that the wooden samples were not completely isotropic could partly explain the deviation between the simulations and measurements.

Throughout the measurements it was difficult to prevent unwanted reflections from entering the receiving antenna. This problem could be reduced by having the antennas placed closer to each other. Shorter distance between the antennas will however imply that one is working in the near field of the antennas where the electromagnetic field is less well described [14].

5. Conclusion

It is shown that effective compensation can be done to reduce the effects of diffraction on wood parameter measurements made in the vicinity of a board edge. This is done by using a correlation function determined by simulating the measurement system. The major advantage is the opportunity to make a higher number of reliable measurements as well as a better chance to measure moisture gradients in the boards, i.e. wet cores.

References

[1] S. Grundberg, An X-ray LogScanner – a Tool for Control of the Sawmill Process, Luleå University of Technology, Skellefteå, 1999.
[2] J.M. Dinwoodie, Timber: its nature and behavior, E & FN Spon, 2000.
[3] S. Geving, J. Holme, The drying potential and risk for mold growth in compact wood frame roofs with built-in moisture, J. Build. Phys. (2010) 249.
[4] B. Esping, Trätorkning 1a, grunder i torkning, Stockholm, 1992.
[5] B. Esping, Trätorkning 2, torkningsfel – åtgärder, Stockholm, 1988.
[6] L. Hansson, Microwave Treatment of Wood, Luleå University of Technology, Skellefteå, 2007.
[7] T. Sjöden, Electromagnetic Modelling for the Estimation of Wood Parameters, Växjö University, Växjö, 2008.
[8] J. Meixner, The behavior of electromagnetic fields at edges, Antennas Propag. IEEE 20 (1972) 442–446.
[9] G.S. Schajer, F.B. Orhan, Microwave non-destructive testing of wood and similar orthotropic materials, Subsurf. Sens. Technol. Appl. 6 (2005).
[10] G.S. Schajer, F.B. Orhan, Measurement of wood grain angle, moisture content and density using microwaves, Holz als Roh- und Werkstoff 64 (2006).
[11] G.I. Torgovnikov, Dielectric Properties of Wood and Wood-Based Materials, Springer-Verlag, 1993.
[12] Comsol AB, Tegnérgatan 23, SE-11140 Stockholm, Sweden. <www.comsol.se>.
[13] R.J. King, Microwave Homodyne Systems, Peregrinus Press, 1978.
[14] R.C. Johnsson, H.A. Ecker, J.S. Hollis, Determination of far-field antenna patterns from near-field measurements, IEEE (1973).

Publication V

INTERNAL HEAT EXCHANGE IN PROGRESSIVE KILNS*

Tommy VIKBERG
Luleå University of Technology, division of Wood Science and Engineering,
Forskargatan 1, SE-931 87 Skellefteå, Sweden/
SP Technical Research Institute of Sweden, Laboratorgränd 2, SE-931 77 Skellefteå, Sweden
Tel: 0046 105 116264, E-mail: tommy.vikberg@sp.se

Tom MORÉN
Luleå University of Technology, division of Wood Science and Engineering,
Forskargatan 1, SE-931 87 Skellefteå, Sweden
E-mail: tom.moren@ltu.se

**Accepted for publication in PRO LIGNO*

Abstract
In this work possible energy savings were investigated by introducing a new layout of a 2-zone progressive kiln. The layout consisted of installing a door between the first and second zone, thereby allowing the two zones to be run at different temperature levels -making internal heat recovery possible. An Optimized Two Stage continuous kiln is dimensioned for drying sideboard of Norway spruce (Picea abies L. Karst) with the aid of a commercial simulation program. Temperature levels of 75/55°C (dry bulb/wet bulb) were chosen at the pressure side of zone 1 and 45/25°C (dry bulb/wet bulb) at the pressure side of zone 2. The capacity of the heat exchanger was assumed to be sufficient to make the suggested design functional and no consideration was given to the increased air flow resistance the introduction of the heat exchanger would cause. The results indicated that roughly 30% of the heat is possible to recover in comparison to a traditional kiln. It was finally concluded that the influence of ingoing process parameters needs to be implemented in the kiln control system to fully utilize the kilns potential.

Keywords: *Wood drying, Energy efficiency, Kiln design, Simulation tools, Kiln ventilation.*

INTRODUCTION

The single largest consumer of heat at a sawmill is the drying process where the heat is used for heating the air in air circulating kilns. Since planks and boards with rectangular cross section are sawn out of logs the volume yield is quite low, normally around 50 % (Ikonen *et al.* 2003, Pinto *et al.* 2006). This leaves a great amount of residuals which is partly used as fuel in boilers to produce the heat demanded in the drying process. Due to an increased price on biofuels in the last decades the sawmills has become more keen on reducing their own consumption, -leaving a larger share to be sold to external customers and thereby increase the profit of the sawmill. To limit the waste of heat, it is important to keep the drying kilns in good condition in terms of limited air leakage and good insulation. As an additional act, it is often possible to decrease the amount of heat in the drying process by increasing the drying temperature and make sure to stop the drying when the target moisture content is reached. Since the value loss of poor drying quality is high, a drying simulation software is useful in this context (Hukka 1996, Salin 2001, Salin 2002, Salin and Wamming 2008). Finally, the used amount of heat can also be limited by installing a heat recovery system. The most common one is the air to air heat exchanger between the warm humid air that is vented out from the kiln and the cold dry air that is let in whereas other solutions is to use condensations panels, heat pumps, open absorption systems, running several kilns as clusters etc. (Johansson and Westerlund 2000, Chua *et al.* 2002, Elustondo and Oliveira 2006, Anderson and Westerlund 2014).

There exist mainly two types of drying kilns in the sawmill industry; the batch kiln and the progressive kiln. In the batch kiln the whole kiln is filled with green timber before the door is closed and the drying starts. The drying then proceeds untill the whole batch is dried and the kiln can be unloaded and ready to be filled up with the next batch of green timber. In the progressive kiln the kiln is always full of timber in different stages of drying. The loading-unloading is done by loading one stack of green timber at the entry of the kiln and simultaneously take out one stack of dried timber at the exit end of the kiln. The three most common types of progressive kilns are the 1-zone progressive kiln, the 2-zone feed-back kiln and the Optimized Two stage Continuous, OTC-kiln (http://www.valutec.se/assets/documents/kanaltorkar/Progressive_kilns.pdf, http://www.muehlboeck.co.at/uploads/media/Kanaltrockner_EN_NEU2011.pdf).

Due to the continuous drying process in a progressive kiln as well as its higher annual drying capacity, a heat recovery system has shorter payback time for a progressive kiln than for a batch kiln (Esping 1982).

OBJECTIVE

In this work possible energy savings are investigated by introducing a new layout of a 2-zone progressive kiln. The layout consists of installing a door between the first and second zone, thereby allowing the two zones to be run at different temperature levels, making internal heat recovery possible.

MATERIAL AND METHODS

A new design of an OTC-kiln is suggested by adding a door between the two zones. By introducing the door the opportunity raises to run the two different zones at very different temperature levels. With one of the zones acting like a heat sink for the other, the amount of heat recovered in the total system can be increased considerably. A schematic sketch of the suggested system is shown in Fig. 1.

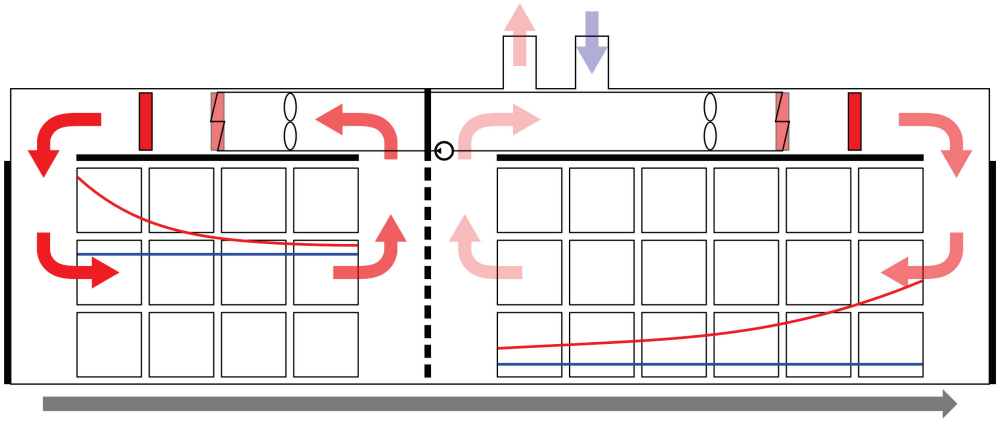

Fig. 1.
Optimized Two stage Continuous, OTC, kiln with heat exchanger and door between the two zones. In each zone, the dark red battery is showing a regular heat battery whereas the faded red battery, schematically connected with pipes, is showing the heat exchangers. The door between the two zones is presented by a dashed line and the directions of airflow in the two zones are illustrated by arrows. The feeding direction through the kiln is illustrated by the gray arrow in the bottom of the figure.

Due to the expense of constructing a kiln and run drying trials in full scale, the drying process was simulated using the commercial software Valusim. A drying schedule for drying Norway spruce *(Picea abies L. Karst)* sideboards from an initial moisture content of 110% to a final moisture content of 17.4% was created with parameters according to Table 1. The dimensioning of the kiln was chosen as to keep the possibility to run it without the door between the two zones.

Table 1

Ingoing parameters to wood drying simulations

Parameter	Zone 1	Zone 2
Dry bulb temperature of the air entering the wood stack [°C]	75	45
Wet bulb temperature of the air entering the wood stack [°C]	55	25
Circulating air [$kg_{dry\ air}$/s]	56	66
No. of trolley positions	3	12
Air leakage [% of $kg_{dry\ air}$/s]	25	25
Air speed in sticker space [m/s]	4.0	3.8
Sticker thickness [mm]	25	
Board thickness (nominal) [mm]	22	
Board average length [m]	4.5	
Package height [m]	1.5	
Package width [m]	6	
Package depth [m]	1.5	
No. of packages on each trolley	3	
Bolster thickness [mm]	90	
Species	Norway spruce	
Wood basic density [kg/m^3]	380	
Drying time [h]	36	
Initial moisture content [%]	110	

With a possible kiln layout and temperature levels of the drying stated, a model determining the conditions of the air was developed by implementing the basic thermodynamic equations of humid air. An amount of air passing the timber without actively taking part in the drying was chosen to represent air going through bolster spaces and around the timber packages.

Throughout the work, it was assumed that a heat exchanger able to transfer the heat from zone 1 to zone 2 could be constructed. Also, no consideration was given to the additional pressure drop over the air circulating fans that would be caused by the introduction of a heat exchanger. The power consumption of fans running the ventilation was also excluded from the calculations.

RESULT AND DISCUSSION

The resulting temperatures, moisture content and heat demand of the drying simulation is summarized in Table 2. Although the heat demand of zone 1 became 1.5 MW, only 1.4 MW was available for zone 2. The difference is explained by the air passing the timber and not taking part in the drying.

Table 2

Results from wood drying simulations. The temperatures after mixing the drying air with the air passing the wood and not taking part in the actual drying are reported.

Parameter	Zone 1	Zone 2
Dry bulb temperature of the air after passing the wood stack [°C]	63	34
Wet bulb temperature of the air after passing the wood stack [°C]	55	25
Moisture content when exiting the zone [%]	65	17.4
Heat demand [MW]	1.5	See Fig. 3.

Ideally, the heat demand of zone 1, caused by the evaporation of water from the timber to the air will be possible to release in the condenser of zone 1. If this is not possible, some of the moist air also needs to be vented out causing the energy efficiency of the kiln to drop. If, on the other hand, the heat demand in zone 2 is higher than what is available from zone 1 some additional heat needs to be added to zone 2 which also will cause the energy efficiency of the kiln to drop. If no ventilation is installed in zone 1and/or no additional heat sink is available, the ideal case would be to design the kiln with a slightly higher heat demand in zone 2. This design would give a high energy efficiency of the

kiln and some safety margin to prevent the process from becoming unstable. It should also be kept in mind that the air circulating fans will add some heat in zone 2 which needs to be taken into account. In practice, some additional heat is also transferred between the two zones, as well as between the kiln and the surroundings when the loading/unloading takes place. The additional heat transfer due to air leakage when the doors are open is not taken into account whereas the heat transfer through the heating of the wood is taken into account in the drying model.

Since air at lower temperature can contain considerably less water vapour, the low temperature in zone 2 implies that a large amount of the circulating air needs to be vented out to keep the assigned drying climate. Of course, the drying air in zone 2 can also be dehumidified by means of other technical solutions but otherwise the functionality of the kiln will be limited by the outdoor climate. The amount of circulating air in zone 2 that needs to be vented as a function of outdoor climate is shown in Fig. 2.

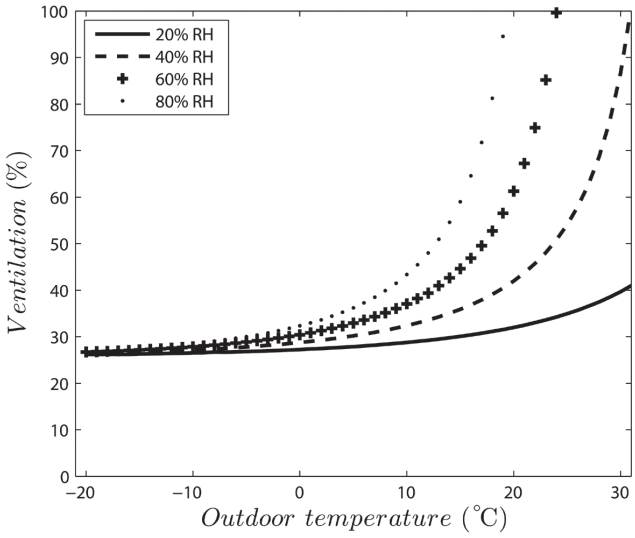

Fig. 2.
Ventilation demand as percentage of the circulating dry air of zone 2 at different outdoor temperatures and relative humidity.

From Fig. 2. it can be seen that the high ventilation demand at the suggested drying temperatures of zone 2 will cause the working range of the kiln to be limited. If the outdoor temperature and relative humidity is high the door between the two zones needs to be opened and the kiln operated as a traditional OTC-kiln.

As the amount of ventilation also affects the amount of outdoor air that needs to be heated in zone 2, the heat demand of zone 2 also becomes a function of the outdoor climate, see Fig. 3.

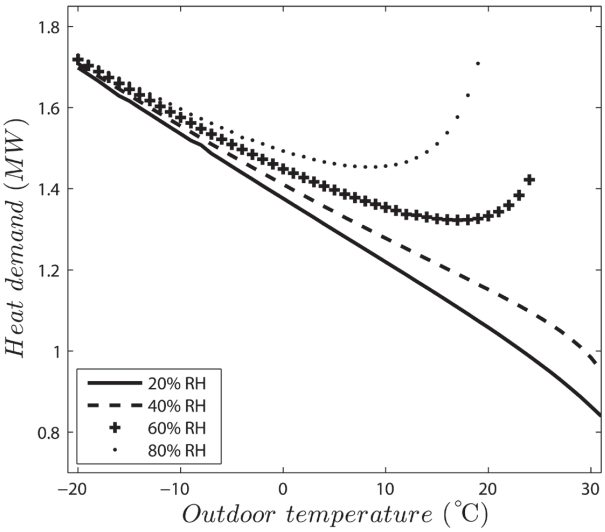

Fig. 3.
Heat demand of zone 2 as function of outdoor temperature and relative humidity.

From Fig. 3. it can be seen that the heat demand of zone 2 decreases approximately linear at low temperatures but as the maximum vapour content increases rapidly at higher temperatures, the heat demand becomes non-linear at higher temperatures. Since the available heat from zone 1 became 1.4 MW in our example and the fan power of zone 2 would add an additional power of approximately 0.1 MW, the suggested kiln design and drying parameters would not work when the heat demand of zone 2 is below 1.5 MW. The exact breakpoint when this happens can be moved slightly by dimensioning the kiln different or by changing some of the drying parameters that were reported in Table 1. As to enhance the working range of the kiln at high outdoor temperatures ventilation of zone 1 should be installed. By this, a part of the circulating air of zone 1 could be vented which would decrease the available heat for zone 2. Thereby, the critical minimum heat demand of zone 2 decreases and it would be possible to run the kiln at higher outdoor temperatures. Ventilation of zone 1 will however always decrease the recovered heat. The exact size of the recovered heat is hard to present due to our partly simplified system. Additional heat savings will also be a result from the fact that a condenser in zone 1 will results in a smaller amount of outdoor air than needs to be heated in zone 1 in comparison to when all the circulating air is dehumidified by ventilation. At an outdoor climate of 0°C and 80% RH where the heat demand of zone 2 is approximately what is available from zone 1, the total heat demand of the suggested system is roughly 1.6 MW. To run the kiln with the door open between the two zones the total heat demand of the kiln becomes roughly 2.2 MW. The total heat savings in our example thereby becomes roughly 30%.The small difference is explained by the fact that the drying in zone 2 becomes more energy efficient at higher temperatures.

As an additional heat recover, it would also be possible to install a traditional air to air heat exchanger for the ventilation air of zone 2. It should however be kept in mind that this heat exchanger would only be possible to use when the heat demand of zone 2 is sufficient high.

Also, either zone 1 or zone 2 can in principle be chosen to be the low temperature zone as long as the ventilation is placed in the low temperature zone. The wet bulb depression and air velocity in the low temperature zone should also be kept reasonable high to prevent mould growth (Esping 1987). The flow direction could also be the opposite of what is presented in Fig. 1, i.e. the kiln could be designed as a 2-zone feed-back kiln. The OTC-kiln layout was chosen since a high wet-bulb depression at the exit side of the kiln enhances the possibility to lower the moisture content of the last package in the kiln before the loading/unloading is done. With a small wet-bulb depression in the exit side of the kiln, hardly any drying will take place and delaying the loading/unloading of the kiln will mostly affect the packages early in the drying process.

To maintain a constant airspeed through the stacks, the electrical power consumption of the motors running the air circulating fans will increase by the introduction of the heat exchanger. If the price of heat generated by the air circulating fans (i.e. electric power) is higher than the price of heat generated by burning residuals, the profitability of the suggested system will decrease. Prior to construction of the suggested kiln, more research needs to be done regarding this matter.

CONCLUSION

Installation of ventilation or other additional ways to dehumidify the air of zone 1 is recommended if the presented kiln design and drying parameters are used. This is due to the fact that the heat demand of zone 2 is often lower than the available heat from zone 1. Furthermore, an installation of an air to air heat exchanger on the ventilation is not recommended since its operational time will be limited.

The suggested kiln design represents a great potential in terms of energy savings. Due to the direct interaction between the first and second zone, the behaviour of the kiln however becomes less intuitive. In contradiction to a traditional two zone continuous kiln, the outdoor climate also becomes an important factor for the kiln's functionality. The influence of ingoing process parameters should therefore be implemented in the kiln control system. This implementation will be a prerequisite to be able to use the full potential of the suggested system.

ACKNOWLEDGEMENT

We would like to acknowledge Valutec AB for sharing their ideas regarding this concept in timber drying and for valuable conversations and comments during our work.

REFERENCES

Anderson J-O, Westerlund L (2014) Improved energy efficiency in sawmill drying system. Appl Energy 113: 891-901.

Chua K.J, Chou S.K, Ho J.C, Hawlader M.N.A (2002) Heat Pump Drying: Recent Developments and Future Trends, Drying Technol 20: 1579-1610.

Elustondo D, Oliveira L (2006) Opportunities to Reduce Energy Consumption in Softwood Lumber Drying, Drying Technol 24: 653-662.

Esping B (1982) Energy Saving in Timber Drying. Wood Technology Report Nr 12. Wood Technology Centre, Stockholm (Sweden).

Esping B (1987) Wood drying 2 Drying defects-actions (in Swedish). TräteknikCentrum, Stockholm.

Hukka A (1996) A Simulation Program for Optimisation of Medium Temperature Drying on an Industrial Scale. Proc of the 5th International IUFRO Wood Drying Conference, Quebec City, (Canada), pp. 41-48.

Ikonen V-P, Kellomäki S, Peltola H (2003) Linking tree stem properties of Scots pine (Pinus sylvestris L.) to sawn timber properties through simulated sawing. Forest Ecology and Management 174: 251–263.

Johansson L, Westerlund L (2000) An open absorption system installed at a sawmill: Description of pilot plant used for timber and bio-fuel drying. Energy 25: 1067-1079.

Pinto I, Knapic S, Pereira H, Usenius A (2006) Simulated and realised industrial yields in sawing of maritime pine (Pinus pinaster Ait.). Holz als Roh- und Werkstoff 64: 30–36.

Salin J. G (2001) Determination of the most economical drying schedule and air velocity in softwood drying. In 3rd COST E15 Workshop, Helsinki, (Finland), pp. 1-10.

Salin J. G (2002) Simulation models as an industrial tool for optimizing the drying of timber. In 4th COST E15 Workshop, Santiago de Compostela, (Spain), pp. 1-8.

Salin J.G, Wamming T (2008) Drying of timber in progressive kilns: Simulation, quality, energy consumption and drying cost considerations. Wood Material Science & Engineering 3: 12-20.

Publication VI

Wood Material Science & Engineering, 2015
Vol. 10, No. 2, 197–204, http://dx.doi.org/10.1080/17480272.2014.995703

Taylor & Francis
Taylor & Francis Group

ORIGINAL ARTICLE

Influence of fan speed on airflow distribution in a batch kiln

TOMMY VIKBERG[1,2], LINUS HÄGG[2], & DIEGO ELUSTONDO[1]

[1]*Department of Engineering Sciences and Mathematics, Luleå University of Technology, Forskargatan 1, SE-931 87 Skellefteå, Sweden,* [2]*SP Wood Technology, SP Technical Research Institute of Sweden, Laboratorgränd 2, SE-931 77 Skellefteå, Sweden*

Abstract
This study reports experimental data of airflow distribution as a function of fan speed in an industrial batch kiln. Measurements were conducted with 20 hot-film anemometers distributed throughout the load at two occasions. The main result was that airflow distribution did not change significantly as the fan speed was reduced, and no positions where the air movement stopped were found. It was also found that relatively more air ran in the bolster spaces in comparison to the adjacent packages as the air ran through the load.

Keywords: *Wood drying, air velocity, hot-film anemometer, power savings*

Introduction

Over the last few decades, the sawmill industry in the Nordic countries has focused on making the production as flexible as possible to rapidly adapt to variations in timber supply and the market situation for the final products. The majority of boards are dried in air circulating batch kilns, and flexibility implies a kiln with the ability to dry boards with different dimensions and initial moisture contents (MCs) produced in the sawing process. The rate at which the hot air transfers heat to the wood and removes the evaporated water depends not only on the temperature and relative humidity of the air but also on the air velocity, to a lesser extent. It is well known from the literature that an increase in the air velocity increases the convective heat and mass transfer coefficients, especially when the flow turns from laminar to turbulent (Incropera *et al.* 2007). Increased air velocity also reduces the temperature drop across the load (Elustondo *et al.* 2009), thereby creating a more homogenous drying climate throughout the load.

In a mature coniferous tree, heartwood is formed in the centre of the trunk. The heartwood dries out because it is not actively taking part in the water transport in the stem. Therefore the heartwood MC in a green tree is in the range of 30–50% whereas the MC in the sapwood is in the range of 100–200%. Green boards originate from the centre of a trunk consisting of both heartwood and sapwood; the centre yield, therefore, naturally contains less water than sideboards from the same trunk. Due to the larger amount of sapwood as well as the larger total wood area facing the air (i.e., normally thinner dimensions of a sideboard), the evaporation rate of a load of side boards is much higher than that from a corresponding load of centre yield boards. To keep the flexibility in the production process (discussed earlier), the heat, ventilation and fan capacity are dimensioned to be able to dry sideboards. This normally results in an 'over dimensioning' of the kiln in the cases where the load consists of centre-yield boards.

Although it is better from a drying point of view to have high air velocity, there is great potential for cost savings, originating from the price difference between electricity and heat from burning residuals if the air velocity can be decreased. The air velocity should therefore be kept as low as possible without risking increased downgrading from the drying process. A customary approach to estimate the effect of

Correspondence: Tommy Vikberg, Department of Engineering Sciences and Mathematics, Luleå University of Technology, Forskargatan 1, SE-931 87 Skellefteå, Sweden. Tel:+46 920 49 10 00. Fax: +46 920 49 13 99. E-mail: tommy.vikberg@sp.se

(*Received 1 September 2014; revised 3 December 2014; accepted 3 December 2014*)

air velocity on fan power consumption is to use the fans' affinity laws (Owen 2012):

$$Q \propto N \tag{1}$$

$$\Delta p \propto \rho N^2 \tag{2}$$

$$W \propto \rho N^3 \tag{3}$$

where Q is the volume of air moved per unit of time (m^3/s), N is the fan rotational speed (1/s), Δp is the total air pressure increase (both static and dynamic) through the fans (Pa), ρ is the air density (kg/m^3) and W is the total power consumed by the fan (W). Equation 1 suggests that the volume of air moved per unit of time only depends on the fan's rotation speed. This is a crude approximation because the fan efficiency is affected by the operating conditions (Bernier and Bourret 1999). To the best of our knowledge, the standard practice in the wood drying industry is however to measure air velocity at ambient temperature.

In addition, Equation 3 suggests that the electric power consumed by the fans increases proportionally to the third power of the air velocity. Assuming that the fans' similarity laws are valid, reducing air velocity by 50% would reduce the power consumption by almost 90%. To reduce power consumption, some researchers have suggested reducing air velocity in the last stages of drying (Esping 1992, Salin 2001, Kudra 2004, Ananias *et al.* 2012). The rationale behind this suggestion is that the evaporation rate is mainly limited by the air heat and mass transfer in the first stage of drying. Therefore, reducing air velocity in the first stage of drying also increases drying time. In the last stages of drying, when the MC is below the fibre saturation point, the drying rate is mainly limited by the diffusive properties of the wood. Therefore, reducing air velocity in the last stages of drying may not significantly reduce drying rate (Esping 1992, Kudra 2004, Ananias *et al.* 2012). Some authors have also developed sophisticated mathematical models to prove the benefits of reducing air velocity in the last stages of drying (Perré *et al.* 2007, Perré 2010), as well as for implementing airflow reversal to compensate for the temperature drop across the load (Perré *et al.* 2012). It should also be mentioned that some authors have found that reducing air velocity is not always beneficial from a cost-saving perspective (Riley and Haslett 1996, Riley and Sargent 2010).

One potential problem with reducing air velocity is that it could also affect the uniformity of the airflow distribution through the load. Some people believe that reducing fan speed could lead to a less uniform airflow distribution and even create dead zones in which the airflow virtually stops. The importance of having a relatively uniform airflow distribution throughout the load is a well-accepted fact in the wood drying industry. This has been demonstrated in the literature through mathematical models (Nijdam and Keey 2000, Pougatch *et al.* 2003) and laboratory studies (Nijdam and Keey 1999), and a number of kiln design recommendations are available (Ledig *et al.* 2007). Probably, the most well-known recommendation is the rule of thumb for the plenum width (the distance in the flow direction between the load and the kiln walls). It has been proposed that the plenum width should be at least equal and preferably twice the sum of all of the gaps between the wood layers (Arnaud *et al.* 1991, Nijdam 1998, Nijdam and Keey 1999). These studies also concluded that the standard rectangular geometry of industrial kilns creates significant recirculation zones in the plenums (Nijdam and Keey 1999), thus resulting in a non-uniform air velocity profile from top to bottom of the kiln chamber.

To assess airflow distribution in industrial kilns, it is customary to measure air velocity at ambient temperature at the exit side of the lumber stack (Cabrera 2007, Steiner *et al.* 2011). This is used for mapping the air velocities coming out from the load in a plane perpendicular to the airflow direction, but it does not show the airflow distribution throughout the load. It is possible that the airflow distribution may change as the air flows through the load (Ledig and Militzer 1999), thus creating a risk of increased downgrading due to poor drying, when trying to reduce the air velocity in practice. Furthermore, many kilns in Sweden are used to dry boards with random lengths, thus introducing a random distortion in the airflow patterns. Consequently, the objective of this study was to implement and test a more comprehensive set-up to measure airflow distribution in industrial kilns as a function of fan rotational speed.

The method used in this study consisted of installing a number of airflow meters at selected positions within the wood packages so that the air velocity could be simultaneously measured at different locations in the load. The reported data are probably unique for kilns with a design similar to the one tested in this study, and provides a measure of how airflow distribution in an industrial kiln is affected when reducing the fan rotational speed.

Materials and methods

The study was performed in an industrial batch kiln operated by a local sawmill in Northern Sweden. The kiln accommodated 28 packages of wood arranged in 7 stacks. The size of each package was

approximately 1.5 m long × 1.5 m high × 5.5 m wide. Figure 1 shows a schematic diagram of the batch kiln loaded with seven columns of lumber packages. Each package contained 21 layers of 50 mm thick scots pine (*Pinus sylvestris*) separated by 21 mm thick stickers. The packages in one stack were separated with bolsters with a dimension of 95 × 95 mm^2. The total cross sectional area available for airflow through the load was approximately 11.4 m^2. The kiln was equipped with three fans for circulating the air with a total maximum power of 66 kW. Each fan was controlled through variable frequency drives capable of arbitrarily reducing the rotation speed. The kiln ceiling space was 2.1 m and the plenum width was 2.0 m.

To measure the airflow distribution, a total of 20 hot-wire anemometers (EE575 from E+E Elektronik) were installed at selected positions inside the lumber load. According to the manufacturer, these anemometers provided a linear relationship between air velocity and voltage within a 0–20 m/s range. Unfortunately, the anemometers could not withstand the warm and humid climate that is required for drying wood; therefore, all measurements were conducted at room temperature with dried wood. A data logger was used to collect the readings of the 20 anemometers simultaneously every 1 s, and each average air velocity reported in this study represents the average of approximately 400 data points.

Two experimental designs were used to test the effect of fan speed on the airflow distribution, hereafter denoted as trial 1 and trial 2. Trial 1 was designed to compare airflow distribution between selected package columns at 30%, 50%, 70% and 90% fan speed, while experiment 2 was designed to compare airflow distribution between selected stack heights at 30%, 40%, 50%, 60%, 70%, 80% and 90% fan speed. Figures 2 and 3 show the anemometer

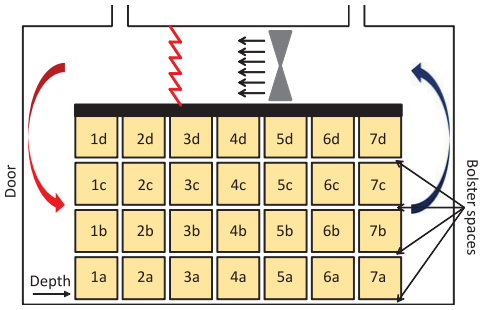

Figure 1. Schematic representation of the kiln and the seven stacks with four packages in each stack. The numbering of the packages is used to identify the position of the gauges in the kiln load.

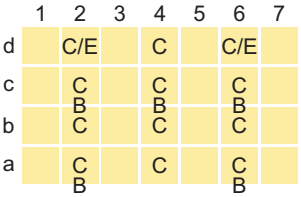

Figure 2. Position of anemometers during trial 1, cf. Figure 1. The capitalized letters in the figure correspond to C, = Centre of the package, E = End of package and B = bolster space.

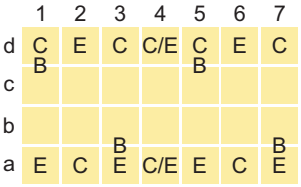

Figure 3. Position of anemometers during trial 2, cf. Figure 1. The capitalized letters in the figure correspond to C = Centre of the package, E = End of package and B = bolster space.

arrangements for trials 1 and 2, respectively, with the letters and numbers used to identify the packages included in the figures. Unfortunately, one of the gauges failed during trial 1 and is therefore excluded from Figure 2 and further analysis.

Most of the anemometers used in trial 1 were placed in the middle of the 5.5 m wide load. In trial 2, the anemometer locations were alternated between the middle of the package (denoted Centre) and a location approximately 50 cm from the end of the packages, where only every second board was present (denoted End). The reason for selecting these two anemometer locations was that wood packages in Sweden typically contain boards of random lengths that are alternated to only reach one of the package's ends. Figure 4 shows the stacking technique of a typical wood package in Sweden, where it can be observed how every second piece is arranged to reach one of the package ends. To prevent the entrance effect from affecting the measurements to a great extent, every anemometer was placed approximately 50 cm deep into the package (dimension denoted 'Depth' in Figure 4).

For each one of the achieved data-sets (i.e. data from trial 1 and trial 2, respectively), a hypothesis test was performed on the mean air velocity at each fan speed for each sensor placed in a 'Centre' position. The applied test assumed normally distributed data with equal variances – prerequisites that seemed reasonably fulfilled after plotting the

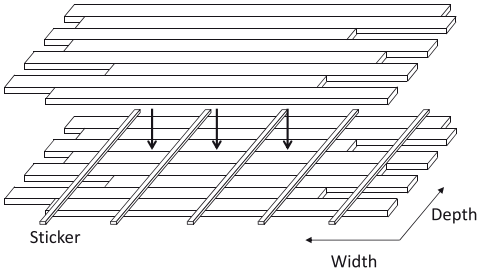

Figure 4. Typical stacking technique in Sweden for a package prior to drying. Note that every second board is aligned to reach one of the package ends. This results in porous package ends and hard determined airflow patterns.

distributions and comparing their sample standard deviations. The null hypothesis that there was no difference in mean between the two distributions was examined with the test statistic:

$$t_0 = \frac{\bar{X}_1 - \bar{X}_2}{S_p\sqrt{\frac{1}{n_1} + \frac{1}{n_2}}} \qquad (4)$$

where t_0 is the t-test score, $\bar{X}$ and n are the mean value and number of observations from distribution 1 and 2, respectively, and S_p is the pooled estimator of the joined variance. As a rejection criterion for the t-test, $\alpha = 0.05$ was used.

Because full-size measurements of the air velocity distribution at different fan speeds can be time-consuming, it is tempting to just make one measurement and then estimate the effect of reducing the fan speed. To get an idea of whether a single measurement is sufficient from an industrial point of view, Equation 1 was applied to estimate the mean air velocities at fan speed 70%, 50% and 30% of the four Centre placed gauges of stack 2, 4 and 6 in trial 1. To perform this examination, the mean air velocity at a fan speed 90% was assumed to be known from measurements.

Results and discussion

The large amount of data achieved from the two trials presented in this paper implies numerous ways to analyse and present the result. The mean air velocity and the corresponding standard deviation at each point of measurement for all tested fan frequencies are therefore presented in Tables I and II.

The result from hypothesis testing of differences in mean air velocity between each anemometer located at a Centre position and at each tested fan speed showed that the null hypothesis could be

Table I. Mean air velocities through packages and bolster spaces at all fan speeds measured in trial 1.

	Average air velocity and standard deviation (m/s)											
Fan speed	30%			50%			70%			90%		
Stack #	2	4	6	2	4	6	2	4	6	2	4	6
d Centre	1.2 (.04)	1.3 (.08)	1.7 (.04)	2.1 (.05)	2.5 (.13)	3.0 (.06)	3.0 (.06)	3.7 (.10)	4.5 (.08)	3.9 (.07)	4.8 (.16)	5.8 (.09)
d End	0.7 (.02)		1.0 (.05)	1.3 (.03)		2.0 (.06)	2.0 (.05)		2.8 (.08)	2.7 (.06)		3.7 (.12)
c Centre	1.5 (.02)	1.5 (.02)	1.4 (.05)	2.6 (.05)	2.7 (.06)	2.5 (.06)	3.8 (.06)	4.0 (.09)	3.6 (.08)	4.9 (.06)	5.3 (.09)	4.7 (.08)
bc Bolster	1.6 (.04)	3.0 (.06)	3.3 (.05)	2.7 (.08)	5.0 (.11)	5.7 (.07)	3.9 (.13)	6.7 (.12)	7.6 (.11)	5.0 (.14)	8.5 (.19)	9.7 (.16)
b Centre	1.6 (.02)	1.5 (.04)	1.6 (.02)	2.9 (.03)	2.6 (.08)	2.7 (.04)	4.1 (.04)	3.7 (.12)	3.9 (.05)	5.3 (.05)	4.7 (.10)	5.0 (.06)
a Centre	1.8 (.03)	1.4 (.04)	1.6 (.02)	3.1 (.04)	2.4 (.04)	2.7 (.03)	4.5 (.05)	3.4 (.06)	4.0 (.03)	5.8 (.06)	4.5 (.06)	5.2 (.04)
0a Bolster	2.0 (.09)		1.4 (.03)	3.8 (.15)		2.4 (.04)	5.7 (.19)		3.7 (.06)	7.3 (.23)		5.1 (.10)

Values enclosed by parenthesis are the corresponding standard deviations.

Table II. Mean air velocities through packages and bolster spaces at all fan speeds measured in trial 2.

Average air velocity and standard deviation (m/s)									
	Stack #								
Row	1	2	3	4	4	5	6	7	Fanspeed
d Centre/End	1.0 C (.13)	1.0 E (.03)	1.2 C (.03)	1.2 C (.03)	0.8 E (.03)	1.5 C (.04)	1.3 E (.06)	1.5 C (.05)	30%
ab/cd Bolster	2.1 cd (.14)		3.2 ab (.08)			3.0 cd (.07)		3.3 ab (.11)	
a Centre/End	1.5 E (.07)	1.8 C (.03)	1.2 E (.04)	1.4 C (.03)	1.0 E (.02)	0.9 E (.03)	1.5 C (.04)	0.8 E (.03)	
d Centre/End	1.5 C (.16)	1.4 E (.05)	1.7 C (.03)	1.6 C (.04)	1.2 E (.04)	2.0 C (.04)	1.8 E (.08)	2.1 C (.04)	40%
ab/cd Bolster	2.8 cd (.21)		4.4 ab (.11)			4.1 cd (.10)		4.6 ab (.15)	
a Centre/End	2.1 E (.10)	2.4 C (.04)	1.7 E (.06)	1.9 C (.03)	1.4 E (.03)	1.3 E (.04)	2.1 C (.04)	1.1 E (.04)	
d Centre/End	1.9 C (.20)	1.8 E (.06)	2.2 C (.04)	2.1 C (.04)	1.6 E (.04)	2.6 C (.06)	2.2 E (.09)	2.7 C (.07)	50%
ab/cd Bolster	3.6 cd (.29)		5.5 ab (.12)			5.1 cd (.12)		5.8 ab (.14)	
a Centre/End	2.7 E (.12)	3.0 C (.04)	2.2 E (.06)	2.3 C (.03)	1.7 E (.03)	1.7 E (.06)	2.6 C (.06)	1.4 E (.04)	
d Centre/End	2.4 C (.24)	2.2 E (.06)	2.6 C (.05)	2.5 C (.06)	2.0 E (.05)	3.2 C (.06)	2.8 E (.11)	3.3 C (.09)	60%
ab/cd Bolster	4.3 cd (.34)		6.6 ab (.16)			6.0 cd (.13)		6.8 ab (.13)	
a Centre/End	3.3 E (.14)	3.7 C (.05)	2.7 E (.07)	2.9 C (.04)	2.1 E (.03)	2.1 E (.06)	3.1 C (.06)	1.8 E (.05)	
d Centre/End	2.8 C (.27)	2.6 E (.09)	3.1 C (.05)	3.0 C (.05)	2.4 E (.07)	3.9 C (.06)	3.3 E (.14)	4.0 C (.08)	70%
ab/cd Bolster	5.1 cd (.41)		7.5 ab (.16)			6.8 cd (.14)		7.8 ab (.20)	
a Centre/End	3.9 E (.17)	4.3 C (.05)	3.2 E (.07)	3.3 C (.04)	2.5 E (.05)	2.5 E (.08)	3.7 C (.08)	2.1 E (.05)	
d Centre/End	3.3 C (.33)	3.0 E (.09)	3.6 C (.07)	3.5 C (.07)	2.8 E (.07)	4.4 C (.06)	3.8 E (.18)	4.6 C (.09)	80%
ab/cd Bolster	5.8 cd (.37)		8.5 ab (.22)			7.7 cd (.18)		8.9 ab (.19)	
a Centre/End	4.5 E (.16)	5.0 C (.05)	3.6 E (.09)	3.8 C (.06)	2.8 E (.04)	3.0 E (.08)	4.3 C (.07)	2.5 E (.07)	
d Centre/End	3.6 C (.33)	3.3 E (.10)	4.0 C (.06)	3.9 C (.07)	3.1 E (.08)	4.9 C (.09)	4.3 E (.17)	5.1 C (.09)	90%
ab/cd Bolster	6.2 cd (.42)		9.2 ab (.22)			8.5 cd (.18)		9.7 ab (.23)	
a Centre/End	4.9 E (.18)	5.4 C (.06)	4.0 E (.09)	4.2 C (.05)	3.1 E (.04)	3.3 E (.09)	4.8 C (.08)	2.8 E (.07)	

Values enclosed by parenthesis are the corresponding standard deviations.
C, Centre of the package; E, End of the package; ab and cd, between packages.

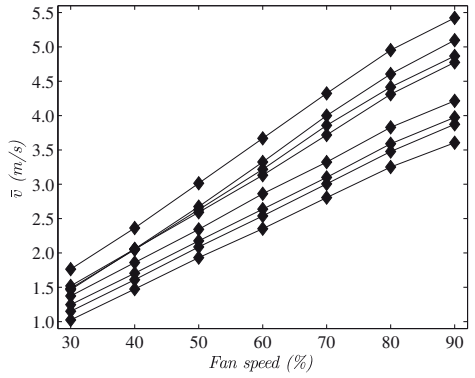

Figure 5. Typical velocity profiles as the fan speed is varied. Each line represents the measured mean air velocity of one of the Centre placed gauges in trial 2.

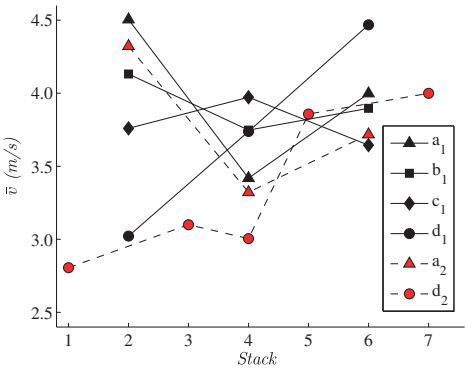

Figure 6. Typical air velocity distribution throughout the kiln load. The values are shown for a fan speed of 70%. The legends refer to the height of the package in the stack and the subscript is referring to trials 1 and 2, respectively.

rejected at the $\alpha = 0.05$ level in 453 cases out of the total number of combinations of 460. It should, however, be noticed that the data are not independent since:

- a high air velocity at time t probably implies that a high air velocity is recorded at time $t + 1$ as well,
- a high air velocity at one gauge at time t probably implies that a high air velocity is recoded at time $t + \tau$ for a gauge placed after the first one in the direction of the airflow.

Still, due to the result of the hypothesis testing, it was concluded that further investigation of the dataset was reasonable. The question of whether the airflow distribution changes as a function of fan speed was investigated in an intuitive way by plotting the mean air velocity for the gauges as a function of the fan speed. As seen in a typical figure of a velocity profile (Figure 5), the parallelism of the velocity profiles indicates that there was no dramatic change in the air velocity distribution as a function of fan speed.

When Equation 1 was applied to estimate the mean air velocity of each stack at fan speeds of 30%, 50% and 70%, the accuracy was remarkably good with a ratio between estimated and measured air velocities between 1.0 and 1.1. The result is summarized in Table III.

In Figure 6, an air velocity distribution is shown at a fan speed of 70%. Because the air velocity distribution did not remarkably change as a function of fan speed, as shown in Figure 5, the values are only presented for one fan speed. In agreement with the previous literature (Ledig *et al.* 2007), the air velocity at the entry side of the airflow tended to increase from the top to the bottom of the load. The global maximum and minimum were found in the

Table III. Mean air velocities of the four gauges placed in stacks 2, 4 and 6 for the four fan speeds run in trial 1.

Measured and estimated air velocity (m/s)												
Fan speed	30%			50%			70%			90%		
Stack #	2	4	6	2	4	6	2	4	6	2	4	6
$\bar{v}$ Centre	1.5	1.5	1.6	2.7	2.6	2.7	3.9	3.7	4.0	5.0	4.9	5.2
$\bar{v}_{est.}$ Centre	1.7	1.6	1.7	2.8	2.7	2.9	3.9	3.8	4.0	–	–	–
$\bar{v}_{est.}/\bar{v}$	1.1	1.1	1.1	1.0	1.1	1.1	1.0	1.0	1.0	–	–	–

The table also shows the estimated mean air velocities at fan speed 30%, 50% and 70% by Equation 1 in which the air velocity at 90% fan speed was assumed to be known by measurements. The bottom row shows the ratio between the estimated and measured air velocity.

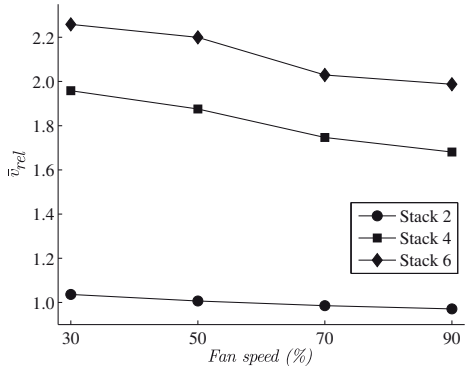

Figure 7. Relative air velocity in the bolster space between packages b and c compared to the average of the two gauges placed in the Centre of package b and c.

first stacks; this is valuable information because those positions are quite easy to access when performing measurements with a hand-held meter. It was also found that the air velocity in the top package increases as the air goes through the load, and there is as well a tendency of diagonal airflow from the bottom to the top of the kiln. These behaviours are expected since the distribution of static pressure in the plenum spaces results in the largest pressure drop (in static pressure) between the bottom of the plenum space at the entry side of the load, and the top of the plenum space at the exit side (Ledig *et al.* 2007). Furthermore, it is interesting to observe that the bottom packages show the lowest air velocity in the middle of the kiln, i.e., stack 4. This behaviour was not fully understood, but because the results from the two trials were consistent, it seems reasonable to assume that the phenomenon is real and not a coincidence. The large differences in air velocity at different positions in the stack might be explained by the ratio between the ceiling height and the plenum width as well as the ratio between the plenum width and the total height of the sticker and bolster spaces. These ratios were 1.1 and 1.0, respectively whereas the design recommendation is to keep both of these ratios at least below 1.0 and preferably below 0.5 (Ledig *et al.* 2007).

Because it is common practice to reverse the flow direction several times during a drying run, it should be kept in mind that what is denoted as stack 1 in this work would in reality experience the reported air velocity of stack 1 only half of the total drying time. The other half of the drying time, i.e., when the fan rotational direction is reversed, it would experience the air velocity that is presented here as the air velocity of stack 7.

The relative air velocity in the bolster space between packages b and c compared to the mean velocity of the same packages is shown in Figure 7. It is clear that the air velocity tends to even out with increasing fan speed, and there is more air run in the bolster spaces as the air flows through the load by comparing stacks 2, 4 and 6. The very low air velocity in stack 2 should be interpreted with care since the package 1b in trial 1 was slightly lower than the rest of the packages. This resulted in a different height of the bolster position between packages b and c in stack 1 compared to the other stacks and thereby the air velocity in the bolster space between packages b and c in stack 2 was lower than it would have been otherwise.

Conclusions

In this study, a relatively simple method was implemented and tested to measure airflow distribution in industrial kilns. The method consisted of installing a number of airflow meters at selected positions within the wood packages so that the air velocity is measured simultaneously at different locations throughout the load. The method was applied to a batch kiln operated by a local sawmill in northern Sweden for drying 50 mm thick pine with random lengths. In this study it was found that:

- The airflow distribution was not remarkably affected by the fan speed.
- The magnitude of the air velocity varied a lot between different positions in the load and measurements of the airflow distribution in a full-size kiln with dimensions that fulfil the design recommendations would be highly interesting. A more uniform airflow distribution would, most probably, result in a higher drying quality.
- The accuracy of the first fan similarity law was good enough, from an industrial point of view, to estimate the effect of reducing the fan speed on the air velocity. It also turned out to be better to carefully examine the airflow distribution at one fan speed and then to estimate the effect of changing the fan speed than to measure the airflow at fewer points but at several fan speeds.
- There was a tendency of a diagonal flow through the batch, going from the bottom to the top of the stack in the airflow direction.

- The most extreme airflow variations in height position was found in the first stack in the flow direction.
- No volumes were found in the batch where the airflow stopped completely, even at the lowest air velocity.
- The air velocity in the bolster spaces relative to the adjacent packages became larger as the fan speed was decreased although the largest difference was noticed between different stacks in the kiln.
- It was possible to considerably reduce the fan energy consumption without affecting the performance of the kiln in terms of the uniformity of the airflow distribution. The critical challenge is to do so without affecting the drying quality and the MC distribution of the load. These matters have to be researched more thoroughly.

Acknowledgements

This work was partly supported financially by Träcentrum Norr, a research programme jointly funded by industrial stakeholders, the European Union (ERDF) and the country administrative boards of Norrbotten and Västerbotten.

Disclosure statement

No potential conflict of interest was reported by the authors.

References

Ananias, R. A., Ulloa, J., Elustondo, D. M., Salinas, C., Rebolledo, P. and Fuentes, C. (2012) Energy consumption in industrial drying of radiata pine. *Drying Technology*, 30(7), 774-779.

Arnaud, G., Fohr, J.-P., Garnier, J.-P. and Ricolleau, C. (1991) Study of the air flow in a wood drier. *Drying Technology*, 9(1), 183–200.

Bernier, M. A. and Bourret, B. (1999) Pumping energy and variable frequency drives. *ASHRAE Journal*, 41(12), 37–40.

Cabrera, M. R. (2007) *Investigation of an air velocity reduction in the kiln drying process*. Master Thesis, Luleå University of technology, Sweden.

Elustondo, D. M., Oliveira, L. and Lister, P. (2009) Temperature drop sensor for monitoring kiln drying of lumber. *Holzforschung*, 63, 334–339.

Esping, B. (1992) *Trätorkning 1a: grunder i torkning* [Wood Drying 1a: Basics in Drying]. (In Swedish). (Stockholm: Trätek).

Incropera, F. P., Dewitt, D. P., Bergman, T. L. and Lavine, A. S. (2007) *Fundamentals of Heat and Mass Transfer* (6th ed.) (Hoboken: John Wiley & Sons).

Kudra, T. (2004) Energy aspects in drying. *Drying Technology*, 22, 917–932.

Ledig, S. F. and Militzer, K. E. (1999) *Measurement and simulation of flow fields in convection timber kilns*. Proceedings of the First COST ACTION E15 Wood Drying Workshop, Edinburgh, UK, October 13–14.

Ledig, S. F., Paarhuis, B. and Riepen, M. (2007) Airflow within kilns. In P. Perré (ed.) *Fundamentals of Wood Drying*, ISBN: 9782907086127. Nancy, France: A.R.BO. LOR, 291–332.

Nijdam, J. J. (1998) *Reducing moisture-content variations in kiln-dried timber*. Ph.D. Thesis, University of Canterbury, New Zealand.

Nijdam, J. J. and Keey, R. B. (1999) Airflow behavior in timber (lumber) kilns. *Drying Technology*, 17, 1511–1522.

Nijdam, J. J. and Keey, R. B. (2000) The influence of kiln geometry on flow maldistribution across timber stacks in kilns. *Drying Technology*, 18, 1865–1877.

Owen, M. S. (ed.) (2012) *ASHRAE Handbook – HVAC Systems and Equipment* (Atlanta: ASHRAE).

Perré, P. (2010) Multiscale modelling of drying as a powerful extension of the macroscopic approach: Application to solid wood and biomass processing. *Drying Technology*, 28, 944–959.

Perré, P., Rémond, R. and Aléon, D. (2007) Energy saving in industrial wood drying addressed by a multi-scale computational model: Board, stack and kiln. *Drying Technology*, 25, 75–84.

Perré, P., Rémond, R., Colin, J., Mougel, E. and Almeida, G. (2012) Energy consumption in the convective drying of timber. *Drying Technology*, 30, 1136–1146.

Pougatch, K., Bian, Z., Gartshore, I., Salcudean, M. and Oliveira, L. (2003) Modelling of airflow and wood drying inside a kiln: A comprehensive approach. *Forest Products Journal*, 53, 46–54.

Riley, S. and Sargent, R. (2010) *Optimising softwood drying schedules*. Proceedings of the 11th International IUFRO Wood Drying Conference, Skellefteå, Sweden, January 18–22, pp. 154–159.

Riley, S. G. and Haslett, A. N. (1996) *Reducing air velocity during timber drying*. Proceedings of the Fifth International IUFRO Wood Drying Conference, Québec, Canada, August 13–17, pp. 301–308.

Salin, J.-G. (2001) *Determination of the most economical drying schedule and air velocity in softwood drying*. Proceedings of European COST ACTION E15 3rd Workshop on Softwood Drying to Specific End-Uses, Helsinki, Finland, June 11–13.

Steiner, Y., Vestøl, G. I., Horn, H. and Sandland, K. M. (2011) Impact of various measures to optimize the air velocity in an industrial wood-drying process. *Wood Material Science and Engineering*, 6, 15–22.